

Electronic Thesis and Dissertation Repository

12-13-2018 10:30 AM

Aversion and Warning Factors for Assessing Existing Reinforced Concrete Structures

Marcie van Weerdhuizen, *The University of Western Ontario*

Supervisor: Bartlett, F. Michael, *The University of Western Ontario*

A thesis submitted in partial fulfillment of the requirements for the Master of Engineering Science degree in Civil and Environmental Engineering

© Marcie van Weerdhuizen 2018

Follow this and additional works at: <https://ir.lib.uwo.ca/etd>



Part of the [Structural Engineering Commons](#)

Recommended Citation

van Weerdhuizen, Marcie, "Aversion and Warning Factors for Assessing Existing Reinforced Concrete Structures" (2018). *Electronic Thesis and Dissertation Repository*. 5979.
<https://ir.lib.uwo.ca/etd/5979>

This Dissertation/Thesis is brought to you for free and open access by Scholarship@Western. It has been accepted for inclusion in Electronic Thesis and Dissertation Repository by an authorized administrator of Scholarship@Western. For more information, please contact wlsadmin@uwo.ca.

Abstract

In a world of aging infrastructure, sustainability initiatives require additional investment in the assessment of existing reinforced concrete structures. Reliability-based assessment should minimize costs by reducing conservatism, while ensuring levels of safety equivalent to those for new designs. Current Canadian and US provisions assign target reliability levels for structural assessment based on criteria including occupancy type, expected failure behaviour, and the effect of element failure on the overall structural integrity. These criteria are defined using discrete and qualitative parameter values. It is shown that the true structural conditions can be better represented by verifying the applicability and completeness of these parameters and associating them with quantifiable structural attributes. Structural risk can be quantified by determining the number of people at risk due to an element failure, and by using the magnitude of deflection at incipient failure as an indicator of the warning of failure. Flexural capacities for assessment can be increased by up to 60% of values used for design using reduction factors calibrated to these parameters.

Keywords: Reinforced concrete, reliability, assessment, ductility, deflection, plasticity

Contents

Abstract	i
List of Figures	vi
List of Tables	ix
List of Appendices	x
List of Symbols	xi
1 Introduction	1
1.1 Introduction	1
1.1.1 Risk and Structural Failure	3
1.2 Background	4
1.2.1 General Probability of Failure	4
1.2.2 Notional Probability of Failure	4
1.2.3 Probability of Failure in Structures	5
1.3 Impact on Structural Assessment Outcomes	6
1.3.1 Economic and Environmental Impact	7
1.4 Objectives	8
1.5 Scope	9
1.6 Organization	9
2 Literature Review	11

2.1	Introduction	11
2.2	Literature Overview	12
2.2.1	Early Application of Reliability Concepts	15
2.2.2	Canadian Building Codes	15
2.2.3	Canadian Bridge Codes	16
2.2.4	American Building Codes	16
2.3	Review of Common Parameters	17
2.3.1	Aversion	18
2.3.2	Ductility	19
2.3.3	Redundancy	19
2.3.4	Other	20
2.4	Summary and Conclusions	20
3	Quantifying the Aversion Factor	22
3.1	Introduction	22
3.2	Analysis	23
3.2.1	Occupant Density	24
3.2.2	Occupancy Duration	26
3.2.3	Live Load Reduction Factor	27
3.3	Results	29
3.3.1	Number of Occupants at Risk	29
3.4	Summary and Conclusions	32
4	Quantifying the Warning of Failure	34
4.1	Introduction	34
4.1.1	Definition of Flexural Limit States	35
4.1.2	Metrics of Warning	35
	Warning by Additional Load Capacity after First Yield	36

	Warning by Visible Deflection	37
4.1.3	Plastic Behaviour of Reinforced Concrete in Flexure	37
	Deflection at Ultimate Limit States	38
4.1.4	Progression toward Failure	39
4.2	Analysis	41
4.2.1	Assumptions	41
4.2.2	Cross Section Analysis	42
	Curvature Ductility Ratio	46
	Shape Factor	46
	Ratio of Moment Capacities	48
4.2.3	Beam Analysis	49
	Load Configuration	49
	End Restraint Conditions	53
	Two-Span Beams	55
4.3	Results	57
4.3.1	Determinate Beams	57
4.3.2	Indeterminate Beams	60
4.4	Definition of Warning Factor	62
4.4.1	Deflection Coefficient	62
4.4.2	Warning Factor	68
4.5	Conclusions	70
5	Calibration Procedure for Assessment	72
5.1	Introduction	72
5.2	Design Basis for Calibration	72
5.3	Application to Assessment Procedure	75
5.3.1	Effects of n and W on Target Reliability Indices	80
5.3.2	Effects of Statistical Parameters on ϕ_a	81

5.3.3	Lifetime Reliability Indices	83
5.4	Draft Code Procedure	84
5.5	Conclusions	86
6	Conclusions and Recommendations	88
6.1	Summary	88
6.2	Conclusions	90
6.3	Recommendations and Future Work	92
	References	95
A	Deflection Calculations	98
A.1	Summary of Deflections and Plastic Hinge Lengths	98
A.2	Example	100
A.2.1	Plastic Hinge Lengths	100
A.2.2	Plastic Deflections	101
B	Warning of Failure Expansions	103
B.1	Ratio of Moment Capacities	103
B.2	Two Span Beam Analysis	104
	Curriculum Vitae	107

List of Figures

1.1	Relationship of probability of failure to load and strength reduction factors . . .	2
3.1	Live load reduction factor as a function of tributary area	30
3.2	Number of people at risk due to structural failure using NBCC and ASCE 7 live load reductions for $\rho_w = 1.0$	31
3.3	Number of people at risk due to structural failure for members carrying large tributary areas using NBCC live load reductions for areas less than 200 m ² . . .	32
4.1	Failure progression of a propped cantilever with concentrated load at midspan .	39
4.2	Plastic hinges at collapse for one- and two-span beams with idealized boundary conditions	40
4.3	Moment-curvature relationship of a reinforced concrete cross section	43
4.4	Beam cross-section dimensions, stress and strain diagrams at YLS and ULS . .	44
4.5	Curvature variation with reinforcement ratio and concrete strength at YLS and ULS	45
4.6	Curvature ductility variation with ρ and f'_c	47
4.7	Shape factor, f , variation with reinforcement ratio and concrete strength	47
4.8	Free body diagram used to compute plastic hinge lengths	49
4.9	Force effects and curvatures for simply supported beams under three load con- figurations	50
4.10	Plastic hinge length for simply supported beams	52
4.11	Simply supported beams with multiple concentrated loads	52

4.12	Plastic hinge lengths for multiple concentrated loads, normalized with respect to the plastic hinge length for a UDL	53
4.13	Force effects for beams with a concentrated load at midspan	54
4.14	Hinge length variation with shape factor, boundary condition, and load configuration	56
4.15	Total normalized deflection of determinate beams at ULS	58
4.16	Total normalized deflection for a simply supported beam	59
4.17	Deflection ratios for determinate beams under uniformly distributed loading	59
4.18	Ratio of ultimate to yield deflections for statically determinate beams	60
4.19	Total normalized deflection of indeterminate beams at ULS	61
4.20	Total normalized deflection for a fixed ended beam	62
4.21	Variation of deflection coefficient, a , with concrete strength for cross sections with $d = 0.95h$	64
4.22	Deflection coefficient variation with reinforcement ratio, and length-to-depth ratio for $f'_c = 25$ MPa	65
4.23	Deflection-length ratios	66
4.24	Deflection-length ratios for elements with $\alpha = 20$	67
4.25	Definition of deflection limits for warning of failure	68
4.26	Warning factor for all end conditions, $\alpha = 20$	69
5.1	Target annual probability of failure variation with design basis and assessment parameters	74
5.2	Target annual target reliability index variation with design basis and assessment parameters	76
5.3	Strength reduction factor variation with load fraction	79
5.4	Normalized strength reduction factor variation with load fraction	80
5.5	Variation of strength reduction factor using alternate statistical parameters	82
5.6	Lifetime (50-year) target reliability indices	84

B.1 Comparison of deflections at incipient failure for M^-/M^+ from 1.0 to 2.0 104

B.2 Load patterns for two-span beams 105

B.3 Elastic curves for two-span beams 106

B.4 Comparison of deflections at imminent failure two span beams with asymmet-
rical loading 106

List of Tables

1.1	Probability of failure and reliability index	5
2.1	Comparison of structural risk concepts in structural design and assessment codes	13
3.1	Occupant density comparison	25
3.2	Occupant density and duration summary	27
4.1	Analysis parameters	42
4.2	Simply supported beam configurations	51
4.3	Fixed-ended beam configurations	55
4.4	Minimum cross section depths, L/h , for deflection control from CAN/CSA A23.3-14 (2014)	63
5.1	Statistical parameters for loads and resistances in Bartlett, Hong, and Zhou, 2003	78
5.2	Extreme values of annual target reliability index for $k = 7.0 \times 10^{-4}$	81
5.3	Extreme values of annual target reliability index for $k = 3.0 \times 10^{-5}$	81
A.1	Elastic deflections and associated loading	98
A.2	Plastic deflections	99
A.3	Plastic hinge lengths; at support ($\ell_{p,1}$), and in span ($\ell_{p,2}$)	99

List of Appendices

Appendix A Deflection Calculations	98
Appendix B Warning of Failure Expansions	103

List of Symbols

a Compression block depth, $\beta_1 c$

A Activity factor

b Width of cross section

c Depth to neutral axis from extreme compression fibre at Ultimate Limit State

d Effective depth

f Shape factor, M_u/M_y

f'_c Concrete compressive strength

f_y Steel yield strength

h Height of cross section

kd Depth to neutral axis from extreme compression fibre at Yield Limit State

$\ell_{p,1}$ Length of plastic hinge at support

$\ell_{p,2}$ Length of plastic hinge in span

L Span length

M Moment

M_y Yield moment

M_u Ultimate moment

n Aversion factor, ratio of elastic moduli for steel and concrete, E_s/E_c , used in determining neutral axis depth; number of concentrated loads applied to a span

P Concentrated load

P_f Probability of failure

V Coefficient of variation

w Uniformly distributed load

W Warning factor

α Ratio of positive and negative flexural yield capacities, M_y^-/M_y^+

β Reliability index

β_T Target reliability index

γ Normalized distance between outermost layers of reinforcing

δ Bias coefficient

Δ Deflection

Δ_e Elastic deflection

Δ_p Plastic deflection

ϵ Strain

ϵ_c Concrete strain

ϵ_{cu} Ultimate concrete strain

ϵ_y Yield strain

ρ Geometric reinforcing ratio, A_s/bd

ρ_w Weighted occupant density

ϕ Curvature

ϕ_u Curvature at Ultimate Limit State

ϕ_y Curvature at Yield Limit State

ϕ_u/ϕ_y Curvature ductility ratio

ω Mechanical reinforcing ratio, $\rho f_y/f'_c$

Chapter 1

Introduction

1.1 Introduction

Concrete buildings can require structural assessment for a number of reasons including increased loading due to change of use or reduced capacity due to deterioration. These circumstances present a wide range of needs that may not all be adequately addressed by a single methodology. The concepts of reliability and risk are inherent in all methods and so can be used to provide consistent results and lead to a uniform acceptance of risk for all buildings. The current state of assessment guidelines in Canada and the USA is generally not unified and not based on consistent standards of reliability. Improvements can therefore be made to the current methods of assessment, specifically, the ways in which design provisions determine the target probabilities of failure for the structural element being assessed.

In the United States, practitioners interested in assessing the capacity of a concrete structure can consult several sources including ACI 562-16 (2016) and ASCE/SEI 7-15 (2015). In Canada, Commentary L to the National Building Code of Canada (NBCC) (2015c) can be used as a basis for building assessment while Chapter 14 of CAN/CSA S6-14 (2014) provides guidance for assessment of bridges.

Load and strength reduction factors, which form the basis for design of structural elements, are calibrated in parallel. Reliability-based methods tie load and strength reduction factors, α and ϕ , respectively, together through the use of a target reliability index, β_T , as shown in Figure 1.1. To have load and strength reduction factors that accurately and consistently represent the state of the structure, the definition of target probabilities of failure must capture the true characteristics of the structure and its behaviour at failure. Various sources (e.g. American Society of Civil Engineers, 2017; Canadian Standards Association, 2014b; National Research Council of Canada, 2015c) state the need to consider the type of failure expected, and the consequences of failure as assessed in a life-safety context. Established codes typically require structural elements to achieve a reliability index ranging from approximately 2 to 4.5 over a 50-year lifespan (American Society of Civil Engineers, 2017; Canadian Standards Association, 2011). The specific load and resistance factor format can also vary. For example, American codes use strength reduction factors that apply to the overall capacity of a particular cross section (ACI Committee 318, 2014), while Canadian codes define partial resistance factors for specific materials (Canadian Standards Association, 2014a, 2014b). The formulation of a more unified basis for assessment of reinforced concrete structures can build from these commonalities to create a simple, usable, and effective assessment procedure.

Figure 1.1 shows the relationship between the structural parameters used for assessment, and the outcomes of that assessment. Structural parameters that are indicative of failure behaviour and occupancy can be used to set appropriate target probabilities of failure, which in turn imply target reliability indices and load and resistance factors. In this way, the assessment outcomes can be made more representative of the observed structural conditions and failure consequences.

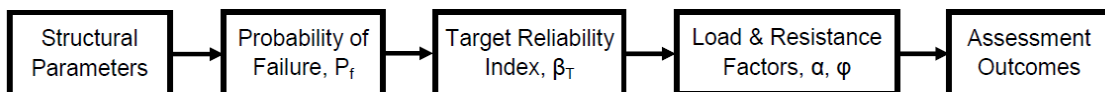


Figure 1.1: Relationship of probability of failure to load and strength reduction factors

1.1.1 Risk and Structural Failure

Risk is often represented as the product of the probability and consequences of a failure event, P_f and C_f , respectively, so that,

$$risk = P_f \times C_f \quad (1.1)$$

or,

$$P_f = \frac{risk}{C_f} \quad (1.2)$$

Using this definition, failures can be categorized according to their consequences. Increasing either the probability of failure or the associated consequences increases the overall perceived risk. Consequences of failure can be further broken down by the completeness or extent of failures, and the rate or suddenness of failure (Aggarwal, 1993). Failures that cause widespread damage or failures that occur without prior warning are not preferred.

Many structural codes use a formulation for risk assessment that echoes this general organization. They use a variety of language to express a relatively consistent understanding of structural concepts. The warning factor, W , is widely used (e.g. Canadian Standards Association, 1981, 2014b) to describe the type of failure both in terms of suddenness, or ductility, and extent of failure, or redundancy. The number of people at risk, n , is also used as a contributor to the consequences of failure (e.g. Canadian Standards Association, 1981, 2014b). The following discussion of failures will connect existing design and assessment codes in ways that will highlight the strengths of current considerations of structural reliability and failures, while also indicating areas where further study is needed to enhance the accuracy and applicability of structural assessment provisions.

1.2 Background

1.2.1 General Probability of Failure

Reliability-based methods have become the basis for ensuring acceptable levels of structural safety in most current structural codes. Ditlevsen and Madsen (1996) identify benefits of this approach, including the second-moment representation of random variables, and a formulation that is not strongly tied to a specific distribution type. A limit state function, g , expressed in terms of random variables, x_i , is

$$g(x_1, \dots, x_i) = R - S = 0 \quad (1.3)$$

where a structural failure occurs when the resistance, R , is less than the demand, S , or $g(x_1, \dots, x_i) \leq 0$.

For a given limit state function, g , the reliability index, β , can be obtained using the inverse of the standard normal distribution, Φ . The acceptable probability of failure, P_f , can be used to define the target reliability index, β_T , as

$$\beta_T = -\Phi^{-1}(P_f) \quad (1.4)$$

Table 1.1 shows target reliability indices and corresponding probabilities of failure over the range appropriate for structures.

1.2.2 Notional Probability of Failure

The notional probability of failure is the component of the total probability of failure that can be attributed to structural safety parameters that are readily quantified, such as applied loads or material strengths. Total probability of failure includes other contributors, including human error, that are much more difficult to quantify statistically (CIRIA, 1977; CAN/CSA

Table 1.1: Probability of failure and reliability index

β_T	P_f
2.0	0.023
2.5	0.0062
3.0	0.0013
3.5	0.00023
4.0	0.000032
4.5	0.0000034
5.0	0.00000029

S6-14, 2014b). These are outside the domain of conventional structural design and assessment provisions, and are therefore not considered in the notional probability of failure used in the remainder of this thesis.

1.2.3 Probability of Failure in Structures

Several formulations to quantify target probabilities of failure are reported in the literature. The exact formulations may vary but the underlying variables are reasonably consistent. CSA S408-81 (1981), for example, provides the following expression for P_f :

$$P_f = \frac{TAk}{W\sqrt{n}} \quad (1.5)$$

where T is the structural lifespan in years, A is an activity factor determined considering the type of structure (1.0 for buildings), k is a calibration factor (10^{-4}), W is a warning factor, and n is the number of people exposed to risk due to failure of an element. W and n vary across codes and based on the type of element being considered, and the designated use of the structure.

In CSA S408-81 (1981), values of n are not explicitly defined, but should “account for public concern” related to the scale of structural failures. Meanwhile W may take on one of four discrete values, selected according to the type of failure expected. An issue with these definitions is that they require a great deal of “engineering judgment” and are not derived from assessed properties of the structure.

CAN/CSA S6-14 (2014) assigns values of n for bridges ranging from $n = 10$ for regular bridge traffic, to $n = 1$ for controlled vehicles because it is anticipated that only one person, the driver of the vehicle, will be at risk during a controlled vehicle passage. Meanwhile, $W = 1.0$ is selected where no warning of failure is expected and failure is likely to cause total collapse, and $W = 0.005$ where the failure is gradual and leads to an isolated, or local, failure only. Similar formats are used in subsequent documents regarding the assessment of bridges (Allen, 1992; Canadian Standards Association, 2014b), and buildings (Allen, 1991; National Research Council of Canada, 2015c).

Qualitative definitions of ductility and redundancy can be problematic for several reasons. First, by creating discrete categories, the designer must decide on the appropriate interpretation of the code language. For example, a decision must be made whether the failure is strictly local, or if it may spread but not lead to collapse, or whether it is local but is likely to impact people (National Research Council of Canada, 2015c). Second, the inclusion of two distinct concepts, ductility and redundancy, in one parameter can be misleading, eliminating the nuances of the interactions of ductility and redundancy on each other. The likelihood of impact on people, and the likelihood of collapse are distinct ideas, and should be treated as such. Similar overlap, and the associated implications for parameter definition, can be observed in ASCE/SEI 7-15 (2015). An example of more ideal parameter definition is in CAN/CSA S6-14 (2014), where element behaviour and system behaviour have separate, though still discrete and qualitative, parameters.

1.3 Impact on Structural Assessment Outcomes

Allen (1991) notes that the reliability level selection for structural assessment should include all available information, where for new design, a more generic set of provisions is appropriate. The following investigation of structural reliability, though useful for general consideration, is particularly helpful when assessing existing structures.

Calibration of load and resistance factors for design or assessment requires the ability to accurately account for the conditions that affect the behaviour of the structure. In the case of aversion factors, the number of people contained within the tributary area of a structural element is a major contributor to the perceived acceptable risk of failure. An increase in this number would necessitate a stricter design, i.e. a lower target probability of failure. Sufficient warning of failure allows more relaxed target probabilities of failure because structural failure will occur after the evacuation of the building and surrounding area, greatly reducing the human impact of the eventual collapse.

1.3.1 Economic and Environmental Impact

When structures no longer meet target levels of reliability, they need either to be taken out of service, or upgraded. This makes the accurate quantification of the probability of failure very important not just for life-safety reasons, but in terms of financial cost and environmental effects. The decisions made to carry out repair work to achieve a target structural reliability are sensitive to the system and parameters used to determine the target probability of failure.

The economic costs associated with increasing reliability for an existing structure are much greater than those for an equivalent increase in new structures. The decommissioning of a structure also has large associated costs. Many are far removed from the actual assessment, design, and construction costs, including costs associated with operational disruptions, relocation, and other business concerns.

As sustainability concerns continue to increasingly dominate corporate decision making processes, the environmental costs of the demolition, disposal, and replacement of the structure become increasingly important. In terms of embodied energy and materials, considerable losses are associated with the total decommissioning of a building. The benefits of continuing to use a structure then become quite substantial, made possible either by a more accurate system for decision-making, or by the rehabilitation of deficient components of the structure to

acceptable reliability levels. In either case, the economy of the entire process can be improved by using assessment measures that truly reflect the particular structure being assessed.

1.4 Objectives

When the maximum acceptable probability of failure is defined by attributes of the structure, it is important that those attributes are quantified simply and accurately. The connection between these attributes and the associated effects on the reliability targets should be rational and objective. Current methods involve mainly qualitative categorization of the consequences of failure, but it is preferable to numerically quantify these factors. The objective of the research reported in this thesis is therefore to refine the metrics that practitioners use to quantify societal risk aversion, cross-sectional ductility, and structural redundancy, and provide continuously defined values for these parameters in a range of structural elements. The betterment of these measures has the potential to change assessment outcomes by better representing the real structural conditions and more appropriately selecting the necessary levels of safety.

The following objectives will direct the research outlined in this thesis:

1. Review current assessment and design codes for reinforced concrete structures to outline the state of reliability-based assessment and design in Canada and the United States.
2. Identify commonly accepted concepts behind the formulation of reliability targets for assessment and design.
3. Propose additional indicators, if necessary, to determine appropriate reliability targets that accurately represent structural behaviour.
4. Analyze the identified parameters to observe their effects on the reliability targets and the outcomes for assessment.
5. Propose a procedure by which the findings can be practically incorporated into assessment provisions.

1.5 Scope

For new design, a lifetime reliability index or acceptable target probability of failure for a structure may be prescribed, or selected using criteria in the design code. For existing structures, various methods can be used to assess the *in-situ* properties of structures and then assign a corresponding reliability index. This can include load or material testing, as-built measurements, and other forms of non-destructive testing. The work that follows will not address the means of quantifying assessed reliability by testing or other methods of determining the load carrying capacity of a structural element. Improvements to these methods are possible and necessary, but outside the scope of this thesis.

The target reliability index, β_T , is tied to the level of risk deemed acceptable for a given structure based on both structural and non-structural attributes, and will be the sole focus of this thesis. The level of acceptable risk is dependent of the consequences of a structural failure. Consequences are element-specific and can vary widely within a structure.

The scope of this work is inclusive of singly reinforced concrete beams, and one-way slabs. Extension to columns with low axial loads is discussed in van Weerdhuizen and Bartlett (2018); this can be applied also to doubly reinforced beams. Further study will required to extend the findings of this research to a wider range of structural elements.

1.6 Organization

This thesis is presented as four main chapters, comprised of a thorough review of current literature, a review of several disparities in, and potential improvements to, current assessment frameworks, and an illustration of the effects of such changes on assessment procedures and outcomes.

In Chapter 2, a review of existing literature and code provisions for assessment will be presented. Review of commonalities and divergences will assist in the development and application of improved methods.

Chapter 3 covers the quantification of life-safety-related consequences of failure. This will include a study of the various aspect of quantifying structural occupancy and the application of tributary-area-based live load reduction concepts to the number of people affected by a failure. These will be combined into one aversion factor to account for societal aversion to risk in reliability analysis.

Chapter 4 presents a study of the deflections expected at incipient failure and their use as a metric for defining a warning factor. This will include an analysis of the effects of the reinforcement ratio, indeterminacy, and applied loading configuration for reinforced concrete elements in flexure.

Chapter 5 presents a brief exploration of the impacts that the findings of Chapters 3 and 4 can have on assessment outcomes, focusing on the calibration of strength reduction factors. A proposed outline of improved assessment procedures is also provided.

Chapter 6 provides general conclusions of this research, along with suggestions for future work.

Chapter 2

Literature Review

2.1 Introduction

Many methods for quantifying the target probability of failure for structural assessment are documented. There are clear commonalities in their organization and criteria. This chapter will provide an overview of some of these documents, focusing on those published in Canada and the US. Each gives a framework for the selection of target levels of reliability for structures. The approaches taken in each vary, but all typically address the achievement of desired reliability levels by the application of suitable load factors and strength reduction factors. These factors modify the nominal loads and resistances in accordance with the certainty and severity of structural conditions.

The calibration of load- and strength-reduction factors is critical to assessment, evaluation and design procedures. Increased accuracy in understanding and representing the behaviour of structures ensures that designs have consistent levels of reliability and are cost effective. Accurate assessment is beneficial because structural strengthening is costly, and so unnecessary conservatism can have negative effects on the economy of building maintenance and repair.

The following discussion of design and assessment documentation will focus on the key parameters used to determine reliability targets. It seeks to identify areas of overlap, points of conflict, and gaps in the range of concepts used to quantify structural risk.

2.2 Literature Overview

In both design and assessment, most documents relate the desired reliability level to some combination of the following factors: the social perception of risk due to structural failure, the type of failure expected, and a calibration factor. The perception of risk, or risk aversion, relates to the inherent danger in the activity for which the structure is used. The type of failure is often discussed in terms of the warning of imminent failure provided and the effect that element failure has on the integrity of the remaining structure. The calibration factor accounts for the time period that the reliability level refers to, as well as some notion of an acceptable probability of failure for the type of structure being considered. Additional considerations include specific factors such as structural inspection, but will not be discussed in detail here.

Table 2.1 summarizes the ways that the reviewed documents incorporate concepts of aversion factors and warning factors. Warning factor has been sub-divided into two categories, ductility and redundancy, although not all sources provide explicit definition of these distinct concepts.

Table 2.1: Comparison of structural risk concepts in structural design and assessment codes

DOCUMENT	RISK/AVERSION/N	DUCTILITY	REDUNDANCY	TARGET RELIABILITY INDEX/PROBABILITY OF FAILURE	OTHER	BASIS
CIRIA 63 (CIRIA, 1972)	<p>Social criterion factor, K_s:</p> <ul style="list-style-type: none"> 0.005: public assembly, dams 0.05: domestic, office, trade, industry 0.5: bridges 5.0: towers, offshore structures <p>Number of people at risk due to structural failure, n_r, assess based on:</p> <ul style="list-style-type: none"> Usage Type of structure Loading Type of failure Environment <p>Usage:</p> <ul style="list-style-type: none"> Number of people supported by element <p>Environment:</p> <ul style="list-style-type: none"> Effects of structure on surroundings 	<p>Type of failure:</p> <ul style="list-style-type: none"> Ductile: clearly visible, visible on inspection, concealed Brittle 	<p>Type of structure:</p> <ul style="list-style-type: none"> Influence of element failure on structure 	<p>$P_f = 10^{-4} K_s n_d / n_r$</p> <p>Loading, correlation with number of people affected:</p> <ul style="list-style-type: none"> Positive: more load, more people Uncorrelated: use average number of people Negative: more load, less people <p>Loading, time variation:</p> <ul style="list-style-type: none"> Quick load build-up Slow load build-up 	<p>Design life of structure, n_d, in years</p>	--
CSA S408-81 (Canadian Standards Association, 1981)	<p>Aversion factor, n:</p> <ul style="list-style-type: none"> Greater public concern for multi-casualty events than equivalent number occurring individually <p>Activity Factor:</p> <ul style="list-style-type: none"> 0.3: Post-disaster 1.0: Normal, buildings 3.0: Bridges 10.0: Construction, offshore <p>Safety Class (based on life safety and economic consequences):</p> <ul style="list-style-type: none"> Not serious Serious Very serious 	<p>Warning factor, W:</p> <ul style="list-style-type: none"> 0.01: failsafe 0.1: gradual failure 0.3: some warning, or gradual but hidden 1.0: sudden without warning 		<p>$P_s = T A 10^{-5} / (W \sqrt{n})$</p> <p>Tabular: Assigned based on type of failure and safety class</p>	<p>T: life span of structure, commonly 50 years</p>	--
CSA S408-11 Annex B (Canadian Standards Association, 1981)	<p>Select from table:</p> <ul style="list-style-type: none"> Not serious Serious (normal) Very serious 	<p>Select from table:</p> <ul style="list-style-type: none"> Gradual Sudden 		<p>Tabular: Assigned based on type of failure and safety class</p>	<p>"might not be appropriate for seismic loads"</p>	CSA S408-81
NBCC (National Research Council, 2016)	<p>Importance Categories:</p> <ul style="list-style-type: none"> Low: low or indirect hazard to human life Medium: other High: post-disaster shelters Post-Disaster: essential services 	<p>Type of failure incorporated by the material resistance factor, ϕ</p>		--	--	--

Table 2.1 Continued: Comparison of structural risk concepts in structural design and assessment codes

DOCUMENT	RISK/AVERSION/N	DUCTILITY	REDUNDANCY	TARGET RELIABILITY INDEX/PROBABILITY OF FAILURE	OTHER	BASIS
NBCC Commentary L (National Research Council, 2016)	N = area*occupant density*duration Risk Category selected by value of N: <ul style="list-style-type: none"> 2: High 1: Medium 0: Low 	System Behaviour: <ul style="list-style-type: none"> 2: failure leads to collapse, likely to impact people 1: failure unlikely to lead to collapse, or unlikely to impact people 0: failure local only, very unlikely to impact people 		Target Reliability Level is the sum of indices for: <ul style="list-style-type: none"> Risk category System behaviour Past performance 	Past Performance: <ul style="list-style-type: none"> 1: No record 0: satisfactory, or dead load measured 	Allen, 1991 CSA S408-81
CAN/CSA S6-14 (Canadian Standards Association, 2014)	Target reliability index may be increased if structure is deemed important (ie. local economic significance, life safety, emergency routes)	Element Behaviour: <ul style="list-style-type: none"> E1: subject to sudden loss of capacity E2: subject to sudden loss of capacity but retains post-failure capacity E3: gradual failure 	System Behaviour: <ul style="list-style-type: none"> S1: Element failure leads to total collapse S2: Element failure probably will not lead to total collapse S3: Element failure leads to local failure only 	Tabular: Assigned based on categories selected to describe element	Inspection Level: <ul style="list-style-type: none"> INSP1: component is not inspectable INSP2: inspection results are satisfactory INSP3: final evaluation calculations account for all inspection results 	CSA S408-81 Allen, 1992
CSA S6-14 Commentary (Canadian Standards Association, 2014)	Activity factor, A: <ul style="list-style-type: none"> 10.0: for "Controlled vehicles" 3.0: for all other traffic Aversion factor n: <ul style="list-style-type: none"> 1.0 for "Controlled vehicles" 10: for all other traffic 	Warning of failure, W: <ul style="list-style-type: none"> 1.0 for no warning of failure expected Can be improved by inspection, alternate load paths, ductility 		$P_{fs} = A K / (W \sqrt{n})$ *probabilities based on 1 year return/service life	--	CSA S408-81
ASCE 7-16 Chapter C1 (American Society of Civil Engineers, 2016)	Occupancy/Risk Categories: <ul style="list-style-type: none"> I - unoccupied, negligible risk to public III - large number of people, or limited mobility, or hazardous storage IV - essential services, and supporting services II - other (each may also be associated with an approximate range of the number of lives at risk due to a failure)	Type of failure: <ul style="list-style-type: none"> not sudden and does not lead to wide-spread progression of damage sudden or leads to wide-spread progression of damage sudden and wide-spread progression of damage 		Tabular: Assigned based on occupancy category and type of failure *probabilities based on 1 year return/service life	--	--
ACI 318-14 (American Concrete Institute, 2014)	Implicit in resistance factor definition (see R.21.2.2) *also refers to ASCE 7	Definition of resistance factor by failure type (via tensile strain): <ul style="list-style-type: none"> compression-controlled transition tension-controlled *also refers to ASCE 7	* refers to ASCE 7	Commentary references ASCE 7-10 (Table C1.3.1a)	--	Mast, 1992
ACI 562-16 (American Concrete Institute, 2016)	Strength reduction factors for: <ul style="list-style-type: none"> design: as in ACI 318 assessment: higher values justified by increased knowledge 			--	Applicable for assessment, repair/rehabilitation design, remedial construction for existing concrete structures	--

2.2.1 Early Application of Reliability Concepts

CIRIA (1972) introduced a framework where reliability concepts and structural parameters could be tied together to give target probabilities of failure for buildings and other structures. The target probability of failure is,

$$P_f = \frac{10^{-4} K_s n_d}{n_r} \quad (2.1)$$

where K_s is a social criterion factor, n_d is the design life of the structure, in years, and n_r is the number of people expected to be at risk during a failure.

Consideration of the social perceptions of risk for different types of structures using the K_s factor is a key part of this definition. Higher risk activities allow for higher failure probabilities in the design of the associated structures. As shown in Table 2.1, K_s varies from 0.003 for areas of public assembly to 5.0 for offshore structures.

2.2.2 Canadian Building Codes

Canadian documentation for structural design began to include similar reliability concepts for assessment beginning with CSA S408-81 (1981). Recall from Chapter 1, the target probability of failure is,

$$P_f = \frac{TA10^{-5}}{W\sqrt{n}} \quad (1.5)$$

Parameter values are determined by the designer or selected from the tables provided, which are summarized in Table 2.1. Equation 1.5 implies incorrectly that the probability of failure for a 50-year lifespan is 50 times the annual probability of failure.

CSA S408-11 (2011) presents a table showing recommended lifetime target reliability indices based on the failure type and safety class of a structural element. The equation provided in CSA S408-81 (1981), Equation 1.5, has been removed, but a table of recommended reliability indices identical to the one provided in CSA S408-81 is presented.

NBCC Commentary L, which evolved from Allen (1991), gives factored load combinations based on computed target reliability levels. Reliability levels are determined from the summation of a variety of factors accounting for system behaviour, risk category, and past performance. The system behaviour categorization mirrors the warning factor in CSA S408-81 (1981), using terminology that describes the impact of failure on the whole structure and the likelihood of impacting people. The risk category addresses risk to life, based on the density of occupants expected, as well as the amount of time the area is expected to be occupied.

2.2.3 Canadian Bridge Codes

CAN/CSA S6-14 (2014) follows a probability of failure format similar to CSA S408-81 (1981). Here, the annual target reliability is presented as,

$$P_f = \frac{Ak}{W \sqrt{n}} \quad (2.2)$$

where the warning factor, W , has a worst-case value of 1.0, and can be reduced due to the frequency of inspection, the presence of alternate load paths, or cross-sectional ductility. The calibration factor, k , is 10^{-4} . The activity factors suggested are larger than those for buildings, 3.0 or 10.0, for normal traffic, or permit-controlled traffic, respectively. These increased risks are appropriate because in using a highway bridge, an individual is willing to accept more risk than when they are inside a building. The bridge evaluator classifies the element as belonging to one of three categories of system behaviour, element behaviour, and inspection frequency and then obtains the target reliability index and live- and dead-load factors from tables given in Clause 14.

2.2.4 American Building Codes

ASCE/SEI 7-15 (2015) provides considerable guidance about risk and probability of failure in a similar format to CSA S408-11 (2011) where lifetime target reliability indices, as well

as annual probabilities of failure, are suggested for various occupancy categories and types of failure.

ACI 562, Code Requirements for Assessment, Repair, and Rehabilitation of Existing Concrete Structures (ACI Committee 562, 2016), provides criteria for assessment in the form of prescribed strength reduction factors. It states that consideration must be given for existing conditions, including as-built dimensions, material properties, and the sufficiency of structural load paths. Physical alterations and changes in loading or occupancy from the original design must also be included in the assessment. If all requirements are satisfied, strength reduction factors larger than those conventionally used for design are allowed, giving an increase in the assessed capacity.

Section R21.1.1 of ACI 318-14 (2014) provides strength reduction factors to reduce nominal strengths for new design, which are intended to account for under-strength members, inaccurate design equations, ductility and reliability, and the importance of the member. The reduction factors for compression-controlled failures, generally columns and heavily reinforced beams, incorporate the effects of relatively low ductility and large tributary areas typically associated with these elements. This results in smaller strength reduction factors, and smaller factored resistances for design of these elements.

ASCE/SEI 7-15 (2015) includes reliability-related criteria through the use of performance-based procedures. The requirements here are that the probability of failure given for a particular risk category should be met, but allow for alternate, equivalent means of achieving this.

2.3 Review of Common Parameters

The main parameters used for quantifying target probabilities of failure tend to fall under two main categories: risk aversion, and warning of failure.

2.3.1 Aversion

Any parameter that reduces the allowable probability of failure in response to a threat to life safety, actual or perceived, should be included in any discussion of risk aversion. The documents discussed previously present such parameters in a variety of ways, including importance factor, activity factor, aversion factor, and occupancy category. Some include more than one factor, and they may be assessed mathematically in different ways. In the NBCC (National Research Council of Canada, 2015a), for example, importance factors are applied when calculating load effects, and are selected based on the degree to which the occupants, and surrounding community would be affected in the event of a failure.

In CSA S408-81 (1981), the aversion factor is defined as \sqrt{n} , where n is the maximum number of people at risk due to a structural failure, to be determined by the designer. Activity factor, A , also an aversion-related quantity, is defined as 1.0 for buildings, and increases to 10.0 for offshore structures, or structural failures during construction. Again, this associates the relative inherent risk accepted by users of a structure with its target reliability.

In ASCE/SEI 7-15 (2015), societal risk aversion is addressed using specific risk categories. Buildings are assigned to a category and then an acceptable target reliability index or probability of failure is determined based on the occupancy type and the function the structure serves during an emergency situation.

These aversion-related factors imply that the level of acceptable risk depends on many factors, including the type of activity performed within the structure and the importance of its functioning in the event of a disaster (Canadian Standards Association, 1981). Aversion is also affected by social factors, such as the increasingly negative public response that can be anticipated as the number of casualties in a structural failure increases (Canadian Standards Association, 1981). This number is either prescribed by the code, or determined by the practitioner, allowing for relative freedom in the quantification of risk aversion.

2.3.2 Ductility

Warning of failure is discussed on a number of different bases. Several of the documents reviewed discuss such failure in terms of suddenness or visibility. ACI 318-14 (2014) classifies failure as tension-controlled and compression-controlled based on strain conditions in the cross section at failure. NBCC Commentary L (2015), focuses on the likelihood of a failure to injure people, which can be interpreted as indirectly describing the suddenness of the failure and the ability to evacuate the structure successfully. The essential quantity being discussed in each instance is the ability for the structure to give users and assessors visible warning of imminent failure.

Ductility can be discussed in terms of curvature, axial strain, or lateral deflection on an element or structural scale. Curvature ductility is most helpful when considering beams in flexure, or other structural elements that can exhibit considerable transverse deflections over their lengths. Axial deformation is most useful for elements that do not exhibit large transverse deformations before failure due to the presence of larger axial loads. The magnitudes of axial deformations are typically small relative to the transverse flexural deflections, and are thus less useful as visible indicators of warning. Storey drift is a metric used to identify lateral sway of entire buildings, often in applications involving seismic or wind loading.

2.3.3 Redundancy

Redundancy is the second main contributor to warning of failure recognized in current literature. Redundancy in current codes is described in terms of single- versus multiple-load-path structures, local failure, and susceptibility to progressive collapse. These concepts of redundancy can be simplified to say that indeterminate, or redundant, elements provide warning of failure by moment redistribution after the first yield occurs. In contrast, determinate structures, with no redundancy, reach their ultimate capacity when the capacity of a single cross section is reached, and so are deemed to give no warning of failure.

The codes and standards reviewed are consistent in recognizing that more redundancy is better. In structural systems where parallel elements provide alternate load paths or where indeterminacy allows some local yielding without collapse, benefits are assumed but not often well quantified. When a lack of redundancy is combined with a sudden brittle failure, the target probabilities of failure must reflect the lack of warning and be reduced.

2.3.4 Other

Other factors are included in some assessment and structural reliability documents. The inspection factor in CAN/CSA S6-14 (2014), can essentially be considered as contributing to warning of failure. This research will not address the effects of inspection on the selection of target reliability indices.

The calibration factor, k , is used to calibrate the probabilities of failure to an acceptable level of risk. For one critical combination of W and n , a specific probability of failure is associated with a particular k value. For other combinations of W and n , this value of k yields distinct target probabilities of failure. This aspect of the selection of a calibration factor will be explored further in Chapter 5.

2.4 Summary and Conclusions

Common themes emerge among existing literature. The primary factors that determine appropriate reliability targets for structural assessment are: the risk to human life, and the warning of failure as indicated by the ductility of the failure mode and the redundancy of the structural element or system. These factors, while generally recognized, are often assigned qualitatively, by the use of judgment on the part of the designer, rather than quantitatively, based on the physical properties and configuration of the structure.

The aversion factor can include several features that are often assigned to different parameters but relate to the perception of risk in structural failures. Prescribing values of n based on

the occupancy type or use of the structure, or providing only limited guidance on the calculation of n are not sufficient provisions for a reliability-based assessment method. Similarly, ductility and redundancy are defined without being quantitatively related to structural properties. Both the discrete categories and the vague language used to quantify warning factor leave opportunity for improvement of this parameter.

The consistency of the concepts used across the literature reviewed indicates their perceived importance when setting reliability targets for assessment. The principles of risk aversion and warning of failure should be starting points from which a more quantitative assessment procedure can be developed. Investigation of possible improvements to these assessment frameworks should focus on determining the veracity and completeness of these widely recognized factors, and should tie target reliability levels for assessment to measurable structural parameters.

Chapter 3

Quantifying the Aversion Factor

3.1 Introduction

In Chapter 2, various forms of risk aversion were identified, including:

- Social criterion factor in CIRIA (1972);
- Activity factor in CSA S408-81 (1981) and CAN/CSA S6-14 (2014);
- Importance factor in NBCC (2015);
- Occupancy categories in ASCE/SEI 7-15 (2015); and
- Number of people at risk in CAN/CSA S6-14 (2014), NBCC Commentary L (2015), CSA S408-81 (1981), and CIRIA (1972)

Risk aversion therefore encompasses a broad range of parameters that account for different aspects of risk. The present investigation will focus on the component of risk aversion that is directly related to the number of people at risk in a structure, here referred to as the aversion factor, which in all cases depends on the occupancy type, duration, and density. While these three factors are not entirely independent, each will be defined to have a unique scope. Occupancy type relates to the defined usage of the space supported by an element. Occupancy

duration addresses the length of time that occupants are present, and is therefore specifically relevant to structures that are unoccupied for large portions of time. For example, nighttime occupancies in a school or office structure may be negligible. Occupant density addresses the average space occupied by a single person, and can also be expressed as the number of people occupying a unit area. This is dependent on the occupancy type, and can be constrained by concerns of safe egress or air quality, and is implicitly included in the derivation of specified live loads.

In Equation 2.2, the probability of failure is inversely related to \sqrt{n} , where n is the aversion factor, essentially the number of people at risk due to structural failure. Larger values of the aversion factor lead to more stringent reliability criteria. Current standards use the aversion factor to define the target reliability by specifying predetermined numbers of occupants at risk (Canadian Standards Association, 2014b), or developing methodologies to explicitly calculate n (National Research Council of Canada, 2015a)). In CIRIA (1972), the designer is free to determine the number of occupants, while the NBCC Commentary L (2015) guides the calculation by providing parameters for both occupant density and occupancy duration.

Underestimating the number of individuals at risk will yield inappropriately high target probabilities of failure, while overestimation leads to excessive strength requirements. The objective of the research reported in this chapter is therefore to propose a simple, rational method for determining the aversion factor, n .

3.2 Analysis

The specified live load and the number of people at risk due to the collapse of a building component should by nature be positively correlated, but historically this positive correlation has not been quantified. In occupancies such as assembly areas, the primary source of live load is the occupants. In contrast, the live loads in storage and industrial occupancies have relatively low occupant live loads. Some occupancies are time-dependent, and may be fully

occupied only a fraction of the time. The total live load may therefore be modeled as the sum of occupant and non-occupant components. The following analysis of live loads and number of occupants will establish an appropriate range of n for the tributary areas and occupant densities of the element under consideration.

3.2.1 Occupant Density

To determine the aversion factor, n , an occupant density for determining the probable number of people in an area with a given occupancy is required. Two possible methods for quantifying this value are as follows:

1. Derive the occupant density based on the use of the structure and appropriate non-structural factors, such as the occupancy limits imposed by emergency egress, or the design of the building's Heating, Ventilation and Air-Conditioning (HVAC) services. These metrics are appropriate because the occupancy limit is directly related to these aspects of safety or comfort. The occupancy limit associated with emergency egress, although dependent on exit pathways and other factors, is primarily determined by the size and use of the structure. The NBCC (2015) and the National Fire Code of Canada (NFCC) (2015b) provide guidance on limiting occupant densities based on egress considerations. Similarly, the American Society of Heating, Refrigerating and Air-Conditioning Engineers (ASHRAE) (2016) provides occupant densities based on the type of occupancy, and the HVAC requirements for the space.
2. Derive occupant density from the live loads specified for structural design. This is more difficult because specified live loads account for human occupancy in addition to other loads, and so can vary widely. For example, the design live loads in storage areas and many assembly areas are both specified at 4.8 kPa in the NBCC (2015), although the implication is obviously not that equivalent numbers of people will be present in each occupancy type. In the storage occupancy, the live load will be primarily due to the

material being stored, while in the assembly area, the live load will be primarily due to occupants.

The densities indicated by these two approaches can vary widely. Table 3.1 provides a summary of occupant densities from the NBCC (2015), NBCC Commentary L (2015), ASHRAE (2016), and the NFCC (2015b). The highest occupant density values are for assembly occupancies where the entire live load is attributed to human weight. In Canada and the US, the average adult mass is 80.7 kg (Walpole et al., 2012). For the specified live load for assembly areas, 4.8 kPa, this corresponds to an occupant density of approximately 6 occupants/m² or 0.17 m²/person. The global average adult mass is 62 kg (Walpole et al., 2012), corresponding to approximately 8 occupants/m², or 0.12 m²/person. This suggests that cultural and geographical variations should be considered when assessing the occupant density in a structure. These densities may also be scaled for cases when the live load due to human weight is only a fraction of the total live load.

Table 3.1: Occupant density comparison

Occupant Density (Occupants/m ²)	Associated Occupancy	Associated Live Load (kPa)	Basis	Source
6	Assembly	4.8	Average adult mass	NBCC, 2015a; Walpole et al., 2012
2.5	Unspecified	–	Fire safety	NFCC, 2015b
1.5	Spectator areas,	4.8	Ventilation rates	ASHRAE, 2016
1	Assembly	4.8	–	NBCC Commentary L, 2015c
0.01	Storage	4.8	–	NBCC Commentary L, 2015c

ASHRAE (2010) provides occupant densities for design of mechanical building services when the actual occupant density is unknown. The range given is from 0.04 occupants/m², or 25 m²/person, in a computer area, to 1.5 occupants/m², or 0.67 m²/person, in an auditorium seating area. These are likely average, not upper bound, values and so may not be appropriate in a life safety context. They should therefore not be used to estimate occupant density for structural assessment.

The NFCC (2015) allocates an area of 0.4 m²/person, which equates to an occupant density of 2.5 occupants/m². This can be considered an appropriate limit for spaces that have maximum capacities limited by the NFCC (2015).

The Ontario Building Code (OBC) Part 3 (Fire Protection, Occupant Safety, and Accessibility) (2012) specifies occupant space allocations for occupancy types that generally correspond with the NBCC Part 4 provisions for specified live loads. The space allocations range from 0.4 m² per person for assembly areas with standing space, to 46 m² per person for a storage area. Within the category of assembly occupancies that have specified live loads of 4.8 kPa, the allocated area per occupant can range from 0.4 m²/person for standing areas to 4.6 or 9.3 m²/person for school laboratories or shops, respectively. It is clear that among occupancy types, the portion of live load attributed to human weight can vary widely.

3.2.2 Occupancy Duration

The number of people at risk due to a structural failure is reduced for structures that are not continuously occupied. NBCC Commentary L (2015) provides a range of occupancy-based densities, which are then combined with a duration factor to determine the number of people at risk due to a structural failure. Duration factors are determined according to the NBCC Commentary L (2015) guidelines by estimating the number of hours per week, out of one hundred, that the area will be occupied. For storage and assembly occupancies, the duration factors suggested are 1.0 and 0.05-0.5 respectively.

Table 3.2 provides a summary of occupant densities and durations. The product of these two can be referred to as a weighted density, ρ_w , and will be used to compute the aversion factor, n , for use in assessment. The number of people at risk is therefore

$$n = \rho_w A_T \quad (3.1)$$

where A_T is the tributary area of the element.

Table 3.2: Occupant density and duration summary

	Occupant Density (occupants/m ²)	Duration Factor (hours per week/100)	Max. Weighted Occupancy, ρ_w (occupants/m ²)
NBCC (2015)			
Assembly - 4.8 kPa	6	0.05 - 0.5	3.0
NBCC Commentary L (2015)			
Assembly	1	0.05 - 0.5	0.5
Mercantile and personal services	0.2	0.5 - 0.8	0.16
Offices/care/detention/manufacturing	0.1	0.5 - 0.6	0.06
Residential	0.05	1.0	0.05
Storage	0.01 - 0.02	1.0	0.02
NFCC (2015)			
Maximum Occupancy	2.5	0.5	1.25
Low density assembly	0.1	0.5	0.05

As shown in Table 3.2, the range of weighted occupant densities is large. The value based entirely on human mass (6 occupants/m²) for a live load of 4.8 kPa exceeds the other occupant density suggestions by a factor of at least 2.4. The assumed duration factor for the NFCC (2015) densities is 0.5, the maximum value suggested by NBCC Commentary L (2015) for assembly areas since the NFCC does not explicitly provide occupancy durations.

While it is possible that occupancies with weighted densities as high as those 3.0 occupants/m² exist, it is unlikely, so 0.02 to 1.25 occupants/m² will be taken as a practical range. An occupant density of 1.0 occupants per square metre will be used for illustration throughout the remainder of this chapter unless noted otherwise. The resulting n values can be easily scaled for other densities as required.

3.2.3 Live Load Reduction Factor

Live loads applied over large areas can be reduced according to the provisions in the NBCC (2015) or ASCE/SEI 7-15 (2015). As the tributary area increases, it becomes increasingly unlikely that the area will be fully loaded. The element can therefore be safely designed for considerably smaller live load effects using the prescribed live load reduction factors (LLRF).

Since the aversion factor, n , is defined by a weighted occupant density applied to the tributary area of an element, the same reduction can be applied to the tributary area used here. The NBCC (2015) allows for the reduction of live load based on the following equations:

$$LLRF = 0.5 + \sqrt{20/A} \quad (3.2)$$

$$LLRF = 0.3 + \sqrt{9.8/B} \quad (3.3)$$

where A and B represent the tributary area in square metres supported by the the element. Equation 3.2 applies for assembly areas with specified live loads greater than 4.8 kPa, or areas designated for storage, manufacturing, retail, garage, or footbridge use. Equation 3.3 applies for all other occupancy areas. No reduction is permitted for A less than 80 m² in Equation 3.2, or for B less than 20 m² in Equation 3.3. Where assembly occupancies are designed for live loads less than 4.8 kPa, no reduction in live load is allowed. Assembly occupancies, as defined by the NBCC (2015), include classrooms, arenas and stadia, theatres and churches, as well as entrance halls, gymnasias and others (National Research Council of Canada, 2015a).

Similarly, ASCE/SEI 7-15 (2015) allows a live load reduction based on:

$$LLRF = 0.25 + \frac{4.57}{\sqrt{k_{LL}A}} \geq 0.4 \quad (3.4)$$

for an element with tributary area, A , and influence area, $k_{LL}A$, in square metres (m²). The live load element factor, k_{LL} , serves to convert tributary area to influence area, and varies from one to four with the type and location of the element being considered. Interior beams, for example, have $k_{LL}=2$, while interior columns have $k_{LL}=4$. Tributary area is the area directly supported by a structural element and in the NBCC is confined by the lines of zero shear in members supported by the element (National Research Council of Canada, 2015a). Influence area, meanwhile, is the area within which the failure of an adjacent element would cause an increase in the demand for the element in question due to the redistribution of load. Reduction

factors from Equation 3.4 are not be applied to specified live loads in areas used for assembly (ASCE 7-16, 2017).

Figure 3.1(a) illustrates these three LLRF models over a range of tributary areas from zero to 1000 m². This upper bound could represent a column supporting a 10 by 10 m tributary area over 10 storeys. The ASCE/SEI 7-15 (2015) provisions show similar reductions to the NBCC (2015) provisions for non-assembly occupancies (Equation 3.3). Figure 3.1(b) shows more clearly the reduction for tributary areas less than 200 m² as k_{LL} varies. Equation 3.2 gives reductions of up to 35% from the full specified live loads for assembly occupancies. For non-assembly occupancies, Equations 3.3 and 3.4 give similar results. Variation due to the use of k_{LL} factors is most notable for tributary areas less than 200 m². The maximum reduction permitted by ASCE 7-16 is 60% of the original live load.

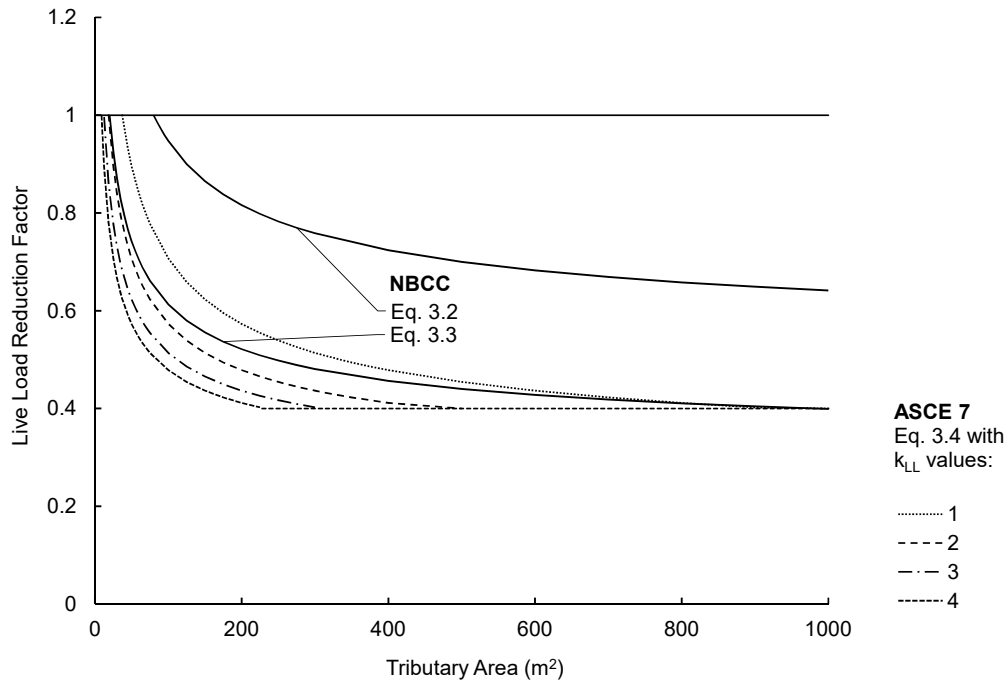
3.3 Results

3.3.1 Number of Occupants at Risk

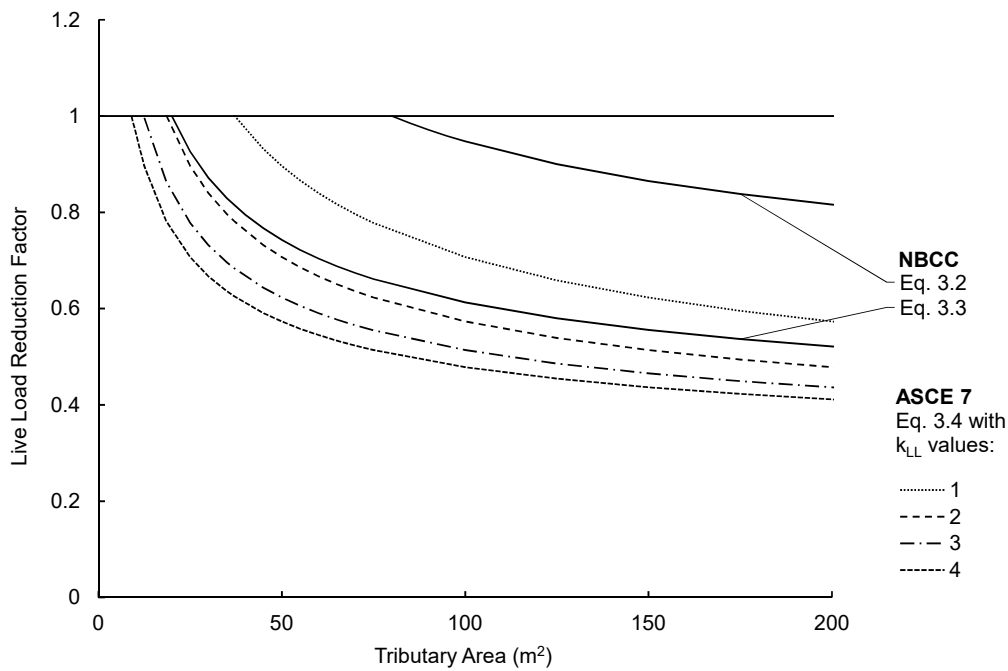
The total number of occupants at risk, n_T , can be quantified in general as a function of the tributary area, A_T using Equation 3.1. The effect of the live load reduction factor for large tributary areas can then be included to determine a reduced number of people at risk, or aversion factor, n :

$$n = \rho_w LLRF A_T \quad (3.5)$$

Figure 3.2 shows the variation of n with tributary area, for a weighted occupant density of 1.0 occupant/m². The assumed upper limit for occupant density is 1.25 occupants/m², in accordance with the NFCC (2015b) provisions and the lower limit is 0.02 occupants/m², in accordance with NBCC Commentary L (2015). Over the range of tributary areas from 0 to 200 m², the effects of using a LLRF are considerable. For example, for a tributary area of 200 m²



(a) 0-1000 m^2 tributary area



(b) 0-200 m^2 tributary area

Figure 3.1: Live load reduction factor as a function of tributary area

and a weighted occupant density of 1.0, the number of occupants is reduced from 200 to less than 100 for all but the assembly areas governed by Equation 3.2.

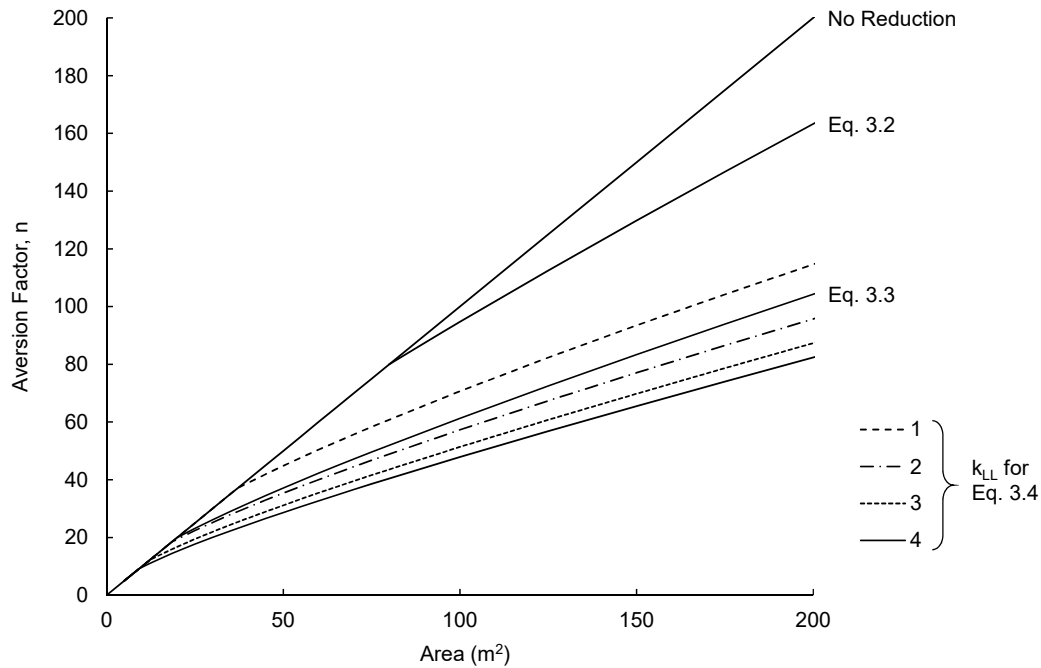


Figure 3.2: Number of people at risk due to structural failure using NBCC and ASCE 7 live load reductions for $\rho_w = 1.0$

Figure 3.3 shows the variation of n using the live load reductions specified in the NBCC (2015) for weighted occupant densities from 0.02 to 1.25 occupants/m². The associated values of aversion factor are quite sensitive to the density used. The selected occupant density and duration factor can therefore have a notable impact on the target probability of failure selected for assessment.

In practice, live load reduction factors can be used to determine the number of people at risk if the weighted occupant density, tributary area, and applicable live load reduction equation are known. The relationship between the number of people and the area supported by a structural element allows the structural evaluation to be based on an upper bound occupancy condition that is consistent with that used in conventional design provisions. It can be assumed for structural assessment that occupant densities are in the range shown above, from 0.02 to

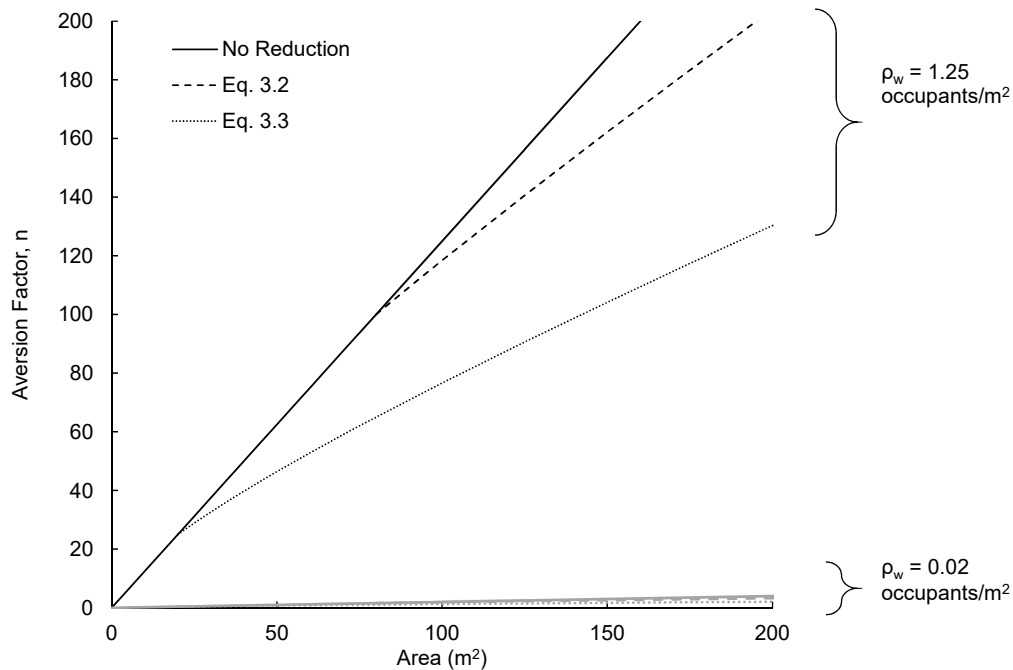


Figure 3.3: Number of people at risk due to structural failure for members carrying large tributary areas using NBCC live load reductions for areas less than 200 m²

1.25 occupants/m². The former represents a storage area, and the latter represents an assembly or other tightly occupied space (National Research Council of Canada, 2015b, 2015c).

3.4 Summary and Conclusions

The number of people affected by a structural failure can be used to quantify the negative perception society has of a particular failure event. The number of people within an area can be conceptualized as an occupant density applied over the tributary area of the element under consideration. The occupant density has been defined and quantified here using explicit and implied densities from structural and non-structural codes. The variation across these sources can be quite large. The occupant density was modified using a factor to account for the relative duration of occupancy. Spaces that spend a large portion of their service life unoccupied are given a lower aversion factor. The tributary area of the element being assessed can be determined with relative ease and used to calculate the number of people it contains.

Application of LLRF to the computation of n can increase the continuity between design and assessment codes. Since reaching the maximum occupancy in large areas is unlikely, the concept of live load reduction can be applied to the tributary area and so used to calculate aversion factor in the same way it is used to calculate the live loads applicable for design. This allows considerable reduction of aversion factors in accordance with a well-defined and widely accepted premise for structural design.

The aversion factor defined in this chapter presents a number of improvements for the quantification of the number of people at risk due to a structural failure. These changes provide a rational and consistent basis for a detailed reliability analysis for structural assessment.

The primary findings of this chapter are as follows:

1. The number of people affected by a structural failure should be quantified directly from the occupancy type and the tributary area supported by the structural element rather than prescribed by a code or determined freely by practitioners.
2. Quantification of the number of people in a tributary area should be based on occupancy data defined by a code whether it is related to fire safety, specified live load, or other limitation on occupancy. The variation of occupant densities across sources is large, due in part to the uses for which they were published.
3. The application of a LLRF to the area supported by an element can provide considerable decreases in the computed number of people at risk, or aversion factor. The use of this reduction factor creates consistency between design and assessment provisions, for both Canadian and American codes.

Chapter 4

Quantifying the Warning of Failure

4.1 Introduction

This chapter will examine the bases that current codes use to determine values of warning factor, and will propose improvements that can more accurately represent structural behaviour as failure approaches. Current documents (e.g. National Research Council of Canada, 2015c; Canadian Standards Association, 2014b; American Society of Civil Engineers, 2017) identify ductility and redundancy as measures of the warning of failure provided. In this chapter, the contributions of both ductility and redundancy to warning of failure will be analyzed. The effect of factors not previously identified, including plastic hinge length, and the effect of loading pattern, will also be considered.

Possible metrics for warning of failure will be compared to determine the most practical and consistent measures for assessment. The effects of varying the reinforcement ratio, concrete strength, configuration of applied loading, and end restraint conditions on the indicators of warning will be studied and used as a basis for quantifying warning factor. The definition of warning factor should include parameters that can be observed or measured from the structure, which also directly relate to observable behaviours as a collapse mechanism is beginning to form.

4.1.1 Definition of Flexural Limit States

The following analysis will consider singly reinforced concrete beams in flexure only, and will focus on behaviour at the yield (YLS) and ultimate (ULS) limit states. The applied moments corresponding to the yield and ultimate limit states are defined simply by moment-curvature analysis of the cross section. Yield corresponds to the reinforcing steel reaching its yield strain in tension, equal to f_y/E_s , where f_y is the yield strength and E_s is the elastic modulus of steel. The YLS of the entire member, then, corresponds to an initial point along the span reaching its yield capacity. This is not a limit state in the traditional sense since yielding may not be directly associated with unacceptable behaviour. The ultimate capacity of a cross section corresponds to its maximum resisting moment and is conventionally assumed to coincide with the onset of concrete crushing. The associated concrete strain in the extreme compression fibre is 0.0035, as in CAN/CSA A23.3-14 (2014). The ULS for an entire element is reached when a collapse mechanism has formed.

4.1.2 Metrics of Warning

The familiar concepts of ductility and redundancy are useful starting points for developing quantifiable metrics for warning. Rather than classifying element failure as discrete degrees of “ductile” or “gradual”, a continuous classification will be derived using physical parameters. Instead of classifying a structure as single- or multiple-load path, the actual support conditions can be idealized and the structural response can be determined analytically. For elements with varying end restraint conditions and configurations of applied loading, there may be common, identifiable behaviours that are independent of the magnitude of loading or the dimensions of the structure. It is desirable to identify behaviour patterns using parameters that are easily observable from a field assessment rather than analyzing every structure in detail to determine the expected failure mode. Identification of such parameters will allow warning of failure to be rationally quantified.

Two possible metrics for characterizing failure behaviours are applied load and deflection. The limits at which structures become unsafe may be quantified using either measure; both load and deflection increase as failure is approached.

Warning by Additional Load Capacity after First Yield

Current codes (e.g. National Research Council of Canada, 2015c; Canadian Standards Association, 2014b) deem single load path structures, in which a single local failure initiates overall collapse, to be undesirable. Multiple load path structures, in which the formation of the first plastic hinge does not lead to collapse, are preferred. Additional load may be applied to an indeterminate beam until a sufficient number of plastic hinges are created to form a collapse mechanism. The load applied between the formation of the first and final plastic hinges can therefore be considered to provide warning of failure. For example, consider a member supporting a uniformly distributed load, w_y , that causes the first plastic hinge to form, and subsequently w_u , that causes failure. The difference can be expressed by a load increment, $\Delta w = w_u - w_y$, or a dimensionless load ratio, w_u/w_y .

Using loads as a metric to define the warning of failure, however, can be problematic. First, loading is complex and the magnitudes and distributions adopted in conventional design practice are always simplified. The representation of structural loading as concentrated or uniformly distributed may be sufficient for design purposes, but for assessment, where the conclusions may be more sensitive to the assumptions made, these simplifications can be misleading. Second, the magnitude of load is not typically visible to an average user. Ongoing monitoring is necessary to track loading as it approaches critical levels. Additional load-carrying capacity due to indeterminacy, while beneficial, does not necessarily provide evidence that the structure is nearing collapse, and therefore is not a useful metric for warning of failure.

Warning by Visible Deflection

Deflection is a more effective measure of warning because it provides visible indication that the condition of the structure could soon become dangerous. Intuitively, the more deflection a structure can sustain without reaching failure, the greater the benefit, or warning of failure. Similarly to load-based measures, various deflection quantities can be defined using the yield and ultimate deflections, Δ_y and Δ_u , respectively. Alternately, deflection can be presented as two components; the linear-elastic deflection, Δ_e , due to curvatures in the regions that have not yielded, and the plastic deflection, Δ_p , due to curvatures in regions where the reinforcement has reached yield. Measures may include ratios between the components of the expected deflection—i.e. elastic, plastic, total. For example, Δ_u/Δ_y , or Δ_p/Δ_e , are unitless ratios of deflection components. The same deflections can also be presented with respect to the span length or height of a particular cross section, as in Δ/L , or Δ/h .

One caution when using deflections to quantify warning of failure is that the deflection of some elements, even at large magnitudes, may be hidden behind finishes, equipment, or other obstructions. Deflection appears to be the superior metric for measuring warning of failure, however, and will be used in the analyses presented in this chapter. As deflections increase in magnitude, users of the structure are able to observe and react to the potentially imminent failure. Additionally, deflections are readily computed, given the material and geometric properties of a structural element, and are therefore practical for structural assessment.

4.1.3 Plastic Behaviour of Reinforced Concrete in Flexure

The magnitudes of deflection considered will include both linear-elastic and plastic, or inelastic, components. Cohn (1965) discusses the need for consideration of inelastic behaviour of reinforced concrete. He emphasizes the rationality of representing the behaviour of structures approaching collapse as accurately as possible, without allowing the uncertainties in material models or structural loads to prevent the adoption of inelastic design concepts. Since reinforced

concrete typically retains considerable capacity beyond the limit of linear-elastic behaviour, he argues that design procedures should recognize and account for the collapse load capacity explicitly.

Cohn (1972) presents a comprehensive set of worked examples to quantify the inelastic behaviour of structural steel and reinforced concrete. These include the calculation of ultimate deflections and rotations, as well as the ratios of these quantities at collapse and at the formation of the initial plastic hinge.

As in Cohn (1972), a plastic hinge will be defined as a region along a span where the applied moment is greater than the yield capacity of the cross section, or where plastic behaviour occurs. At a plastic hinge location, the plastic rotation capacity will be assumed sufficient to develop a full collapse mechanism. In reality the rotation capacity may be limited, particularly by the concrete reaching its ultimate strain in compression.

Deflection at Ultimate Limit States

The Moment-Area Method can be used to approximate the deflection of an element as it reaches its collapse load (Cohn, 1972). This essentially allows the simplified double integration of curvature to determine deflection. The Moment-Area Method is based on the assumption of small deflections, where the arc length along the elastic curve is approximately equal to the chord length along the undeformed element (Leet, Uang, & Gilbert, 2011). The integration therefore underestimates the total deflections because the elastic curve is in fact longer than the undeformed length. It is acceptable to use the Moment-Area Method to compute deflections at incipient failure in the present study as the underestimation of the true deflection and associated warning will be conservative. The consistent use of the Moment-Area Method will also allow for appropriate comparisons of the relative deflections for a variety of structural conditions.

The curvature diagram of the element at ULS is used to compute the plastic deflections occurring in the hinging regions of the span. Example calculations of deflections for a fixed end beam under a uniformly distributed load (UDL) can be found in Appendix A. The total

deflection at ULS is the sum of both the plastic and elastic deflections. Although material behaviour at ULS can be beyond the linear-elastic limits, the elastic portion of deflection can be well represented using elastic beam theory (Cohn, 1972).

4.1.4 Progression toward Failure

In a statically indeterminate element, collapse does not occur when the first plastic hinge forms if the flexural and shear reinforcement are detailed to allow large plastic rotations. When a sufficient number of hinges have formed to create a collapse mechanism, the element is no longer stable and deflections increase rapidly. For a simply supported beam, the formation of a mechanism requires a single plastic hinge, while in a fixed-ended beam, three hinges must be formed before instability occurs.

Figure 4.1 shows the distributions of moment through the progression of a propped cantilever beam toward collapse. The first plastic hinge forms under negative moment at the support. The beam responds to additional load as a simply supported beam until the formation of the second plastic hinge under positive moment at midspan. These two hinges create a failure mechanism.

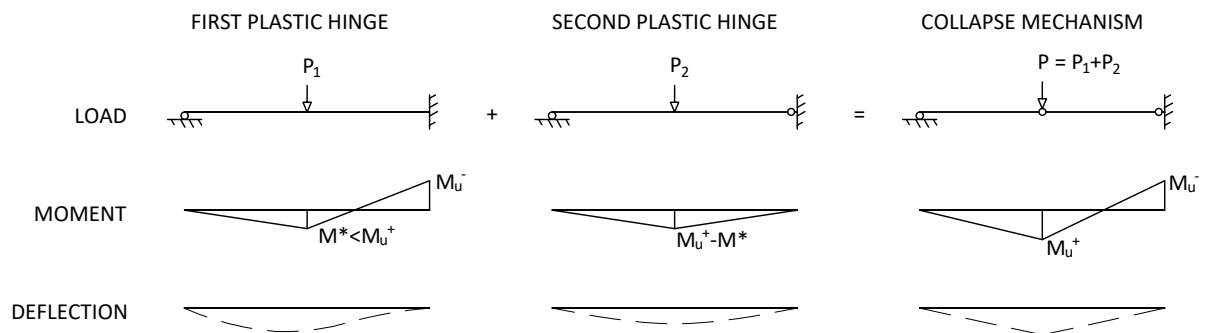


Figure 4.1: Failure progression of a propped cantilever with concentrated load at midspan

A structural element under increasing transverse loading will eventually form a plastic hinge at each location where the moment reaches a local maximum value. These extreme values fall into two categories: maximum positive moments, which occur at critical midspan locations, and maximum negative moments, which occur at support locations where rotational restraint is present.

All locations of local maximum moments are dependent on loading and boundary conditions. As hinges begin to form, rotational restraints are eliminated and the moment distribution is altered.

Figure 4.2 shows elastic deformed shapes and plastic collapse mechanisms for simply supported (SS), cantilever (CA), fixed-ended (FE), propped cantilever (PC), and two-span (TS, TA) boundary conditions. Two-span beams may be loaded symmetrically (TS) or asymmetrically (TA). It is possible to have several hinges form simultaneously at a given load level, for example, at the fixed ends of a symmetrically loaded beam. Although three plastic hinges are needed to create a failure mechanism, the two end hinges form simultaneously. Since warning depends on the actual visibility of the impending failure, classifying warning based solely on the level of redundancy or degrees of indeterminacy may not be sufficient.

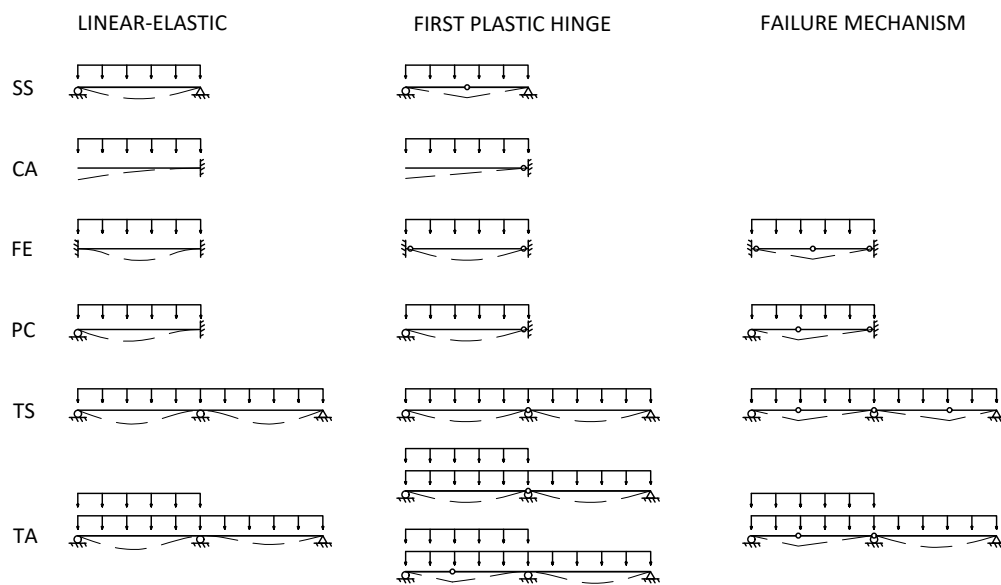


Figure 4.2: Plastic hinges at collapse for one- and two-span beams with idealized boundary conditions

4.2 Analysis

4.2.1 Assumptions

The following assumptions, which are commonly adopted for simple reinforced concrete flexural analysis, will be used in analyzing warning of failure in reinforced concrete beams:

1. Plane sections remain plane and perfect bond exists between concrete and reinforcing steel

Plane sections must remain plane to achieve linear strain profiles for cross sectional analysis. Perfect bond between the concrete and reinforcement ensures the compatibility of strains across the cross section.

2. Linear-elastic, cracked response up to yield

All strain occurring before yielding of reinforcing steel is assumed recoverable. Concrete in tension is ignored.

3. Rectangular stress block at ultimate flexural capacity

The behaviour of concrete at the ultimate moment capacity can be well represented by assuming a uniform distribution of stress in the compression region. Strain hardening of reinforcement is ignored.

4. No catenary action

Elements will be assumed to have reached their capacity when the flexural collapse mechanism occurs. Possible additional capacity or deformation due to catenary action is ignored.

5. Flexural failure

Failures due to shear or axial load effects exhibit fundamentally different behaviour patterns and are ignored.

4.2.2 Cross Section Analysis

Singly reinforced cross sections can be classified by reinforcement ratio, either geometric, $\rho = A_s/bd$, or mechanical, $\omega = \rho f_y/f'_c$, where A_s is the area of reinforcing steel, b is the cross section width, d is the effective depth of the cross section, and f'_c is the concrete strength. The mechanical reinforcement ratio allows for the direct inclusion of concrete strength variation in the analysis output. The geometric reinforcement ratio has the benefit of being a more familiar quantity that can be easily conceptualized, and so will be used to present results.

Table 4.1 includes the range of parameters used for cross-sectional analysis. A geometric reinforcement ratio from 0.002 to 0.012 represents a range that may be expected for a typical flexural element. The lower limit of 0.002 may be present in lightly reinforced two-way slabs, whereas 0.012 represents an approximate limit where the linear-elastic assumption of concrete stress-strain behaviour at YLS becomes doubtful.

Table 4.1: Analysis parameters

Parameter	Symbol	Range	Units
Geometric reinforcement ratio	ρ	0.001-0.012	-
Concrete Strength	f'_c	25-50	MPa
Reinforcing Steel Strength	f_y	400	MPa

The strength of the reinforcing steel has been assumed constant at 400 MPa. Concrete strengths have been selected across a common range, from 25 to 50 MPa.

Figure 4.3 shows a moment-curvature diagram generated by Response-2000 (Bentz & Collins, 2001) for a cross section using 35 MPa concrete, 400 MPa reinforcing steel, with a reinforcement ratio of 1% and a ratio of effective depth to height, d/h , of 0.9. The true moment-curvature response, shown by the dotted line, has been simplified as two linear segments for the analyses presented in this chapter. This idealized bilinear moment-curvature relationship provides a clear distinction between linear-elastic and plastic behaviour. Tension stiffening between cracks will be ignored, so the fully cracked moment of inertia, I_{cr} , will be adopted to calculate linear-elastic deformations. The slight overestimation of curvature caused

by this assumption has little effect on the resulting deformations at the yield limit state. It will also be assumed that the distribution of curvature between the yield and ultimate moments, shown as the rigidity EI_p , is linear.

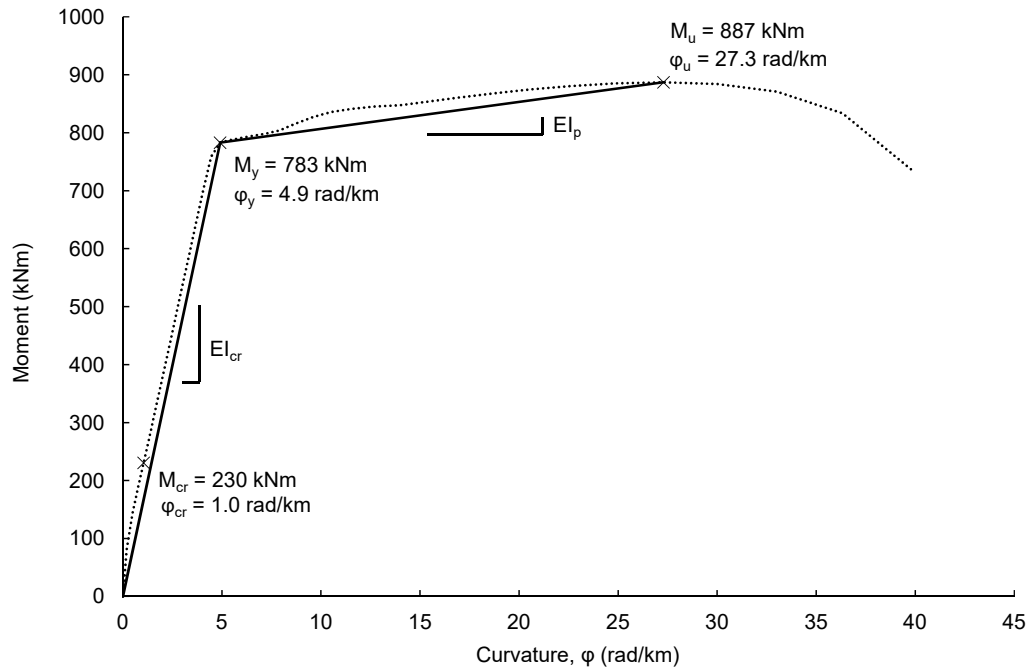


Figure 4.3: Moment-curvature relationship of a reinforced concrete cross section

For the simple beam cross section shown in Figure 4.4, a set of equations can be derived to compute the curvature and moment in a cross section. The elements considered will be rectangular cross sections under flexural load with only tension reinforcement. At the yield limit state, the distribution of concrete compression stress is linear. At ultimate, it is represented as a rectangular stress block defined in CAN/CSA A23.3-14 (2014) by parameters α_1 and β_1 where,

$$\alpha_1 = 0.85 - 0.0015f'_c \quad (4.1)$$

$$\beta_1 = 0.97 - 0.0025f'_c \quad (4.2)$$

Equilibrium requires that the tension force in the reinforcing steel at yield must be equal to the compression force in the concrete. Figure 4.4 shows the stress and strain states in a beam at YLS and ULS. At both limit states, the curvature depends on the depth of the neutral axis and, at yield, the steel yield strain, ϵ_y , or at ultimate, the concrete crushing strain, ϵ_{cu} . High concrete compressive strengths mean that smaller stress block depths are required to resist compression forces. If the section width remains constant, greater compressive strengths are associated with smaller compression block depths, a , and therefore larger ultimate curvatures, $\varphi_u = \beta_1 \epsilon_{cu} / a$.

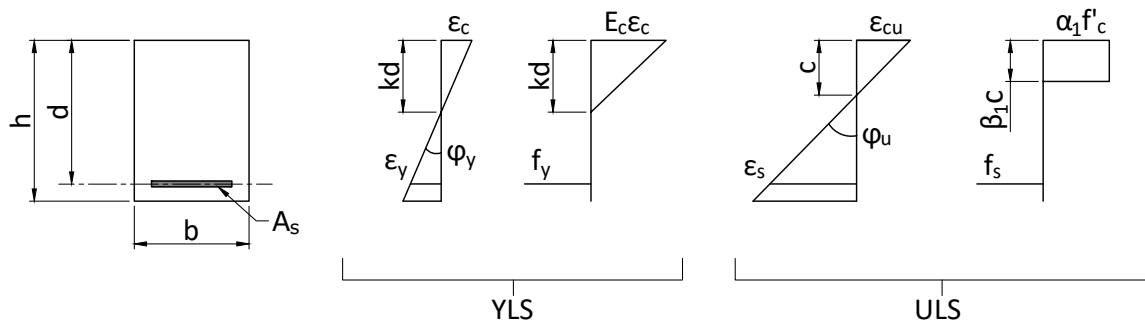


Figure 4.4: Beam cross-section dimensions, stress and strain diagrams at YLS and ULS

The effective depth, defined as kd at YLS, and c at ULS, defines the strain profile in the cross section. At YLS,

$$k = \sqrt{(\rho n)^2 + 2\rho n} - \rho n \quad (4.3)$$

where ρ is the reinforcement ratio, and n is the modular ratio, or the ratio of the elastic moduli of reinforcing steel and concrete, E_s/E_c . At ULS, the compression block depth is $\beta_1 c$. Each of the strain conditions defined by these parameters has an associated cross-sectional curvature.

Curvature is defined according to these generic strain profiles. At yield and ultimate limit states the curvatures, φ_y and φ_u , respectively, are:

$$\varphi_y = \frac{\epsilon_y}{(1 - k)d} \quad (4.4)$$

and

$$\varphi_u = \frac{\alpha_1 \beta_1 f'_c \epsilon_{cu}}{\rho f_y d} \quad (4.5)$$

Equation 4.5 can be written as $\varphi_u = \frac{\alpha_1 \beta_1 \epsilon_{cu}}{\omega}$, showing that the ultimate curvature is inversely proportional to the mechanical reinforcement ratio, ω .

Figure 4.5 shows the relationship between geometric reinforcement ratio, ρ , and curvature normalized by cross-section depth, φd . Curvatures are associated with cross-sectional properties alone and are independent of boundary conditions, loading, and other element-level parameters. The ultimate curvature, φ_u , is quite sensitive to the quantity of reinforcing steel present in the cross section, primarily because it is approximately proportional to $1/\rho$, or $1/\omega$. Low reinforcement ratios produce markedly greater ultimate curvatures than the same cross section with more reinforcing. The yield curvature is relatively insensitive to the reinforcement ratio.

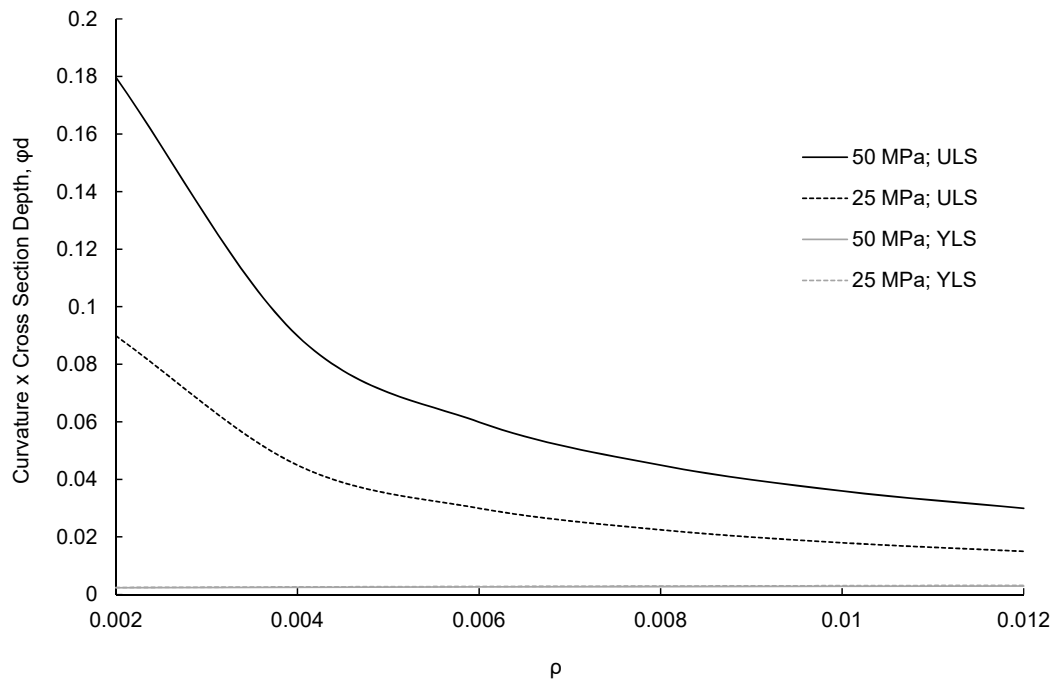


Figure 4.5: Curvature variation with reinforcement ratio and concrete strength at YLS and ULS

The flexural capacity at each limit state can also be determined using this basic set of assumptions and parameters. At yield, the moment capacity is,

$$\frac{M_y}{bd^2} = \rho f_y \left(1 - \frac{1}{3}k\right) \quad (4.6)$$

where the capacity is normalized by the cross-section dimensions. Similarly, the normalized moment capacity at failure is

$$\frac{M_u}{bd^2} = \rho f_y \left(1 - \frac{\rho f_y}{2\alpha_1 f'_c}\right) \quad (4.7)$$

These quantities can be used to define metrics for comparison of elements with varying cross-sectional dimensions. The two unitless quantities that will be used to identify cross sections are the curvature ductility ratio and shape factor.

Curvature Ductility Ratio

The curvature ductility ratio, φ_u/φ_y , from Equations 4.4 and 4.5, is simply,

$$\frac{\varphi_u}{\varphi_y} = \left(\frac{\alpha_1 \beta_1 f'_c \epsilon_{cu}}{\rho f_y}\right) \left(\frac{1-k}{\epsilon_y}\right) \quad (4.8)$$

Figure 4.6 shows the relationship between curvature ductility and concrete strength over a range of reinforcement ratios. Ductility is large at low reinforcement ratios, and increases with concrete strength. The changes due to increased concrete strength are relatively minimal for higher reinforcement ratios, while for lightly reinforced cross sections, the concrete strength is more influential.

Shape Factor

The shape factor, f , is the ratio of flexural capacities, M_u/M_y . For singly reinforced beams, Equations 4.6 and 4.7 give,

$$f = \frac{1 - \frac{\rho f_y}{2\alpha_1 f'_c}}{1 - \frac{1}{3}k} \quad (4.9)$$

Figure 4.7 shows the variation of shape factor with both the concrete strength and the mechanical reinforcement ratio, ω . Over the parameter ranges studied, shape factors can reach maximum values of approximately 1.054, increasing as concrete strength is increased.

For each concrete strength shown, there is a value of ρ that maximizes the value of f . After this point f decreases until a critical stage where the assumption of linear-elastic behaviour

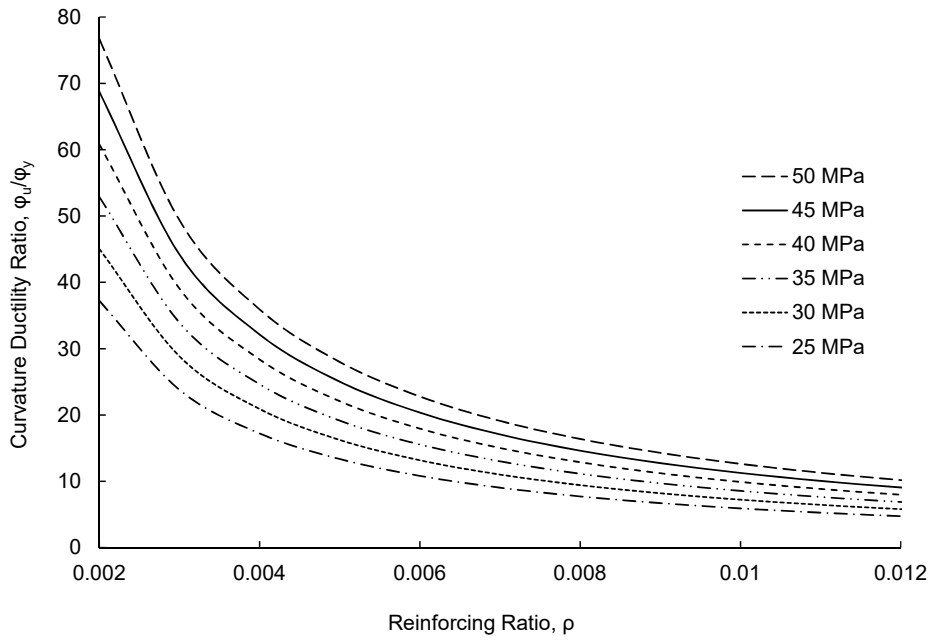


Figure 4.6: Curvature ductility variation with ρ and f'_c

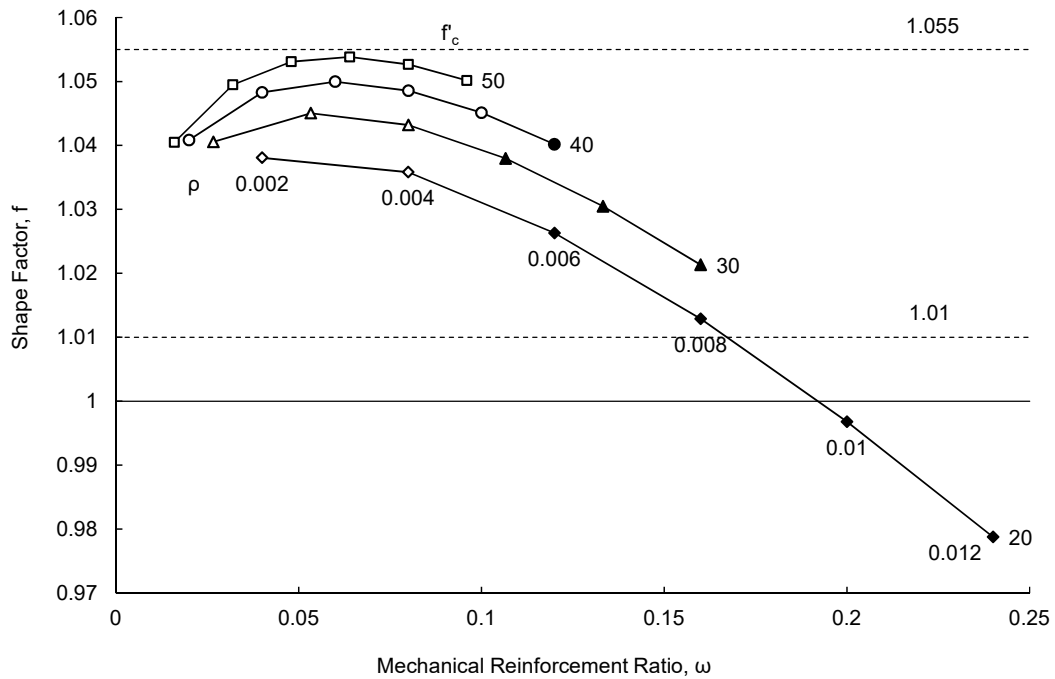


Figure 4.7: Shape factor, f , variation with reinforcement ratio and concrete strength

of concrete at YLS no longer holds. A maximum concrete stress of $0.7f'_c$ will be considered the limit of the validity of this assumption. For higher stresses, Equation 4.3 is no longer representative of actual concrete material behaviour. Figure 4.7 shows in solid markers the reinforcement ratios that are inadmissible by this constrained concrete stress. These will not be strictly used to limit possible values for f , but were influential in selecting a lower bound of 1.01 for f .

Ratio of Moment Capacities

Statically indeterminate elements introduce the possibility of cross sections with different flexural capacities existing in a single element. For the investigation presented in this chapter, all cross-sections in an element, whether in positive or negative bending, will be taken to have identical flexural capacities, or $|M^+| = |M^-|$. In a fixed ended beam under a concentrated load, the moments at midspan and the supports are identical, $PL/8$, so identical positive and negative flexural capacities mean that all three hinges form simultaneously. In the same beam under a uniformly distributed load, the support moments, $wL^2/12$, are larger than the span moment, $wL^2/24$, so the failure mechanism is formed in two stages. In the design of reinforced concrete beams, this assumption is unlikely to be valid, and the negative moment capacity will be larger than the positive moment capacity such that $|M^-| = \alpha |M^+|$, where $\alpha \geq 1$.

Based on the moment distributions for elastic beams, the capacity of cross sections at maximum moment locations can be assumed to be proportional to the factored moment and an appropriate range of α is 1.0 to 2.0 for single spans. Applying this range of moment ratios to the deflection results for indeterminate beams will cause the total deflections to decrease, due increased end stiffness. This analysis is briefly outlined in Appendix A.

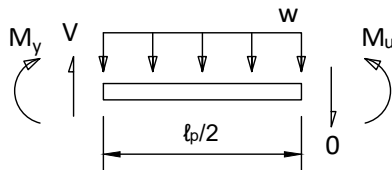
For the remainder of this analysis, $|M^-/M^+|$ will be assumed to be one. The results in terms of warning of failure will therefore be upper bound values. Though the impacts of this parameter will be ignored in this chapter, the impact on outcomes is relatively minimal. These

effects can easily be incorporated in the future in the same way as other deflection-altering parameters.

4.2.3 Beam Analysis

Deflections at failure can be obtained by the analysis of the entire flexural element. While the cross section plays a role in the resulting deflection magnitudes, the configuration of loads, and the boundary conditions are also significant factors.

The plastic hinge length, ℓ_p , for a given moment variation can be determined using simple static analysis, setting the magnitude of the maximum applied moment to the ultimate moment capacity, M_u . For example, Figure 4.8 shows a beam segment under a uniformly distributed load. Applying the known force effects in the midspan plastic hinge region, as in Figure 4.8, the hinge length, ℓ_p , can be determined. Appendix A includes an example of this calculation procedure.



$$V = \frac{w\ell_p}{2}$$

$$M_u - M_y = \frac{V\ell_p}{2} - \frac{w\ell_p^2}{8}$$

where for a simply supported beam,

$$M_u = \frac{wL^2}{8}$$

therefore,

$$\ell_p = \sqrt{1 - \frac{M_y}{M_u}}L$$

Figure 4.8: Free body diagram used to compute plastic hinge lengths

Load Configuration

Figure 4.9 shows the three loading conditions that will be analyzed to derive warning factor metrics. Beams with concentrated and uniformly distributed loads, Cases (a) and (b), will be

studied. Case (c) with two equally spaced loads will further illustrate the effects of spans with long zero-shear regions in beams with symmetrical boundary conditions. These cases represent large variations in the magnitudes and distributions of shear and bending moments. Case (a) gives the largest midspan shears and has a small plastic hinge length, while Case (b) has a much longer plastic hinge length, with shears that increase from zero at the midspan. Case (c) has the longest plastic hinge length, that extends slightly beyond the zero shear region between the two concentrated loads.

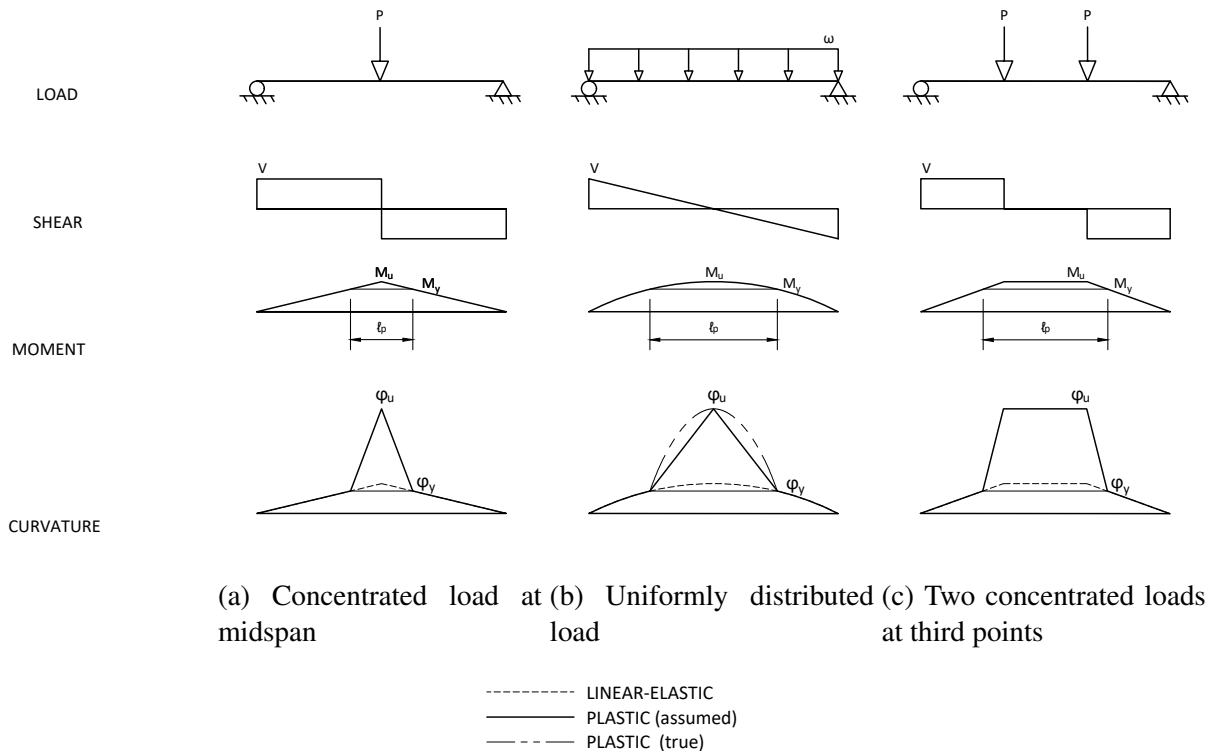


Figure 4.9: Force effects and curvatures for simply supported beams under three load configurations

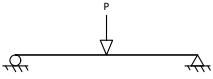
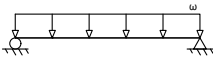
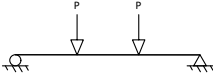
Figure 4.9 also shows the curvature diagrams necessary to determine the total deflections by the Moment-Area Method. For curvatures under distributed loads, the true parabolic distribution of plastic curvature will be simplified to vary linearly between yield and ultimate curvatures as shown in Figure 4.9(b).

Table 4.2 shows the resulting hinge lengths for simply supported beams with each load configuration. All hinge lengths are reduced as the shape factor, f , decreases. Increasing the

reinforcement ratio, ρ , therefore reduces the deflection at incipient failure because both the ductility ratio and the plastic hinge length are reduced.

Figure 4.10 shows the variation of the normalized plastic hinge lengths, ℓ_p/L , with the shape factor. The longest hinge lengths occur with two concentrated loads, and range from 34-36% of the span. Under a uniformly distributed load, the plastic hinge length can vary from 10-22% of the span length, and under a single concentrated load at midspan, the range is only 1-5% of the span length. Plastic hinge lengths increase with the shape factor, most dramatically for beams under uniformly distributed loading.

Table 4.2: Simply supported beam configurations

Configuration	Plastic Hinge Length
	$(1 - \frac{1}{f})L$
	$\sqrt{(1 - \frac{1}{f})}L$
	$(1 - \frac{2}{3f})L$

A similar procedure may be followed to determine plastic hinge lengths for beams with additional equally spaced concentrated loads as shown in Figure 4.11. The number of loads may be even or odd as shown.

Figure 4.12 shows the plastic hinge lengths for simply supported elements with increasing numbers of equally spaced concentrated loads, normalized by ℓ_p for the UDL case. Increasing the number of load points leads to longer hinge lengths for odd numbers of loads, while the opposite is true with even numbers of loads. As the number of load points increases, whether odd or even, the load effects become increasingly similar to those for a uniformly distributed load and the normalized hinge lengths converge to 1.0. The least plastic hinge length is for the

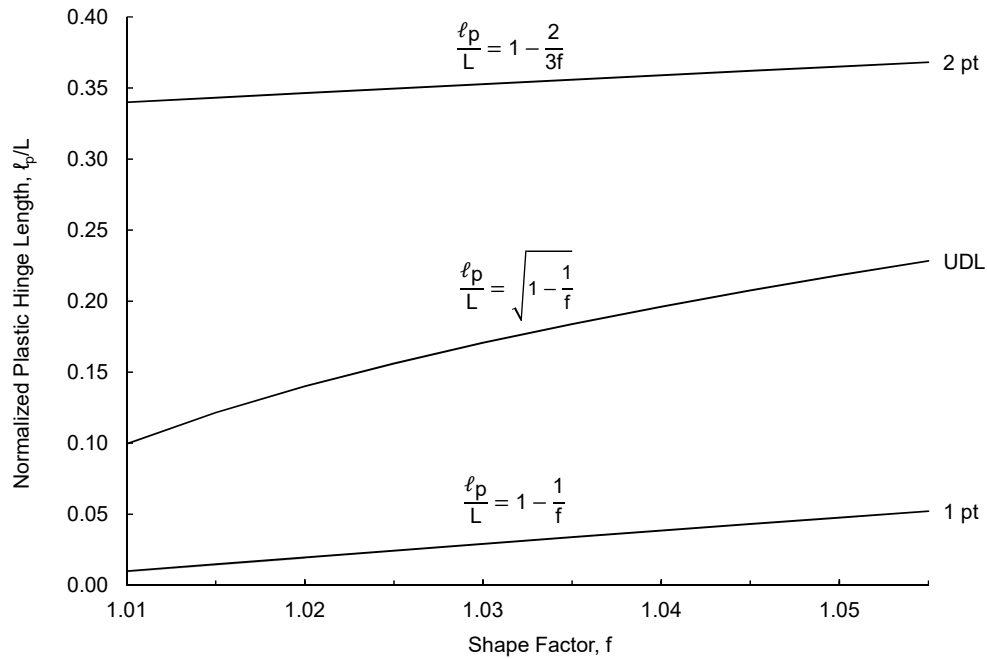


Figure 4.10: Plastic hinge length for simply supported beams

case with one concentrated load, and the largest plastic hinge length is for the case with two concentrated loads.

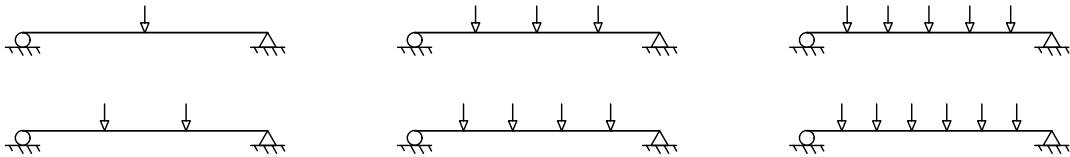


Figure 4.11: Simply supported beams with multiple concentrated loads

Although the effects of load configuration on warning of failure are not necessarily intuitive, and do not appear in current assessment documents, they appear to be important in determining the length of plastic hinges, and therefore the deflection at imminent failure. The above patterns should be considered when simplifying conditions to a conservative state. In general, long hinge lengths may be expected where even numbers of concentrated load points cause zero-

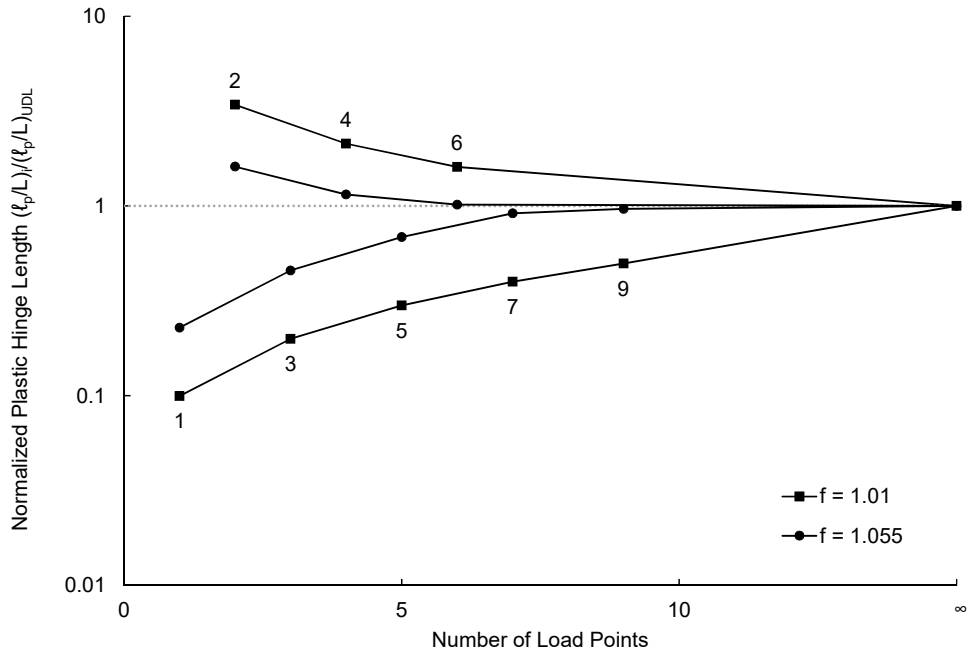


Figure 4.12: Plastic hinge lengths for multiple concentrated loads, normalized with respect to the plastic hinge length for a UDL

shear regions between the central load points. Increasing even numbers of load points create shorter plastic hinges. With odd numbers of concentrated loads, the opposite trend can be observed, where increases in the number of load points in odd numbers causes a flattening of the moment-distribution diagram and therefore longer hinge lengths.

End Restraint Conditions

Beam deflections, being dependent on distribution of moment along the member, will also vary with end restraint conditions, which can be assumed to have zero rotational restraint, as in a pinned condition, or complete rotational restraint, as in a fully fixed end. Pinned ends cause large linear-elastic deformations, while increased rotational restraint generally corresponds to smaller linear-elastic deformations.

End conditions affect the total deflections of a beam both through the elastic component of deflection, and the plastic component. Plastic hinge locations can be determined by the

locations of local maximum moments, and their lengths depend on the applied shear and the shape factor of the cross section at the hinge location.

Figure 4.13 shows the end conditions considered: simply supported, cantilever, propped cantilever, and fixed ended. While the shear force distributions in the plastic hinge regions for each are effectively the same, the moment distributions vary greatly. Each end restraint therefore impacts the general deflection response. The cantilever case, while relatively uncommon, is associated with large free end deflections, while the propped cantilever represents an intermediate case between simply-supported and fixed-ended beams. A propped cantilever also behaves identically to a two-span element with pin supports and symmetrical loading, Case TS in Figure 4.2.

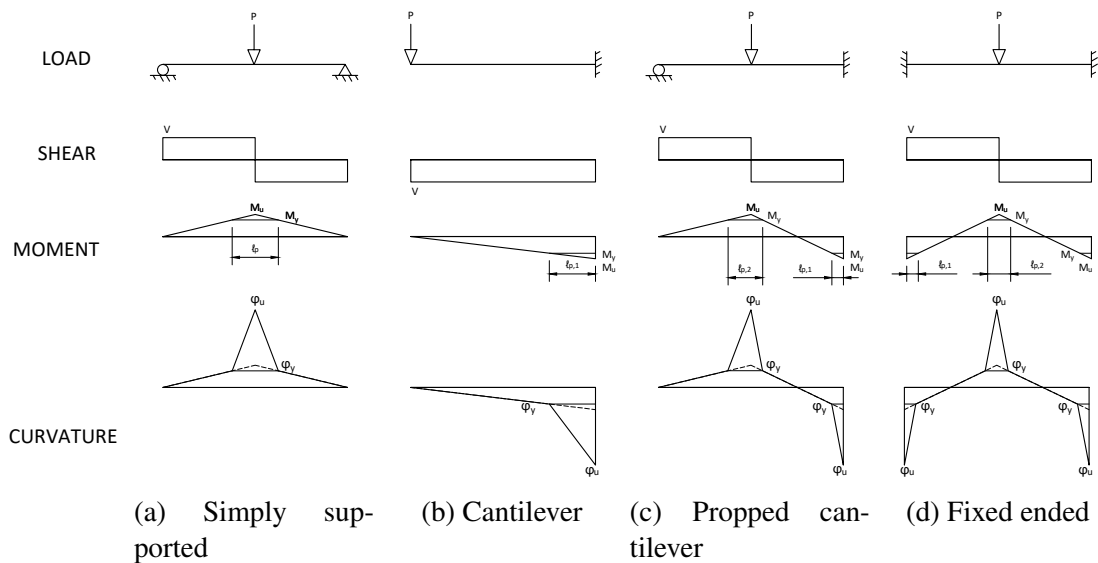
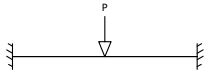
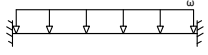
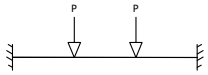


Figure 4.13: Force effects for beams with a concentrated load at midspan

Each of these end restraint conditions may be studied under any configuration of loading to observe patterns in the resulting deflections. Here, each will be studied under a single concentrated load, as well as a uniformly distributed load over the whole span. The cantilever beam will have a concentrated load applied at the free end, while for the other end conditions it will be applied at midspan.

Table 4.3 summarizes the expressions for plastic hinge lengths in in single span beams with fixed boundary conditions. The plastic hinge length expressions for all boundary conditions and load configurations are shown in Appendix A. Using these plastic hinge length expressions, as well as those for cantilevers and propped cantilevers, the total deflections at incipient failure can be calculated for all beam support conditions.

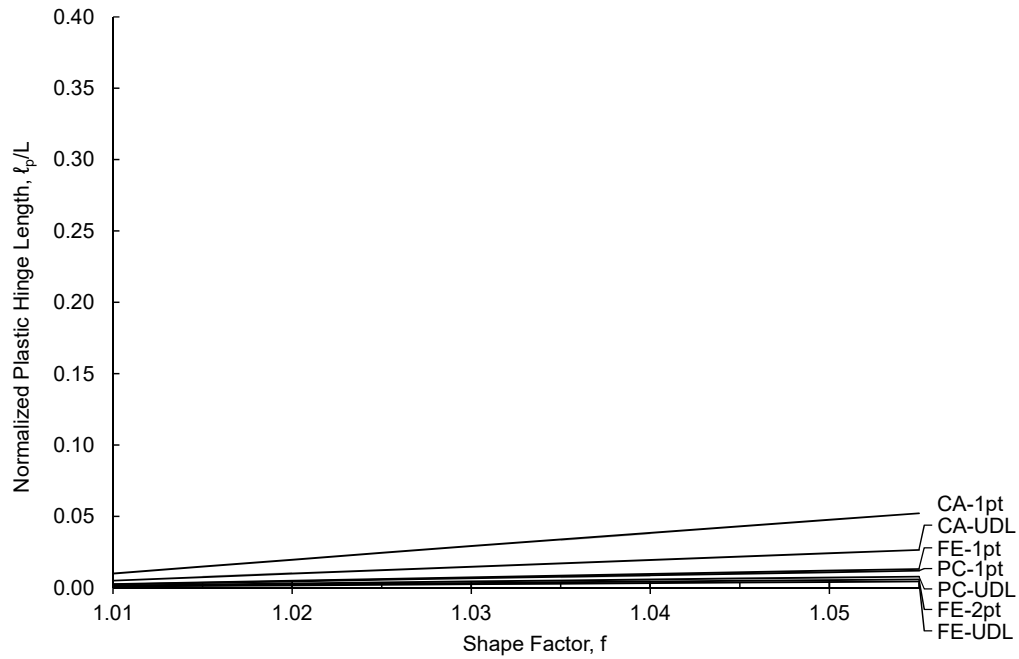
Table 4.3: Fixed-ended beam configurations

Configuration	Plastic Hinge Length	
	Support	Span
	$\frac{1}{4}(1 - \frac{1}{f})L$	$\frac{1}{2}(1 - \frac{1}{f})L$
	$\frac{1}{2}(1 - \sqrt{\frac{1}{3}(2 - \frac{1}{f})})L$	$\sqrt{\frac{1}{3}(1 - \frac{1}{f})}L$
	$\frac{1}{9}(2 - \frac{1}{f})L$	$\frac{1}{9}(5 - \frac{2}{f})L$

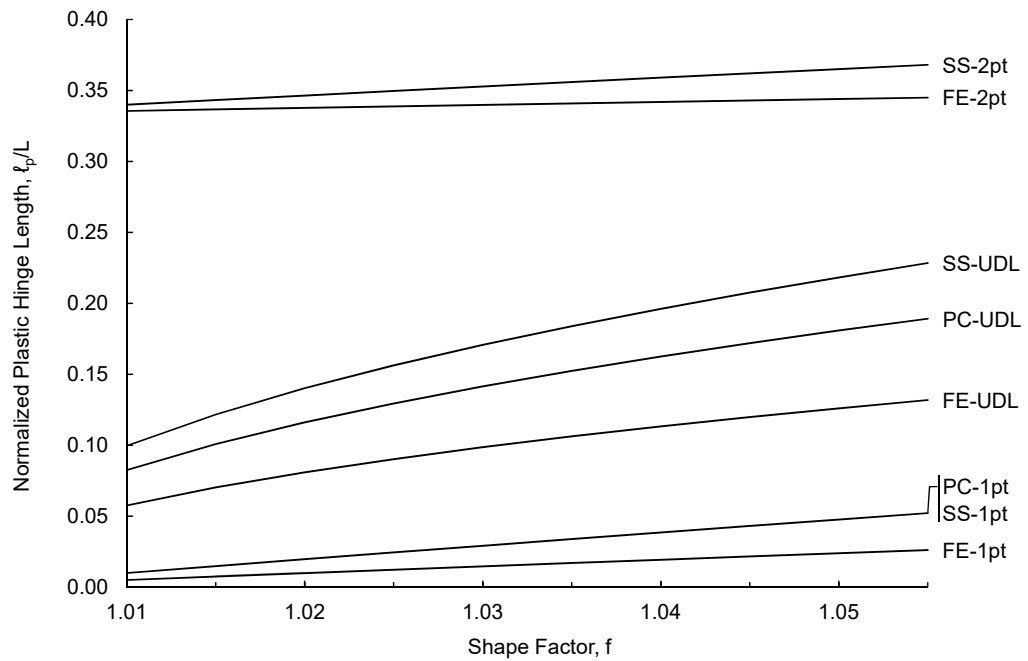
Figures 4.14a and 4.14b illustrate the differences in plastic hinge length as the shape factor varies from 1.01 to 1.055 for hinges that form at supports and in the span, respectively. The longest plastic hinges at the supports occur in cantilevers. The support hinges in general tend to be shorter than the span hinges, since they form in regions of high shear. For span hinges, beams with concentrated loads at third points produce plastic hinges that remain in excess of 33% of the span length. The length of plastic hinges in spans are more sensitive to the shape factor, and thus to the reinforcement ratio.

Two-Span Beams

Two-span beams can be examined under similar variations to determine the effects of continuity on the patterns observed above. The procedure, similar to that for single span beams, and the results will be presented in Appendix B. The symmetrical load combination gives results equal



(a) Support hinge length



(b) Span hinge length

Figure 4.14: Hinge length variation with shape factor, boundary condition, and load configuration

to those for propped cantilevers, so the discussion of two-span beams will focus on systems where one span is more heavily loaded than the other.

4.3 Results

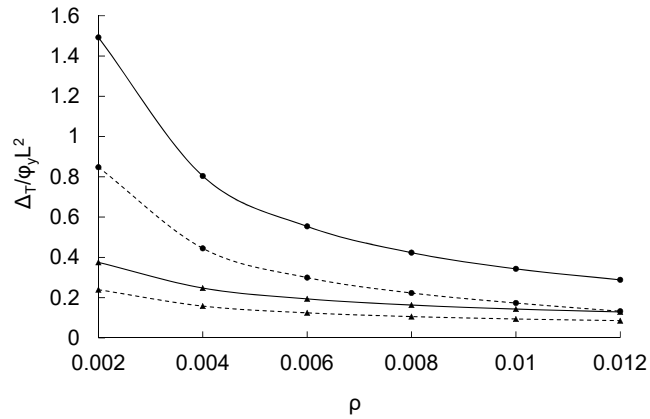
Using the Moment-Area Method and the plastic hinge length expressions derived above, the deflections of beams at incipient collapse can be determined. Deflection magnitudes can then be used to quantify warning of failure. Results will be presented first for determinate beams to indicate the effect of loading configuration, reinforcement ratio, and end restraint conditions on the ultimate deflection. Results will then be presented for indeterminate beams, to further illustrate the effects of the end restraint conditions.

4.3.1 Determinate Beams

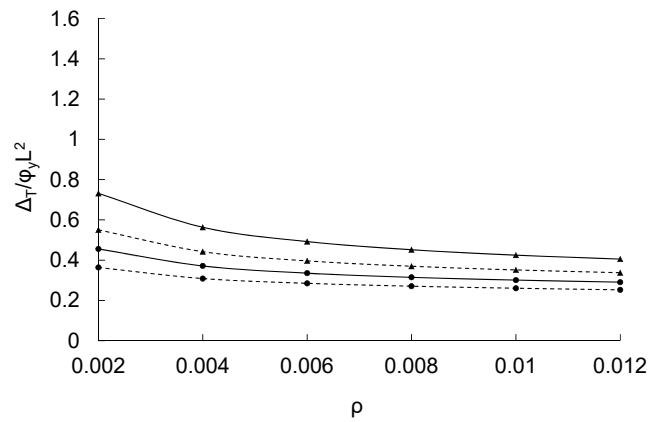
Consider first the simply supported beam and the cantilever beam. Each requires the formation of a single plastic hinge to create a collapse mechanism.

Figure 4.15 shows the total normalized deflections at ULS for determinate beams under a single concentrated load, and a uniformly distributed load. For each, the total deflection at ULS is greatest for low reinforcement ratios and high concrete strengths. As concrete strength decreases, or reinforcement ratio increases, the total deflection at incipient failure becomes less. The magnitudes of deflection however, are quite different. The overall deflections in cantilevers are less than in the simply supported beams and show less variation with reinforcement ratio. The maximum deflection magnitude for cantilevers occurs under a concentrated load, rather than a uniformly distributed load because the length of the plastic hinge at the support location is longer. The length of the plastic hinge in the cantilever is always shorter than that in the simply supported beam due to the larger shear forces at the support.

Figure 4.16 shows the deflections for the two concentrated load configuration alongside those for a UDL and single concentrated load on a simply supported beam. The longer hinge



(a) Simply supported



(b) Cantilever



Figure 4.15: Total normalized deflection of determinate beams at ULS

lengths for the beam subjected to two concentrated loads produce notably larger ultimate deflections. This illustrates the importance of considering the load idealization for assessment. The case with two concentrated loads produces much larger deflections, indicating greater warning of failure, and lower risk to occupants.

The most common loading configuration for beams in reinforced concrete buildings is uniformly distributed, so the subsequent comparisons will focus on this configuration. Figure 4.17 shows the differences in total deflections for determinate beams under a UDL. The differences

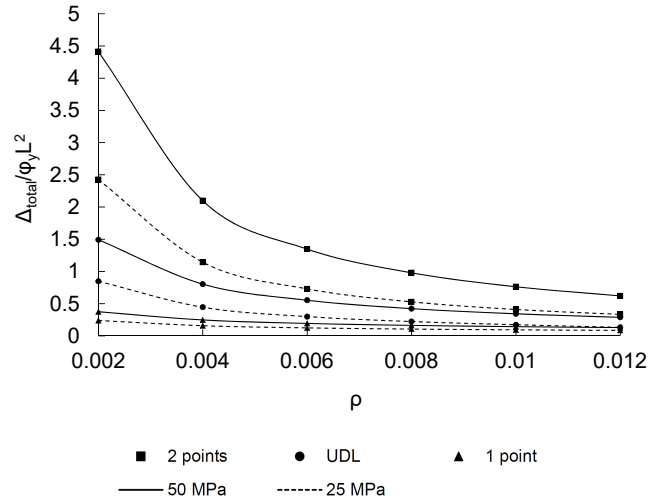


Figure 4.16: Total normalized deflection for a simply supported beam

in deflections can be attributed to the differences in plastic hinge lengths as well as the shape of the elastic curves. At low reinforcement ratios, the simply supported beams give much larger total deflections, but as ρ increases, the cantilever case becomes much more comparable, or even preferable. These observations indicate that indeterminacy on its own is not necessarily a helpful indicator of failure. These two systems could both be classified as having a single load path, or zero degrees of indeterminacy, but the deflections they exhibit, and therefore the warning they can provide, is markedly different.

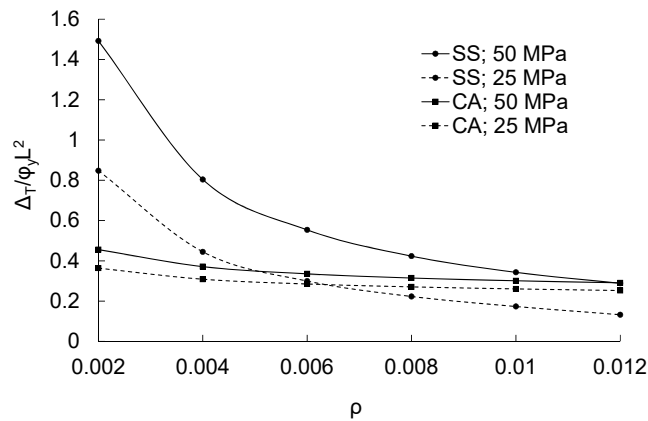


Figure 4.17: Deflection ratios for determinate beams under uniformly distributed loading

Figure 4.18 shows the ratios of total deflection to yield, or linear-elastic, deflection for determinate elements as the reinforcement ratio is varied. The cantilever beam deflections are comprised primarily of linear-elastic deflection over the entire range, while the simply supported beam experiences primarily plastic deflection at low reinforcement ratios but primarily linear elastic deflections at high reinforcement ratios.

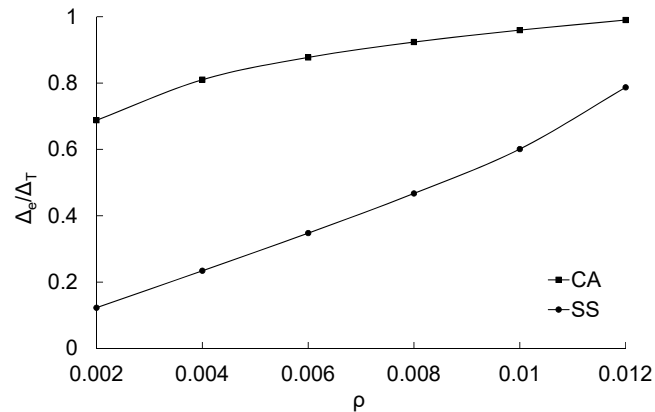
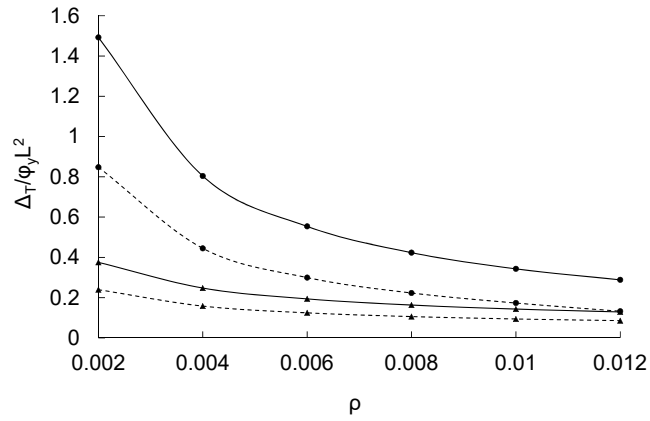


Figure 4.18: Ratio of ultimate to yield deflections for statically determinate beams

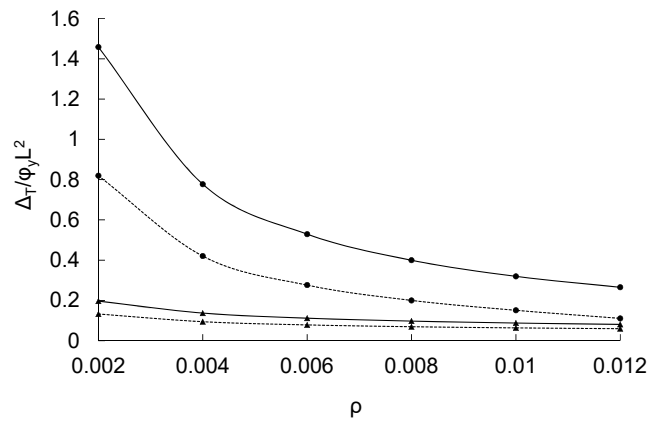
4.3.2 Indeterminate Beams

Figure 4.19 shows normalized deflections for cases of simply supported, propped cantilever, and fixed-ended beams subjected to single concentrated and uniformly distributed loads. Similar trends can be observed as in the previous section: total deflection decreases with decreasing concrete strength and increasing reinforcement ratio.

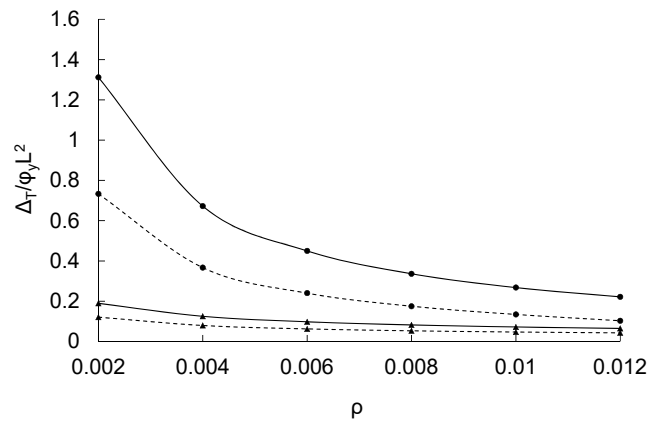
Figure 4.20 shows the effects of expanding the fixed ended beam results to include the two concentrated load case. Again, the deflections for this case are much larger, providing considerable warning of failure. In assessment, the case with a single concentrated load is the most severe, giving the least warning of failure, and requiring the most stringent assessment criteria. The case with two concentrated loads provides ample warning of impending failure due to large deflections.



(a) Simply supported



(b) Propped cantilever



(c) Fixed ends



Figure 4.19: Total normalized deflection of indeterminate beams at ULS

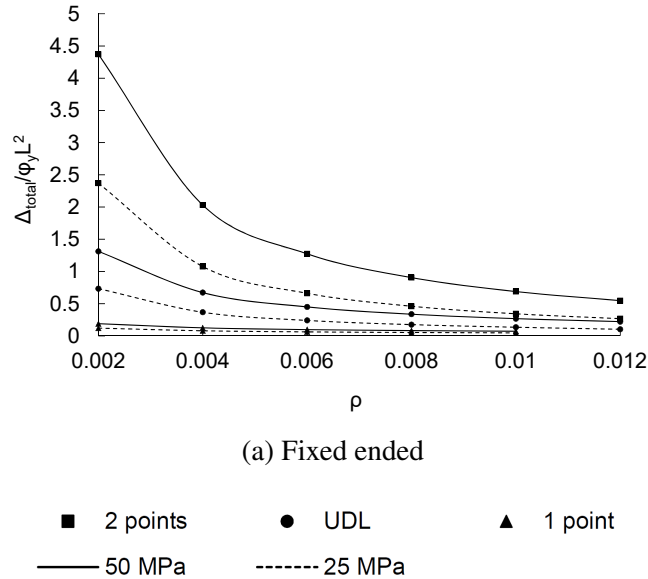


Figure 4.20: Total normalized deflection for a fixed ended beam

4.4 Definition of Warning Factor

In Chapter 3, a procedure to compute the aversion factor is presented. Practitioners can select occupant density, occupancy duration, and tributary area to determine the number of people that may be at risk if the element under consideration fails. Similarly, using information about cross section geometry, load configuration, and end conditions, the total normalized deflection at incipient failure, $\Delta_T/\varphi_y L^2$, can be predicted. From this prediction, warning factors may be determined using a known relationship between deflection and warning.

4.4.1 Deflection Coefficient

To move from $\Delta_T/\varphi_y L^2$ to a warning factor, it is helpful to consider the deflections in terms of the deflection-span ratio, Δ/L , which is conventionally used to specify acceptable deflection limits for Serviceability Limit States. It can also be conveniently used for the definition of

warning factor using deflection limits. A deflection coefficient, a , can be implemented, where

$$\frac{\Delta_T}{L} = a \frac{\Delta_T}{\varphi_y L^2} \quad (4.10)$$

so $a = \varphi_y L$. This will be defined for a given beam using dimensionless ratios, L/h , and d/h , and the normalized yield curvature, $\varphi_y d$, so that:

$$a = \varphi_y L = \frac{\varphi_y d}{d/h} (L/h) \quad (4.11)$$

Span to Depth Ratio, $\alpha = L/h$

This ratio is easily determined, either by field survey or drawing review, for an existing structural element. Beams and one-way slabs generally satisfy the limits specified in CAN/CSA A23.3-14 (2014) for deflection control shown in Table 4.4. These limits are essentially identical to those in ACI 318-14 (2014) for the range of end conditions considered and have remained unchanged since the 1970s (Cement Association of Canada, 2016).

Table 4.4: Minimum cross section depths, L/h , for deflection control from CAN/CSA A23.3-14 (2014)

Boundary Conditions	<i>L/h</i>	
	One-way Slabs	Beams
Simply Supported	20	16
Propped Cantilever	24	18
Fixed Ended	28	21
Cantilever	10	8

Yield Curvature, φ_y

Curvatures at yield, defined by Equation 4.4, can be determined for a beam given the effective depth, d , the reinforcement ratio, and the modular ratio. For the purposes of illustration, the following discussion will use a range of effective depths from 0.65h to 0.95h.

Deflection Coefficient, a

Figure 4.21 shows the variation of a for cross sections with $d = 0.95h$ for reinforcement ratios ranging from 0.002 to 0.012. The parameter a is most sensitive to $\alpha = L/h$, and slightly sensitive to ρ , while the effect of changing f'_c is relatively minimal. Higher concrete strengths correspond to smaller values of a , and are therefore associated with the smallest deflections that provide the least warning of failure. However, the presentation of deflection coefficients using the slightly larger values for 25 MPa concrete will be adopted to remain consistent with previous simplifications.

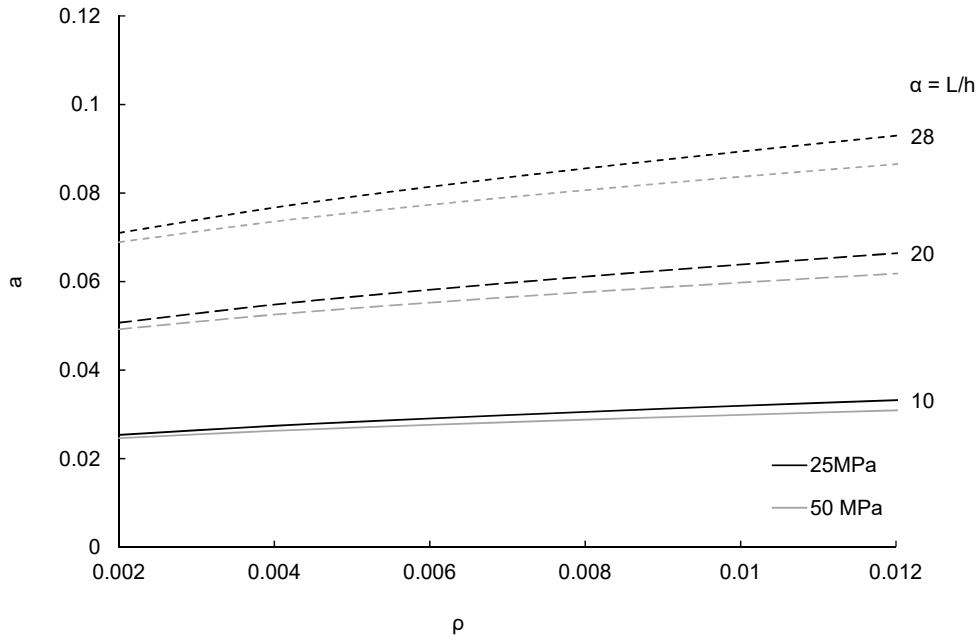


Figure 4.21: Variation of deflection coefficient, a , with concrete strength for cross sections with $d = 0.95h$

Figure 4.22 shows the range of a for slabs with α varying from 10 for cantilevers to 28 for fixed-ended slabs in accordance with Table 4.4, and with d/h ratios of 0.95 and 0.65, where f'_c is 25 MPa. The resulting multipliers are between 0.022 and 0.140 and can be applied to the previously computed $\Delta_T/\phi_y L^2$ magnitudes to give Δ/L ratios at ULS.

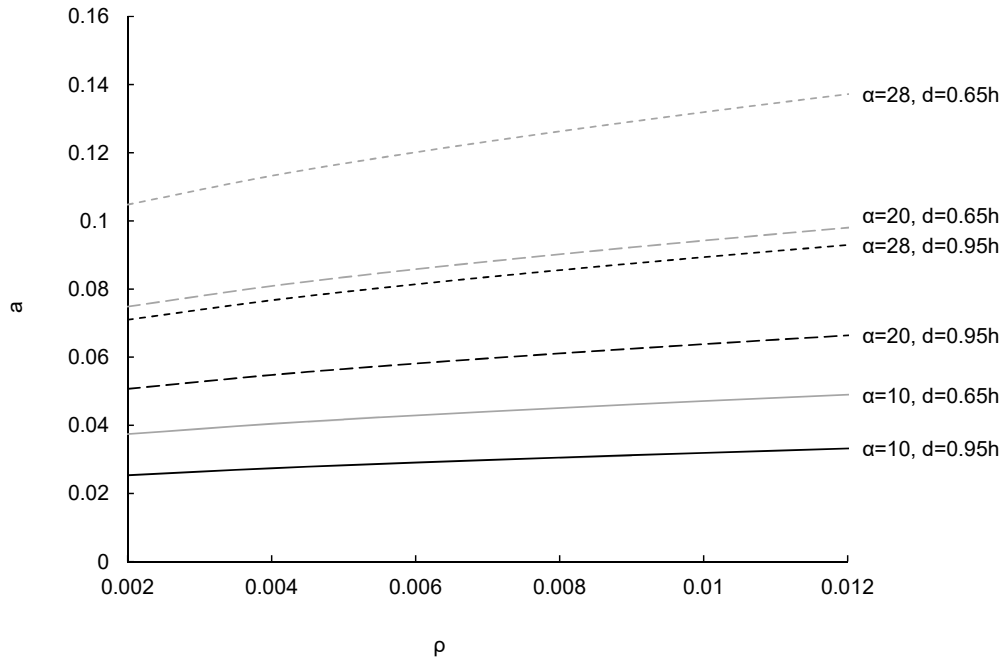
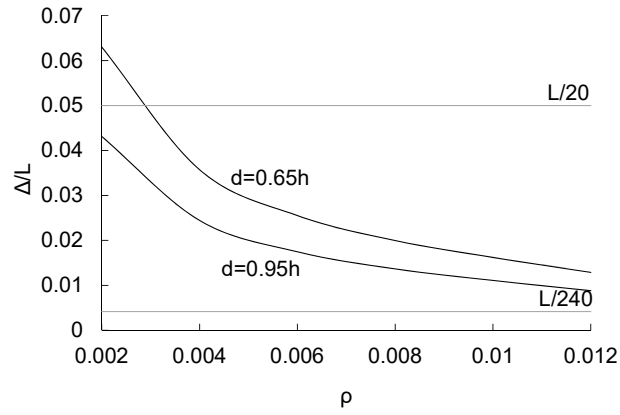


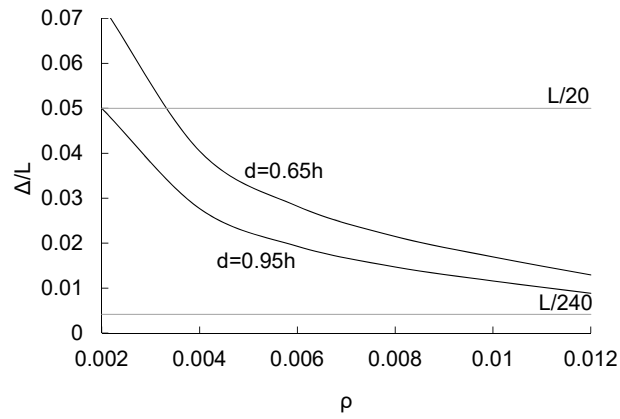
Figure 4.22: Deflection coefficient variation with reinforcement ratio, and length-to-depth ratio for $f'_c = 25$ MPa

Figure 4.23 shows the variation of deflection, Δ/L , with ρ for one-way slabs that just meet the L/h limit shown in Table 4.4. The largest deflections corresponds to the fixed-ended case, reaching a maximum of approximately 7.5% of the span length at $\rho = 0.002$, where the corresponding maximum for the simply supported case is approximately 6.3% of the span length. The commonly used SLS limit of $L/240$ is shown for reference, and all minimum deflections in this range of reinforcement ratio are well above this level. Comparing the values of α for each beam type, it is observed that the simply supported beam has a depth that is 40% greater than the fixed-ended beam, giving an uncracked moment of inertia that is 2.74 times larger. This creates a discrepancy between the values used for comparison.

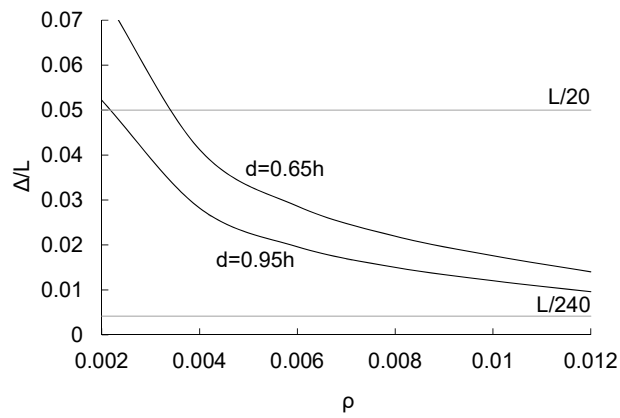
Figure 4.24 shows the variation of Δ/L with ρ , using $\alpha=20$ for all end conditions. The simply supported beam now gives the largest deflections, whereas in Figure 4.23, the largest deflections occur in fixed-ended beams. The maximum deflection for a simply supported beam is still approximately 6.3% of the span length, while the corresponding value for the fixed-ended



(a) Simply Supported, $\alpha=20$

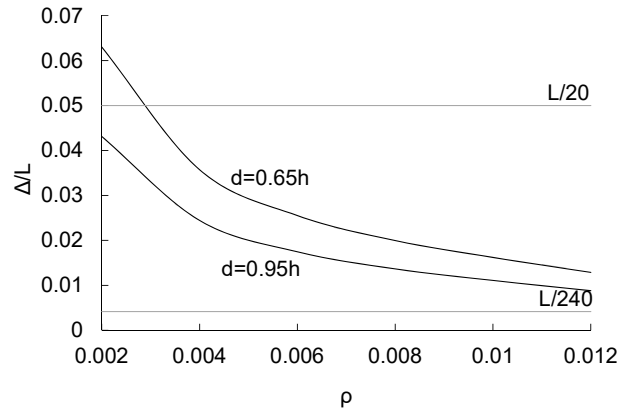


(b) Propped Cantilever, $\alpha=24$

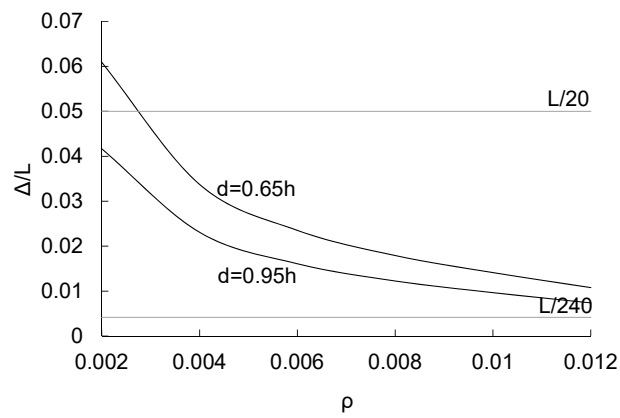


(c) Fixed-Ended, $\alpha=28$

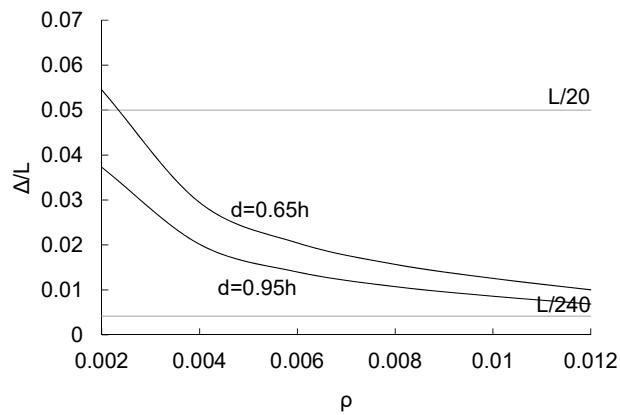
Figure 4.23: Deflection-length ratios



(a) Simply Supported



(b) Propped Cantilever



(c) Fixed-Ended

Figure 4.24: Deflection-length ratios for elements with $\alpha = 20$

beam is approximately 5.4%. The previous results are skewed by the tendency for elements to be designed with lower stiffness (smaller depth) where there is element-level stiffness provided by end fixity.

4.4.2 Warning Factor

Figure 4.25 shows a possible linear relationship between deflection and warning that gives a usable output for determining probability of failure. The exact form of this relationship may be the subject of further study, but for the purposes of this chapter, this simple correlation is sufficient. The key to this mapping is the identification of deflection limits that can provide warning of failure.

A deflection of magnitude $L/240$ at incipient failure is clearly insufficient to provide meaningful warning of failure because standards such as CAN/CSA A23.3-14 (2014) deem this deflection to be acceptable at Serviceability Limit States (SLS). Larger deflections become visible to occupants, and so provide warning. An arbitrary upper limit is $L/20$, or 5% of the span length, which is quite large. When this mapping is applied to the deflections from Figure 4.24, a continuous range of warning factors for use in the assessment procedure can be determined.

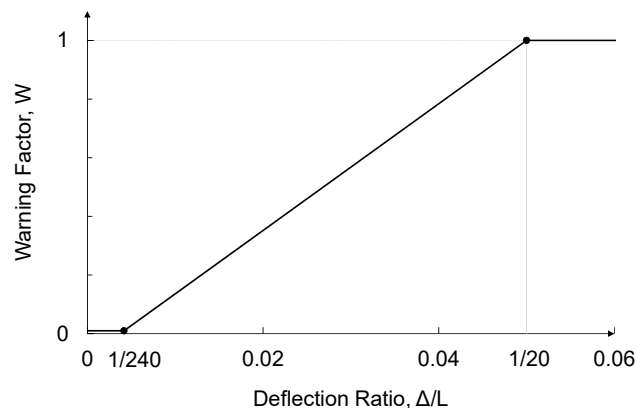


Figure 4.25: Definition of deflection limits for warning of failure

Figure 4.26 shows how the resulting warning factors vary for beams with a range of reinforcement ratios, effective depths, and end conditions. The end conditions considered (SS, PC, FE, and fixed-fixed) cause relatively little change in the associated warning factor. The typical magnitude of the difference in W between the fixed-ended case and the simply supported case is on the order of 0.1 across the range of reinforcement ratios. The effective depth, ranging from 65 to 95% of the cross section depth, gives changes in the warning factor of, on average, 0.17. This range of effective depths is quite large, and in reality, most cross sections will tend to fall in the higher end of this range, i.e. $d/h \geq 0.85$.

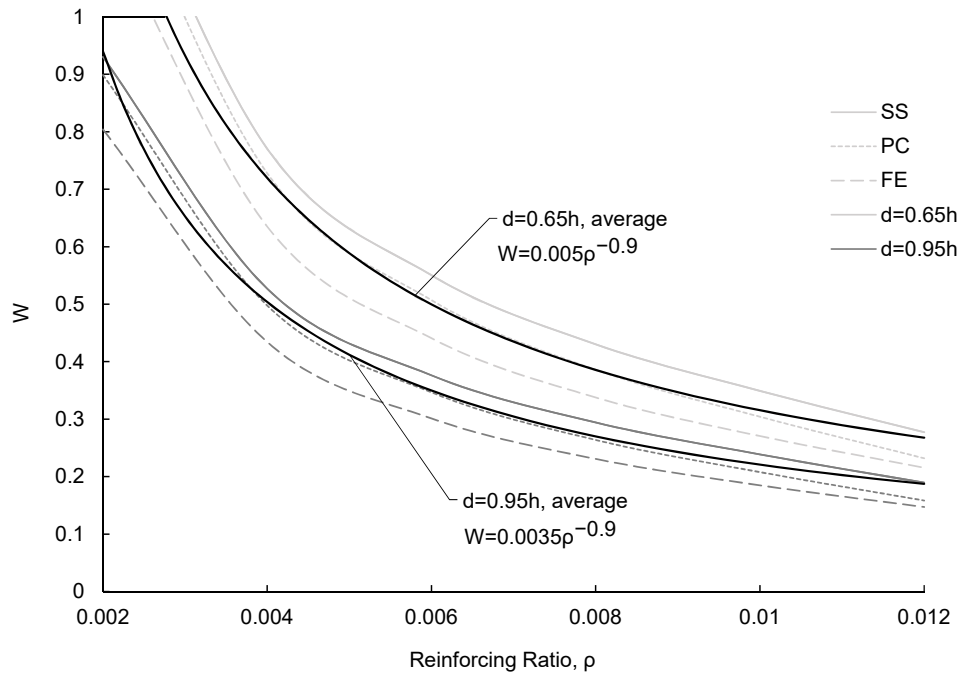


Figure 4.26: Warning factor for all end conditions, $\alpha = 20$

Given the magnitudes of the effects of these two factors on the overall results and the accuracy of the deflection-to-warning mapping, the simplification of these six curves to average curves for each d/L ratio is appropriate. The average curves shown in Figure 4.26 represent an aspect ratio, α or L/h , of 20. Since both d/h and α are linearly related to deflection magnitude (Eq. 4.10, 4.11), and therefore W , a general equation can be formulated for all values of d/h

and L/h so that,

$$W = 1.625 \times 10^{-4} \rho^{-0.9} \frac{L/h}{d/h} = 1.625 \times 10^{-4} \rho^{-0.9} \frac{L}{d} \leq 1.0 \quad (4.12)$$

Using this equation, the warning factor, W , can be estimated if the reinforcement ratio and dimensions are known.

4.5 Conclusions

In this chapter, the warning of failure provided by beams subjected to flexure has been studied under the influence of several convenient structural parameters. It was determined that deflection at incipient failure is the most useful measure of warning of failure. Both plastic and elastic deflections contribute to the total deflection at incipient failure.

The analysis considered variation of the reinforcement ratio, as well as the member length and depth. The cross-section variables impact deflection through the curvature ductility ratio, and shape factor. As the reinforcement ratio is increased, the deflection at incipient failure decreases and warning is reduced.

The effects of variations in the load configuration and end restraint conditions were also investigated. Three configurations of load— a UDL, a single concentrated load, or two concentrated loads— were investigated to determine their impact on ultimate deflections. The largest deflections occur for beams subjected to two concentrated loads, and the smallest for beams subjected to one concentrated load. Since most structural loads on reinforced concrete structures are idealized as uniformly distributed, the primary focus was on this configuration. Extreme cases for end restraint conditions are simply supported, and fixed ended. Results for elements with partial end fixity can be assumed to fall between these two.

The normalized ultimate deflections determined from these analyses were used to formulate a translation from Δ/L to W . Using a simple linear mapping, an equation for warning factor was developed, requiring the reinforcement ratio, span length and effective beam depth as

input. This proposed equation may be used in place of previous categorizations for warning of failure based on ductility and redundancy.

The major findings of this chapter are as follows:

1. The magnitudes of total deflections at incipient failure are a function of cross-section geometry, loading configuration, and end conditions. The consideration of plastic hinge formation is a key addition to the proposed procedure for determination of W .
2. Redundancy by itself is not necessarily an effective indicator of warning of failure. When measuring redundancy using the degree of indeterminacy, the results are not only inconsistent, but can also be misleading. For example, the differences between the deflections of simply supported beams and cantilevers are quite large.
3. Deflections at incipient failure challenge the conventional code assumption that increased redundancy enhances the warning of element failure. It has been shown that total deflection, and therefore warning of failure, decreases when additional degrees of indeterminacy are added to an element.
4. Plastic hinge length, which has previously not been identified as a factor in the determination of warning of failure, has been shown to contribute in a significant way to ultimate deflection magnitudes. Plastic hinge length is a function of load configuration and boundary conditions, as well as the shape factor associated with the cross section. Large deflections can be attributed to a combination of long plastic hinge lengths, and large shape factors due to low reinforcement ratios.
5. The warning factor, when linearly related to the magnitude of deflection at imminent failure, can be well represented without consideration of the specific end conditions of a flexural element. This does not negate the influence of end conditions altogether, but means that at the level of refinement of the current assessment procedure, its impact is minimal.

Chapter 5

Calibration Procedure for Assessment

5.1 Introduction

This chapter will synthesize the conclusions of the previous chapters to develop a procedure to quantify risk and calibrate strength reduction factors for improved structural assessment procedures. In Chapter 2, literature relating to assessment procedures and reliability were shown to have strong underlying bases, but are qualitative in nature. Chapters 3 and 4 outline improvements to the means of quantifying both aversion and warning factor, respectively, and therefore demonstrate that continuous, rationally derived factors are possible. Chapter 5 will integrate the full range of these and other new concepts into improved assessment procedures. The new definitions of n and W can be used to compute the target probabilities of failure and associated target reliability indices to be used for structural assessment.

5.2 Design Basis for Calibration

Target probabilities of failure are determined primarily by the values assigned for n and W , but are scaled using calibration factors. In CAN/CSA S6-14 (2014), the calibration factor, k , is set to 10^{-4} per year, based on Allen (1992). Similar implied calibration factors may be calculated using the annual probabilities of failure for a given set of conditions. In ASCE/SEI

7-15 (2015), lifetime target reliability indices and annual probabilities of failure are given for each of the occupancy classes and types of failure discussed, which are implicitly related to n and W , respectively. With assumed values for n and W based on the description of failure for a given reliability level, the associated k can be determined using Equation 5.1.

The following formulation for P_f is slightly modified from Equation 2.2 because warning factor in this thesis has been defined between zero (no warning) and 1.0 (considerable warning), which is opposite to the definition used in CSA S408-81 (1981) and CAN/CSA S6-14 (2014). Here, W is positively correlated to warning, so that higher values are associated with beneficial behaviours as failure approaches.

$$P_f = \frac{AkW}{\sqrt{n}} \quad (5.1)$$

or,

$$k = \frac{P_f \sqrt{n}}{WA}$$

Reliability targets from ASCE/SEI 7-15 (2015) will be used because they are clearly outlined for various types of structures, and state associated failure behaviours. Canadian codes such as CAN/CSA S6-14 (2014) discuss target reliability indices, but do not associate them with specific behaviours, making calibration to these targets more arbitrary.

Using the most stringent reliability targets ($\beta_{T,50} = 4.0$) in ASCE/SEI 7-15 (2015) for normal (Class II) occupancy, and an expected failure that is sudden and causes widespread damage, a baseline will be determined to use in the illustrative examples to follow. A sudden failure causing widespread damage indicates little warning, so let $W = 0.01$. Similarly, the large scale of the failure indicates a large number of people at risk, so let $n = 100$. The activity factor A is equal to 1.0 for buildings (Allen, 1992). These are equated with the target annual probability of failure, equal to 7.0×10^{-7} , giving a calibration factor, k , of 7.0×10^{-4} . This calibration factor can now be used to determine reliability indices and strength reduction factors for other combinations of W and n .

Selection of another design-basis from ASCE/SEI 7-15 (2015) may also be appropriate. Varying any of the initial inputs will change the magnitude of the calibration factor, and thus the resulting target probabilities of failure and strength reduction factors. For example, other normal occupancy buildings with less critical failure types give lifetime β_T values of 3.5, or $P_{f,1}$ of 5×10^{-6} , and 3.0, or $P_{f,1}$ of 3×10^{-5} (American Society of Civil Engineers, 2017). If these are associated with $n = 10$ and 1 and $W = 0.1$ and 1.0, respectively, the associated calibration factors are 1.58×10^{-4} and 3.00×10^{-5} .

Figure 5.1 shows the variation of target annual probability of failure with the assessment-stage W and n values, in the combined form, W/\sqrt{n} . The three curves illustrate the target probabilities of failure obtained from the use of the three design bases in ASCE/SEI 7-15 (2015).

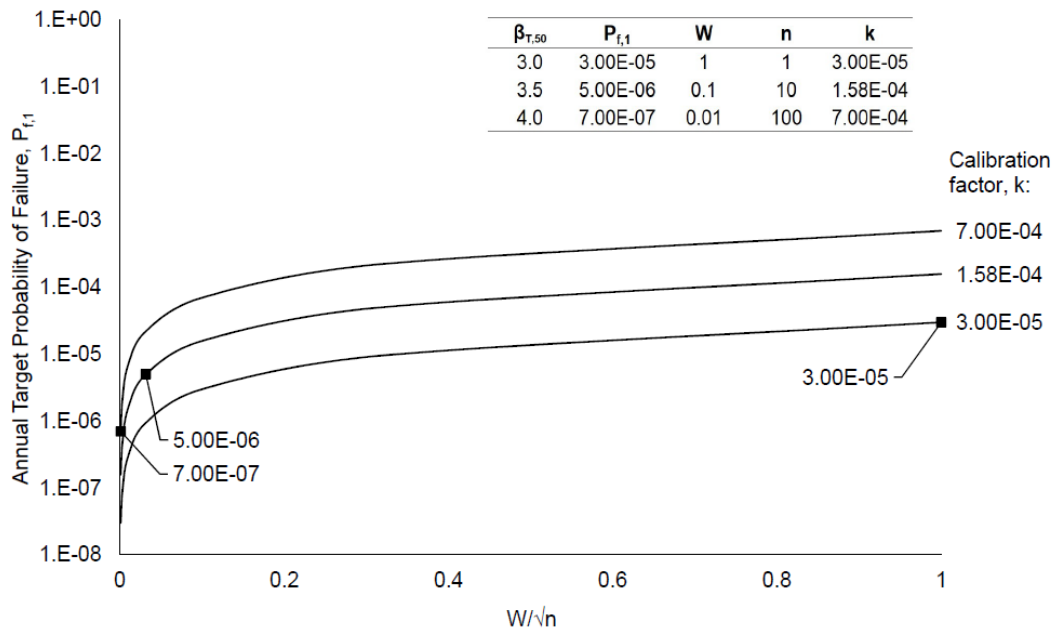


Figure 5.1: Target annual probability of failure variation with design basis and assessment parameters

The inset table shows the parameters assumed for each case. The marked calibration points indicate where the assessment-stage n and W are the same as those assumed for the design-basis condition. Using one of these three calibration factors, annual target probabilities of failure,

$P_{f,1}$, are easily determined. The following analysis will use k of 7.0×10^{-4} to calibrate target reliability indices for assessment, corresponding to a design-basis $P_{f,1}$ of 7.0×10^{-7} and conditions where failure is “sudden and results in wide spread progression of damage” (American Society of Civil Engineers, 2017). Any reliability targets determined by the proposed assessment procedure using this k will be more favourable, since the warning will be greater than or equal to 0.01 and the aversion factor will generally be less than or equal to 100. These more favourable conditions will give higher allowable target probabilities of failure and therefore lifetime target reliability indices lower than the 50-year design-basis value, 4.0.

5.3 Application to Assessment Procedure

Given both a warning factor, W , an aversion factor, n , and a calibration factor, k , the target probability of failure can be computed. From an annual probability of failure, the corresponding annual target reliability index, $\beta_{T,1}$, is also known, since

$$\beta_T = -\Phi^{-1}(P_f) \quad (5.2)$$

where Φ^{-1} is the inverse cumulative normal distribution function.

Figure 5.2 shows the annual target reliability indices associated with the probabilities of failure in Figure 5.1 for the calibration factor $k = 7 \times 10^{-4}$. The lowest annual target reliability index occurs when warning is high and aversion is low, or $W/\sqrt{n} = 1.0$. As warning and aversion factor conditions become less favourable, or approach zero, $\beta_{T,1}$ increases, approaching 5.0. The calibration point at $W/\sqrt{n} = 0.01/\sqrt{100} = 0.001$ gives an annual target reliability index of 4.8, which is consistent with a lifetime value, $\beta_{T,50}$, of 4.0.

Warning factor has been defined over a range from 0.01 to 1.0, representing elements with deflections at incipient failure from $L/240$ to $L/20$, respectively. Depending on the reinforcement ratio, span length, and effective depth, a flexural element can be assigned any value in

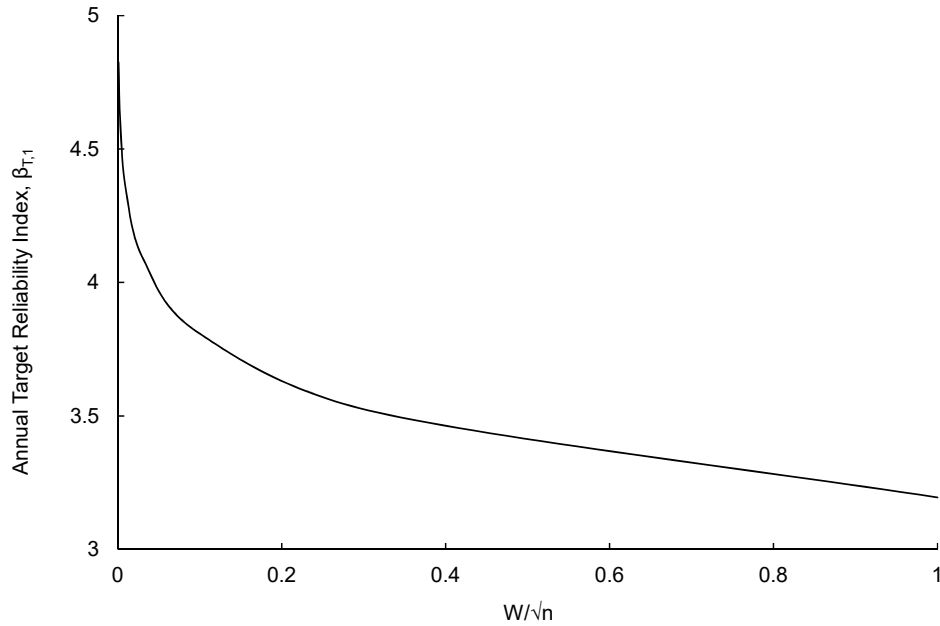


Figure 5.2: Target annual target reliability index variation with design basis and assessment parameters

this range. The values of W/\sqrt{n} therefore range from 0.01 to 1.0 for an aversion factor of 1.0, and approach zero as the aversion factor increases.

Strength reduction factors for assessment may be derived from known target reliability indices in accordance with Appendix B of CSA S408-11 (2011). Strength reduction factors, applied to the flexural capacity of the entire cross section, are determined by the following equation,

$$\phi = \delta_R \frac{\sum_i \alpha_i S_i}{\bar{S}} \ln \left(-\beta_T \sqrt{V_S^2 + V_R^2} \right) \quad (5.3)$$

where δ_R , V_R , and V_S are the bias coefficient for the resistance, and the coefficients of variation for the resistance and demand, respectively. The summation of factored load effects normalized by the average load effect, $\sum_i (\alpha_i S_i) / \bar{S}$, gives an approximate load factor for the total load effect. The target reliability index, β_T , whether annual or lifetime, selected according to W and n , sets the level of acceptable risk for the element. If an annual target probability is being con-

sidered, the associated statistical parameters must be defined on an annual basis. In particular, the live load parameters should be converted to represent a one-year return period.

Equation 5.3 accounts for the bias and variability of the demands and resistances, but does not account for the underlying distribution of each random variable. Higher-order reliability methods are available (i.e. Madsen, Krenk, and Lind, 1986) that do account for the underlying distribution. For the present study, Equation 5.3 is recommended in CSA S408-11 (2011) and so is suitable for this purpose.

Although in Canadian code documents, flexural resistance is a function of partial resistance factors for both concrete and reinforcing steel, ϕ_c and ϕ_s , the steel behaviour governs in flexure and modification of the single factor ϕ_s is appropriate. For other load effects such as axial or shear force, calibration using both ϕ_c and ϕ_s is necessary.

Table 5.1 outlines the statistical data for this analysis. Bartlett, Hong, and Zhou (2003) give the bias coefficients and coefficients of variation for both load effects and resistances to be used for analysis. The live load is assumed to follow an Extreme Value (Type I) or Gumbel distribution so its parameters can be transformed, using the log-shift principle, from a 50-year lifetime value to an annual value (Bartlett, Hong, & Zhou, 2003). The resulting annual live load distribution is Extreme Value (Type I) but this is ignored when using Equation 5.3. The bias coefficient and coefficient of variation for the resistance have been modified by applying a professional factor as suggested in Nowak and Szerszen (2003) to account for differences in the actual section capacity and that obtained by analysis.

The coefficient of variation for the demand, V_S , depends on the dead load fraction, γ , being investigated. In general,

$$V_S = \frac{\sigma_S}{\bar{D} + \bar{L}} = \frac{\sqrt{V_D^2 \delta_D^2 \gamma^2 + V_L^2 \delta_L^2 (1 - \gamma)^2}}{\delta_D \gamma + \delta_L (1 - \gamma)} \quad (5.4)$$

where the dead load fraction is $\gamma = D/(D + L)$, and therefore $L = D(1 - \gamma)/\gamma$. The bias coefficients and coefficients of variation for live and dead loads are δ_L , δ_D , V_L , and V_D , respectively.

Table 5.1: Statistical parameters for loads and resistances in Bartlett, Hong, and Zhou, 2003

Load	Bias Coefficient, δ_R	Coefficient of Variation, V	Distribution
Live Load (50 year)	0.9	0.17	Gumbel
Transform to load effect	1.0	0.206	Normal
Live Load (1 year, transformed)	0.433	0.409	\sim Normal
Dead Load	1.05	0.1	Normal
Resistance			
Professional Factor, P	1.02	0.06	Normal
Reinforcing Steel	1.17	0.108	Normal
Resistance ($R_n P$)	1.19	0.124	Normal

The range of V_S for one-year live loads is 0.097 to 0.409, and for 50-year live loads, 0.094 to 0.267. The coefficient of variation tends to decrease with increasing γ , but begins to increase again when the critical load combination changes from 1.25D+1.5L to 1.4D at $\gamma=0.91$.

Figure 5.3 shows the strength reduction factor for assessment, ϕ_a , as a function of the dead load fraction, γ , or the nominal dead load divided by the total load. After determining an annual target reliability index, $\beta_{T,1}$, an appropriate strength reduction factor can be selected for the given dead load fraction.

Strength reduction factors can vary quite markedly with both $\beta_{T,1}$ and γ . When the annual target reliability index is less than or equal to three, the strength reduction factors are typically greater than 1.0, and so increase the factored flexural resistance from its nominal value. This may seem counterintuitive but, as shown in Table 5.1, the bias coefficient is 1.19, which implies that the mean resistance is 19% greater than the nominal resistance. Further, the load factors, α_i , in Equation 5.3 are greater than 1.0 and do not vary with β_T . The change in reliability must therefore be achieved by varying the resistance factor only, which is why the variation shown in Figure 5.3 is so large. Where $\beta_{T,1}$ is greater than 3.0, ϕ_a can range from 0.5 to 1.15. Generally, lower target reliabilities can be associated with large values of ϕ , and therefore have factored flexural resistances larger than the nominal flexural strength. Conversely, high target reliabilities are associated with small increases, and sometimes notable decreases in the design

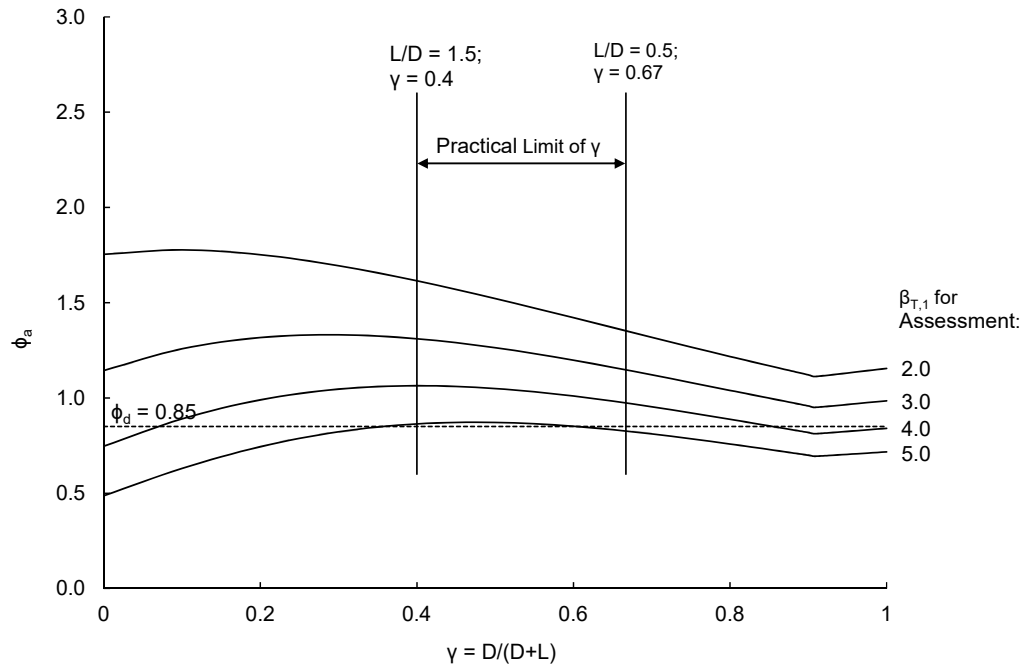


Figure 5.3: Strength reduction factor variation with load fraction

resistance from the nominal value. This is particularly visible where the dead load fraction is low, and the live load, which is more highly variable, contributes more to the overall variability of the loading.

The large range in ϕ_a can be limited by the practical range of γ as shown in Figure 5.3. If the range of live loads varies from 50% to 150% of the dead load, the corresponding γ range is from 0.67 to 0.4. While the full range of ϕ is 0.5 to 2.7, a more practical range is from 0.82 to 1.61.

The effects of using these ϕ_a factors on the flexural capacity of the structure can be illustrated by comparing the suggested strength reduction factors for assessment, ϕ_a , with those used for design, ϕ_d . In CAN/CSA A23.3-14 (2014), the strength reduction factor used for reinforcing steel in the design stage, ϕ_d , is 0.85. This will be used to normalize the ϕ_a values from Figure 5.3. Figure 5.4 shows the ratio ϕ_a/ϕ_d over the full range of γ . Again considering the practical range of dead load ratios, the resulting assessment capacities from the use of ϕ_a fall between 0.97 to 1.9 of the design-stage capacities.

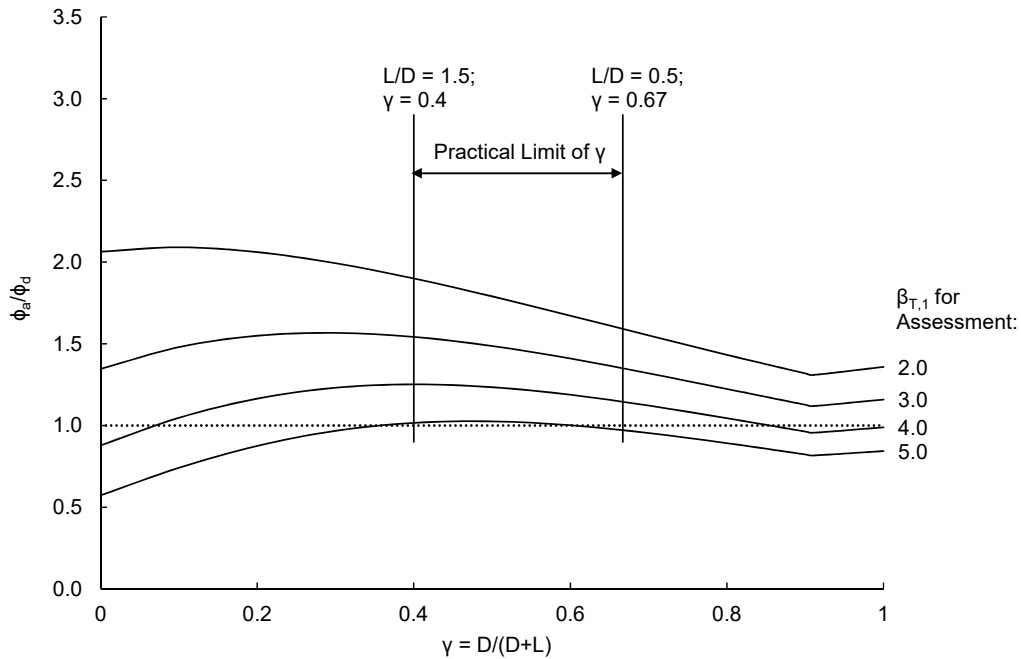


Figure 5.4: Normalized strength reduction factor variation with load fraction

When reliability targets are low, for example $\beta_{T,1} = 2.0$, the flexural capacity can increase by 60 to 90% of the factored value used for design. Meanwhile, for higher reliability targets, where $\beta_{T,1} = 5.0$, the flexural capacity in the assessment stage will be 97 to 102% of the values given by design provisions.

5.3.1 Effects of n and W on Target Reliability Indices

Applying the ranges of n and W from Figures 3.2 and Equation 4.12 to the computation of P_f and subsequently $\beta_{T,1}$ yields a wide range of annual target reliability indices. The resulting extreme values of these reliability targets are shown in Table 5.2. For a calibration factor equal to 7.0×10^{-4} , $\beta_{T,1}$ can fall between 3.19 and 4.83. The variations associated with an order of magnitude change in W are much larger than an equal change in n because P_f is proportional to W and inversely proportional to \sqrt{n} . Each parameter has a range that spans two orders of magnitude. The changes in $\beta_{T,1}$ associated with this W variation are 1.15 and 1.02, while the

changes due to the n variation are approximately half as large, or 0.61 and 0.48.

Table 5.2: Extreme values of annual target reliability index for $k = 7.0 \times 10^{-4}$

	$\beta_{T,1}$	n		$\Delta\beta_{T,1}$
		1	100	
W	1	3.19	3.81	0.61
	0.01	4.34	4.83	0.48
$\Delta\beta_{T,1}$		1.15	1.02	

Table 5.3 shows annual target reliability indices that illustrate the less dramatic effects of using a smaller calibration factor, k , on the reliability targets over the lifetime of a structure.

Table 5.3: Extreme values of annual target reliability index for $k = 3.0 \times 10^{-5}$

	$\beta_{T,1}$	n		$\Delta\beta_{T,1}$
		1	100	
W	1	4.01	4.53	0.51
	0.01	4.99	5.42	0.43
$\Delta\beta_{T,1}$		0.98	0.89	

5.3.2 Effects of Statistical Parameters on ϕ_a

The sensitivity of ϕ_a to the selection of statistical parameters can be observed in Figure 5.5. For each parameter shown in Table 5.1, maximum and minimum values for sensitivity analysis were set at a 25% greater than or 25% less than the value reported in literature, respectively. The values shown are for $\beta_{T,1} = 3.0$.

Overall, changing the statistical parameters can have notable impacts on ϕ_a . Specifically, increasing the bias coefficient for resistance causes an increase in ϕ_a , which results in larger flexural resistances. The variations in ϕ_a are relatively uniform over the entire range of gamma. This is expected, because in Equation 5.3, ϕ is proportional to δ_R . Similarly, the variation of ϕ_a with changes in the coefficient of variation for resistance and is relatively uniform over the

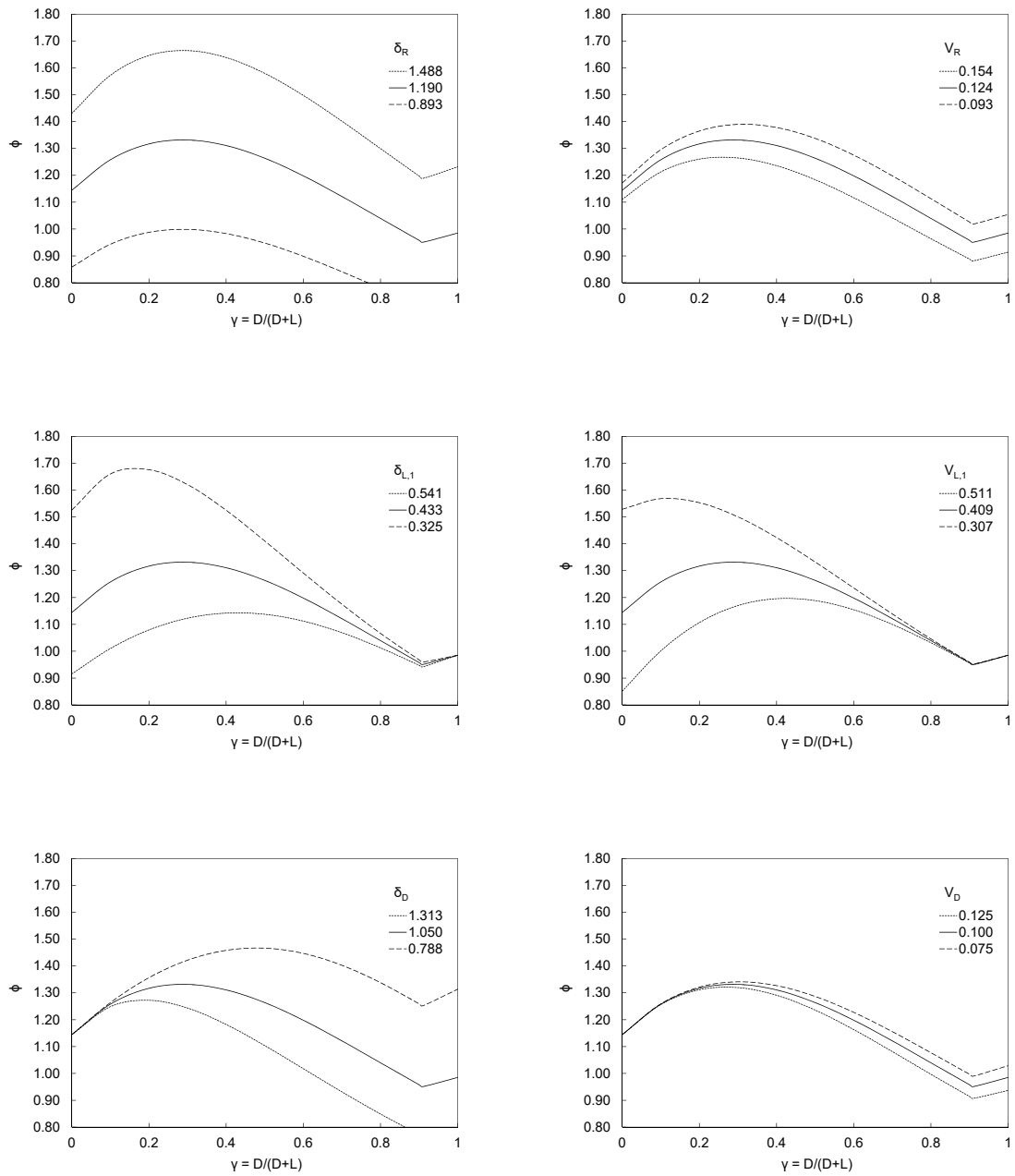


Figure 5.5: Variation of strength reduction factor using alternate statistical parameters

range of γ . The overall impact of a 25% increase or decrease in V_R is much less than that for a 25% change of the bias coefficient.

Increasing the bias coefficient for either dead or live load causes a reduction in the ϕ_a factor, resulting in smaller factored flexural resistances. The effects of the respective bias coefficients are most notable when the load associated with the varied bias coefficient constitutes most of the total load. For example, the ϕ_a results are most sensitive to variations in live load bias coefficient when γ is small, or the load is comprised largely of live load, and vice versa.

The coefficient of variation for live load can cause large variations in ϕ_a , but only in the region where live loads are considerable, or γ is less than approximately 0.5. The coefficient of variation for dead loads are similarly notable only in areas where dead loads are large, but the scale of the changes is much smaller.

5.3.3 Lifetime Reliability Indices

Figure 5.6 shows the lifetime equivalent $\beta_{T,50}$ values for the strength reduction factors in Figure 5.3. These lifetime reliability indices can be compared directly with the target reliability indices used for design. For example, ASCE/SEI 7-15 (2015) uses $\beta_{T,50}$ for design between 3.0 and 4.0 for a normal-occupancy structure, while the range may expand to include values from 2.5 to 4.5 for structures in other occupancy categories. Similarly, CSA S408-11 (2011) gives lifetime target reliabilities of from 2.5 to 4.0 for gradual failures, and from 3.0 to 4.5 for sudden failures. These cover structures in safety classes from “not serious” to “very serious”.

Higher lifetime target reliability indices are necessary when the loading is primarily dead, which has a higher bias coefficient than live load, or primarily live, which is much more variable than dead load. Dead loads are often assumed not to vary in time. This means that $\beta_{T,50}$ and $\beta_{T,1}$ are equal when only dead loads are present, $\gamma=1.0$. The smallest lifetime target reliability indices occur in the range from $\gamma=0.2$ to 0.45 where both dead and live loads contribute meaningfully to the total. The target lifetime reliability index begins to increase in the lower γ region where the coefficient of variation for live loads becomes increasingly influential.

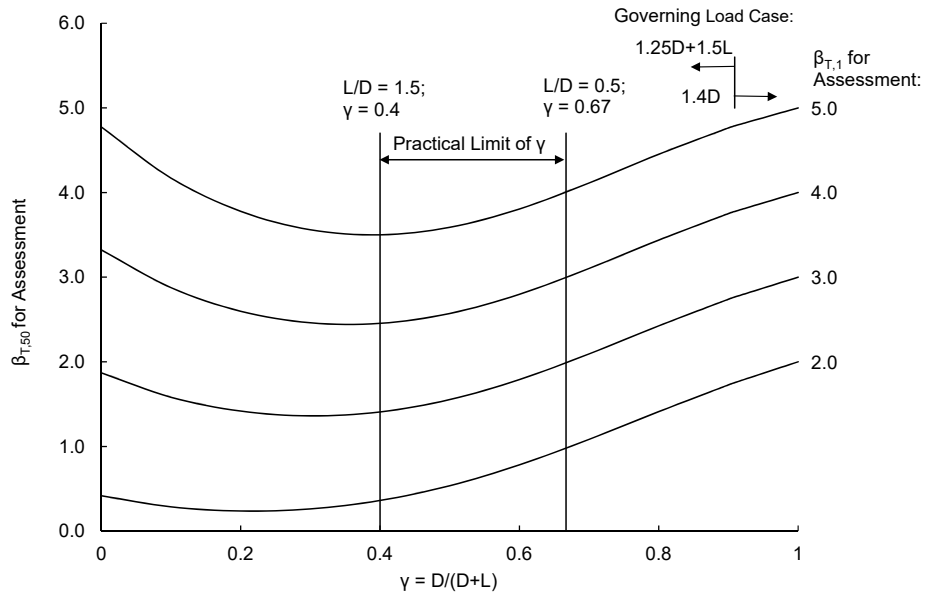


Figure 5.6: Lifetime (50-year) target reliability indices

Converting the target reliability indices in Tables 5.2 and 5.3 to lifetime values using Figure 5.6 yields results in the general range of those used for design, approximately 2.5 to 4.5 (American Society of Civil Engineers, 2017, 2017). This means that the results achieved by the proposed changes are in the range of lifetime reliability indices that are commonly accepted for structural design.

5.4 Draft Code Procedure

A general procedure can be proposed for adoption in codes for the assessment of concrete structures based on the previous illustration. The input parameters include:

- occupant density, occupancy type, duration factor, tributary area;
- reinforcing ratio, cross section geometry, concrete strength, load configuration, boundary conditions

Aversion Factor, n :

1. Obtain occupant density (occupants/m²) based on occupancy type, examples in Table 3.2.
2. Obtain duration factor from Table 3.2 or based on building study.
3. Compute weighted density, $\rho_w = \rho d$, or select directly from Table 3.2.
4. Compute tributary area of element.
5. Compute appropriate LLRF based on A_T and occupancy type from Equation 3.2 or 3.3.
6. Compute n from Equation 3.5.

Warning Factor, W :

1. Identify reinforcing ratio, ρ .
2. Identify span length, L , and effective depth, d , from field measurements, as-built drawings, or non-destructive testing.
3. Compute applied (dead and live) loads as per NBCC (2015) and dead load ratio $\gamma = D/(D + L)$.
4. Compute warning factor, W , from Equation 4.12.

When n and W are known, the following steps can be taken to determine the appropriate strength reduction factor for structural assessment of a flexural element:

1. Using n and W from above, compute W/\sqrt{n} .
2. Determine value of $\beta_{T,1}$ corresponding to W/\sqrt{n} from Figure 5.2 or Equation 5.1.
3. Use $\beta_{T,1}$ and γ (determined previously) to determine ϕ_a from Figure 5.3.
4. Compute the flexural capacity for assessment, $M_{r,a}$, of the cross section using ϕ_a :

$$M_{r,a} = \phi_a f_y A_s \left(d - \frac{\phi_a A_s f_y}{\phi_c \alpha_1 \lambda f'_c b} \right) \quad (5.5)$$

where ϕ_c is the strength reduction factor for concrete from design provisions, or 0.65 as per CAN/CSA A23.3-14 (2014).

5. Compute factored moment, M_f , in accordance with NBCC (2015).
6. Compare $M_{r,a}$ to M_f to determine if action required.

$$\begin{aligned} M_{r,a} &\geq M_f && \text{Acceptable} \\ M_{r,a} &< M_f && \text{Unacceptable, action required} \end{aligned}$$

5.5 Conclusions

In this chapter, the basis of current design was used to calibrate the assessment procedure to achieve reliability levels that are consistent with those in current design codes. Using a calibration factor, k of 7.0×10^{-4} , the effects of W and n on the target reliability indices for design, as well as the resulting strength reduction factors for assessment, were observed.

Conversion of annual to lifetime target reliability indices was used as a means of comparing the proposed assessment procedure to the reliability index range expected for structures.

The major findings of this chapter are as follows:

1. Warning factor, W , has the most direct impact on assessment outcomes, but aversion factor, n , is important and can also contribute meaningfully. For an equivalent order of magnitude change in W or n , the change in β_T is approximately half as large when changing n than when changing W .
2. Calibration of the assessment framework outlined here gives reliability targets that are in line with accepted reliability-based codes. The possibility of increasing ϕ for assessment has the potential to improve assessment outcomes, while maintaining appropriate reliability levels. For a calibration factor of 7.0×10^{-4} , the resulting lifetime target reliability indices are between 3.2 and 4.8.

3. In most cases, the proposed changes to the assessment procedures lead to increases in the factored flexural capacity when comparing to the values used in design. The overall range of ϕ_a within a practical range of dead load ratio ($\gamma=0.4$ to 0.67) is approximately 0.8 to 1.6, so generally greater than the value used for design, $\phi_s = 0.85$.

Chapter 6

Conclusions and Recommendations

6.1 Summary

The main goal of this thesis is to enhance reliability-based structural assessment provisions in Canada and the United States by identifying parameters that accurately quantify the probability of structural failure. Significant costs are associated with the repair or replacement of a structure, so rational bases for connecting structural risk to measurable structural parameters can have cost benefits in addition to safety benefits.

Current and historical structural risk assessment methods were compared to determine common metrics. The primary means of classifying structural risk, risk aversion and warning of failure, are often defined qualitatively rather than quantitatively. Risk aversion includes a range of factors, including the type of occupancy and the number of people expected to be impacted by a structural failure. Warning of failure, defined further in terms of ductility and redundancy, addresses the type of structural behaviour expected at failure and therefore the likelihood that occupants could recognize and respond to an incipient failure. Risk aversion and warning of failure can define a target probability of failure and overall level of acceptable risk using a calibration factor.

The analysis of risk aversion in Chapter 3 led to the formulation of an aversion factor, n , which is essentially the number of people that would be harmed by the failure of an element. The aversion factor is a function of the occupancy type of the area supported by the element, as well as the tributary area. Existing data regarding occupant density and occupancy duration were aggregated and used to suggest applicable weighted occupant densities for the determination of n . Reduction of the number of people at risk can be justified by the tributary area reductions allowed for live loads in new design. Live load reductions decreased the number of people at risk in some cases by up to 60%.

In Chapter 4 the analysis of warning of failure yielded a set of metrics to determine the warning factor, W . Curvature ductility ratio provides the basis for quantifying ductility in cross sections of flexural elements, where the curvature at first yield can be compared to that at incipient failure. Curvature ductility is a property of the cross section determined primarily by the reinforcement ratio. The total deflection at incipient failure includes plastic deflections due to hinge formation, which contribute positively to the perceptible warning of failure and therefore should be included in assessment provisions. The deflections at incipient failure are dependent on the configuration of loading applied to the element, as well as the end restraint conditions. These affect the location and length of plastic hinges as well as the elastic deflection profile, neither of which are explicitly considered in current assessment provisions. The warning factor is then assumed to be proportional to the magnitude of total deflection and can be well approximated as a simple function defined by reinforcement ratio, span length, and effective depth.

The target probability of failure for assessment is determined from the computed values of n and W , using a calibration factor, k , determined using reliability parameters from design provisions. For each combination of n and W , a strength reduction factor, ϕ_a , for calculating the assessment-stage moment capacity may be determined. This provides the basis upon which repair or replacement decisions can be made for the structure.

6.2 Conclusions

The following primary conclusions have been reached with regard to the quantification of the target probability of failure and the corresponding assessment provisions:

1. In current assessment codes and standards, aversion and warning factors are often described qualitatively and quantified using a set of discrete values. It would be preferred that both be defined as continuous functions of measurable parameters.
2. Aversion and warning, two primary factors used to define target reliability levels, are widely used in assessment codes, and are appropriate factors to define suitable reliability targets.
3. The metrics currently used to identify target levels of reliability to assess existing structures can more accurately reflect structural conditions by applying readily available principles, data, and structural parameters to the calculation procedure. This allows target reliabilities to be defined using a continuous numerical scale rather than the existing judgment-based classification of structural behaviour, and ensures greater consistency in the application of reliability methods for assessment.
4. Social aversion to risk is directly related to the number of people affected by a structural failure. Tributary-area-based live load reduction, allowed for new design based on the notion that full occupation of large areas is unlikely at any given time, is a valid basis for quantifying the number of people at risk. This number can be reduced according to the live load reduction schemes in NBCC (2015) or ASCE/SEI 7-15 (2015), bringing assessment procedures in line with the rationale used for structural design.
5. The number of people present in the tributary of a structural element can be computed using occupant density. Data from literature regarding occupant density comes from a range of intended uses, and should not be viewed as prescriptive or fully representative of real structural occupancies.

6. Warning factors in current code documents are assigned based on a description of the expected failure mode and the extent of its effects on the structure as a whole.
7. Warning factor should quantitatively account for the visibility of an incipient failure. It is dependent on the flexural reinforcement ratio in the cross section, the configuration of applied loading, and the end restraint conditions of the element. The reinforcement ratio is the primary influencing parameter for, and for a given concrete and steel strength is inversely proportional to, the total deflection expected at incipient failure.
8. A simple formulation for W can be created using the reinforcement ratio, the span length, and the section depth. Concrete strength, and end restraint conditions do affect the deflection at incipient failure, and so on the warning factor, but their influences are relatively small and have therefore been removed from the proposed warning of failure definition.
9. Loading configuration is an important consideration when determining the magnitude of plastic deflection. In previous formulations for warning factor, this has not been accounted for, but can be critical, especially in high shear locations where concentrated loads are applied to flexural elements. Only uniformly distributed loads have been used for illustration in this thesis, with the understanding that this is not a valid assumption in all cases.
10. Computing target probabilities of failure for structural assessment using n and W is dependent on calibration factors that are consistent with those used for design. The calibration of assessment methods to the current reliability levels used for design are based on interpretation of the code language and the application of newly defined W and n to the structural conditions described. The definition of acceptable probabilities of failure and the corresponding structural conditions are loosely implied in ASCE/SEI 7-15 (2015), but are otherwise unclear.

11. The ϕ factors associated with the new n and W values generally cause the flexural capacity for assessment to be greater than those used for design. In contrast to assessment codes such as NBCC Commentary L (2015) where load factors for assessment are varied in accordance with target reliability levels, these strength reduction factors are intended to be used alongside the load factors for design.

6.3 Recommendations and Future Work

It is recommended that the above results be integrated into code provisions for the assessment of reinforced concrete structures. In NBCC Commentary L (2015), this transition can be relatively smooth, since its procedures for determining the target reliability levels for assessment closely parallel those presented in this work. Changing the current procedure to align with the provisions discussed in Section 5.4 will require that the assessment procedures no longer achieve target reliability levels by changing the factored load combinations, but rather use design load combinations alongside a revised strength reduction factor.

In documents such as ACI 562-16 (2016), the transition to a reliability-based assessment method of this form will require a more thorough change in the code provisions. The end result will still be the computation of a strength reduction factor for determining the assessment capacity of an element, but the steps used to obtain it will be more involved. Rather than the current assignment of ϕ factors based on the type of element or critical failure mode, the selection of ϕ will be based on the results of a basic structural investigation.

With these goals in mind, suggestions for future work emerge in two main areas: the application of these concepts to a wider range of elements and load effects, and the refinement of aversion and warning factor parameters.

To create widely applicable procedures for structural assessment, a wide array of element types and load effects should be addressed. The following steps are suggested for future expansion in this area:

1. Address failure types that are typically considered brittle, such as shear and axial load dominated failures, the inclusion of warning of failure parameters may need to be formulated using alternate metrics. The expansion of warning of failure concepts for column assessment has been partially addressed in van Weerdhuizen and Bartlett (2018) for columns with low axial loads. Further research in column reliability assessment should include the consideration of axial loads beyond the balanced failure point in the column. In these cases, curvature ductility in a column will not be an effective or visible measure. Brittle elements require the development of alternate visible means by which to observe an approaching failure condition.
2. Calibrate material-specific strength reduction factors corresponding to load effects that are sensitive to both concrete and steel material strengths.
3. Use higher-order reliability methods (e.g. Madsen et al., 1986) to more accurately represent the distributions of applied loads and material properties.

The parameters that are used as metrics to describe risk aversion and warning of failure have been largely redefined, but refinement of the parameters through reliability-focused studies is needed. The following are areas of improvement that would address some of the assumptions made about available data in the proposed assessment procedures:

1. Study the occupant density and duration for the occupancy types outlined in structural codes to provide a more consistent basis upon which aversion factors can be determined. The values used should be the result of a focused investigation for structural reliability, rather than be interpreted from provisions created for other purposes.
2. Define the influence of loading configuration on warning of failure more fully. Due to scope limitations in this thesis, the most common configuration for reinforced concrete structures was assumed to be uniformly distributed loading. The results presented do not outline the effects of concentrated loading on warning of failure and the resulting assessment provisions. The presence of concentrated loads, especially a single concentrated

load, can greatly decrease the length of the plastic hinging region, and therefore the total deflection expected at incipient failure and warning of failure.

3. Redefine the relationship between warning of failure and the deflections at incipient failure. Both the deflection limits that can provide warning and the form of the relationship can be improved through further empirical study.

References

- ACI Committee 318. (2014). *Building Code Requirements for Structural Concrete (ACI 318-14) and Commentary (ACI 318R-14)*. Farmington Hills, MI: American Concrete Institute.
- ACI Committee 562. (2016). *Code Requirements for Assessment, Repair, and Rehabilitation of Existing Concrete Structures (ACI 562-16) and Commentary*. Farmington Hills, MI: American Concrete Institute.
- Aggarwal, K. K. (1993). *Reliability Engineering*. Norwell, MA: Kluwer Academic Publishers.
- Allen, D. E. (1991). Limit states criteria for structural evaluation of existing buildings. *Canadian Journal of Civil Engineering*, (18), 995–1004.
- Allen, D. E. (1992). Canadian highway bridge evaluation: reliability index. *Canadian Journal of Civil Engineering*, (19), 987–991.
- American Society of Civil Engineers. (2017). *Minimum Design Loads For Buildings and Other Structures (ASCE 7-16)*. Reston, VA: American Society of Civil Engineers.
- American Society of Heating, Refrigerating and Air-Conditioning Engineers. (2016). *ANSI/ASHRAE Standard 62.1-2016 Ventilation for Acceptable Indoor Air Quality*. Atlanta, GA: American Society of Heating, Refrigerating and Air-Conditioning Engineers.
- Bartlett, F. M., Hong, H. P., & Zhou, W. (2003). Load factor calibration for the proposed 2005 edition of the National Building Code of Canada: Statistics of loads and load effects. *Canadian Journal of Civil Engineering*, (30), 429–439.

- Bentz, E., & Collins, M. P. (2001). *Response-2000 Shell-2000 Triax-2000 Membrane-2000 User Manual*. Toronto, ON: University of Toronto.
- Canadian Standards Association. (1981). *CAN/CSA S408-81 Guideline for the development of limit states design*. Rexdale, ON: Canadian Standards Association.
- Canadian Standards Association. (2011). *CAN/CSA S408-11 Guideline for the development of limit states design standards*. Mississauga, ON: Canadian Standards Association.
- Canadian Standards Association. (2014a). *CSA A23.3-14 Design of Concrete Structures*. Mississauga, ON: Canadian Standards Association.
- Canadian Standards Association. (2014b). *CSA S6-14 – Canadian Highway Bridge Design Code*. Mississauga, ON: Canadian Standards Association.
- Cement Association of Canada. (2016). *Concrete Design Handbook 4th Edition*. Ottawa, ON: Cement Association of Canada.
- Cohn, M. Z. (1965). Why nonlinear analysis and design? *American Concrete Institute Special Publication, SP-12*, 591–593.
- Cohn, M. Z. (1972). *Analysis and Design of Inelastic Structures, Volume 2: Problems*. Waterloo, ON: University of Waterloo Press.
- Construction Industry Research and Information Association. (1977). *Rationalisation of safety and serviceability factors in structural codes*. London, UK: Construction Industry Research and Information Association.
- Ditlevsen, O., & Madsen, H. O. (1996). *Structural Reliability Methods*. West Sussex, England: John Wiley & Sons.
- Leet, K. M., Uang, C.-M., & Gilbert, A. M. (2011). *Fundamentals of Structural Analysis (4th)*. New York, NY: McGraw-Hill.
- Madsen, H. O., Krenk, S., & Lind, N. C. (1986). *Methods of Structural Safety*. Englewood Cliffs, NJ: Prentice-Hall.
- Mast, R. F. (1992). Unified Design Provisions for Reinforced and Prestressed Concrete Flexural and Compression Members. *ACI Structural Journal*, (89), 185–199.

- National Research Council of Canada. (2015a). *National Building Code of Canada*. Ottawa, ON: National Research Council of Canada.
- National Research Council of Canada. (2015b). *National Fire Code of Canada*. Ottawa, ON: National Research Council of Canada.
- National Research Council of Canada. (2015c). *Structural Commentaries (User's Guide – NBC 2015: Part 4 of Division B)*. Ottawa, ON: National Research Council of Canada.
- Nowak, A. S., & Szerszen, M. M. (2003). Calibration of Design Code for Buildings (ACI 318): Part 1— Statistical Models for Resistance. *ACI Structural Journal*, *100*(3), 377–382.
- Ontario Ministry of Municipal Affairs and Housing. (2012). Ontario Building Code. O Reg. 332/12, s.4.1.2. Toronto, ON: Queen's Printer for Ontario.
- van Weerdhuizen, M., & Bartlett, F. M. (2018). Curvature Ductility of Concrete Columns with Low Axial Loads. In *Proc. CSCE 2018 Fredericton Annual Conference*. Canadian Society of Civil Engineers.
- Walpole, S. C., Prieto-Merino, D., Edwards, P., Cleland, J., Stevens, G., & Roberts, I. (2012). The weight of nations: an estimation of adult human biomass. *BMC Public Health*, *12*(439), 1–6.

Appendix A

Deflection Calculations

A.1 Summary of Deflections and Plastic Hinge Lengths

Table A.1: Elastic deflections and associated loading

	1 Concentrated Load	UDL	2 Concentrated Loads
SS	$\Delta_e = \frac{1}{12}\varphi_y L^2$ $P = 4M/L$	$\Delta_e = \frac{5}{48}\varphi_y L^2$ $w = 8M/L^2$	$\Delta_e = \frac{23}{216}\varphi_y L^2$ $P = 3M/L$
FE	$\Delta_e = \frac{1}{24}\varphi_y L^2$ $P = 8M/l$	$\Delta_e = \frac{1}{16}\varphi_y L^2$ $w = 24M/L^2$	$\Delta_e = \frac{5}{144}\varphi_y L^2$ $P = 9M/2L$
CA	$\Delta_e = \frac{1}{3}\varphi_y L^2$ $P = M/L$	$\Delta_e = \frac{1}{4}\varphi_y L^2$ $w = 2M/L^2$	–
PC	$\Delta_e = \frac{7}{120}\varphi_y L^2$ $P = 32M/5L$	$\Delta_e = \frac{1}{12}\varphi_y L^2$ $w = 16M/L^2$	–

Table A.2: Plastic deflections

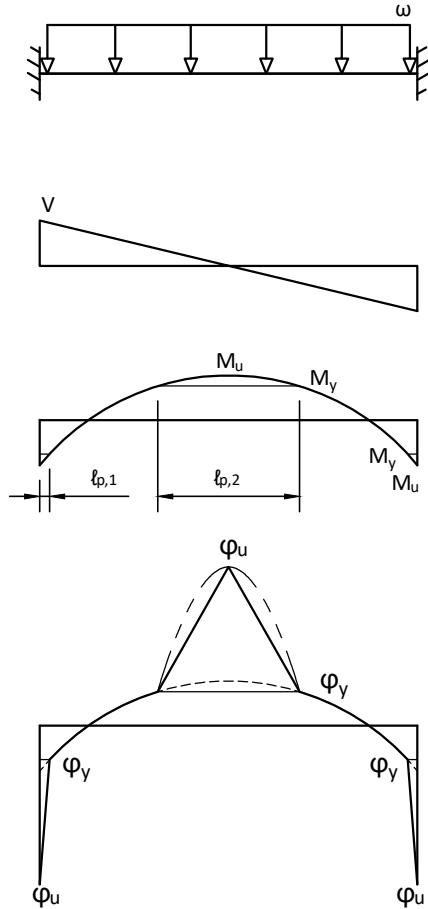
	1 Concentrated Load & UDL	2 Concentrated Loads
SS	$\frac{\Delta_p}{\varphi_y L^2} = \left(\frac{\varphi_u}{\varphi_y} - 1\right) \left[\frac{1}{8} \left(\frac{\ell_{p,2}}{L} - \frac{1}{3} \left(\frac{\ell_{p,2}}{L} \right)^2 \right) \right]$	$\frac{\Delta_p}{\varphi_y L^2} = \left(\frac{\varphi_u}{\varphi_y} - 1\right) \left[\frac{1}{3} \left(\frac{1}{9} + \frac{1}{3} \frac{\ell_{p,2}}{L} - \frac{1}{8} \left(\frac{\ell_{p,2}}{L} \right)^2 \right) \right]$
FE	$\frac{\Delta_p}{\varphi_y L^2} = \left(\frac{\varphi_u}{\varphi_y} - 1\right) \left[\frac{1}{6} \left(\frac{\ell_{p,1}}{L} \right)^2 + \frac{1}{8} \left(\frac{\ell_{p,2}}{L} - \frac{1}{3} \left(\frac{\ell_{p,2}}{L} \right)^2 \right) \right]$	$\frac{\Delta_p}{\varphi_y L^2} = \left(\frac{\varphi_u}{\varphi_y} - 1\right) \left[\frac{1}{6} \left(\frac{5}{18} + \left(\frac{\ell_{p,1}}{L} \right)^2 - \frac{1}{4} \left(\frac{\ell_{p,2}}{L} \right)^2 + \frac{1}{2} \frac{\ell_{p,2}}{L} \right) \right]$
CA	$\frac{\Delta_p}{\varphi_y L^2} = \left(\frac{\varphi_u}{\varphi_y} - 1\right) \left[\frac{1}{2} \left(\frac{\ell_{p,1}}{L} - \frac{1}{3} \left(\frac{\ell_{p,1}}{L} \right)^2 \right) \right]$	–
PC	$\frac{\Delta_p}{\varphi_y L^2} = \left(\frac{\varphi_u}{\varphi_y} - 1\right) \left[\frac{1}{24} \left(\frac{\ell_{p,2}}{L} \right)^2 + \frac{1}{4} \frac{\ell_{p,1}}{L} - \frac{1}{6} \left(\frac{\ell_{p,1}}{L} \right)^2 \right]$	–

Table A.3: Plastic hinge lengths; at support ($\ell_{p,1}$), and in span ($\ell_{p,2}$)

	1 Concentrated Load	UDL	2 Concentrated Loads
SS	–	–	–
	$\ell_{p,2} = \left(1 - \frac{1}{f}\right)L$	$\ell_{p,2} = \sqrt{1 - \frac{1}{f}}L$	$\ell_{p,2} = \left(1 - \frac{2}{3f}\right)L$
FE	$\ell_{p,1} = \frac{1}{4} \left(1 - \frac{1}{f}\right)L$	$\ell_{p,1} = \frac{1}{2} \left(1 - \sqrt{\frac{1}{3} \left(2 - \frac{1}{f}\right)}\right)L$	$\ell_{p,1} = \frac{1}{9} \left(1 - \frac{1}{f}\right)L$
	$\ell_{p,2} = \frac{1}{2} \left(1 - \frac{1}{f}\right)L$	$\ell_{p,2} = \sqrt{\frac{1}{3} \left(1 - \frac{1}{f}\right)}L$	$\ell_{p,2} = \frac{1}{9} \left(5 - \frac{2}{f}\right)L$
CA	$\ell_{p,1} = \left(1 - \frac{1}{f}\right)L$	$\ell_{p,1} = \left(1 - \sqrt{\frac{1}{f}}\right)L$	–
	–	–	–
PC	$\ell_{p,1} = \frac{5}{22} \left(1 - \frac{1}{f}\right)L$	$\ell_{p,1} = \frac{1}{8} \left(5 - \sqrt{17 + \frac{8}{f}}\right)L$	–
	$\ell_{p,2} = \left(1 - \frac{1}{f}\right)L$	$\ell_{p,2} = \frac{1}{4} \left(1 + \sqrt{9 - \frac{8}{f}}\right)L$	–

A.2 Example

- Plastic deflections and plastic hinge lengths for FE beam subjected to UDL



$$M_{end} = M_{max} = \frac{\omega L^2}{12}$$

$$M_{mid} = M_{collapse} = \frac{\omega L^2}{24}$$

Therefore the UDL that causes the upper limit of plastic deflection is,

$$\omega_{collapse} = \frac{24M}{L^2}$$

where $M = M_u^+ = M_u^-$ for the cross section.

A.2.1 Plastic Hinge Lengths

SUPPORT HINGE LENGTH, $l_{p,1}$

$$\Sigma M_R = 0 = M_u - M_y - \frac{1}{2}\omega l_{p,1} + \frac{1}{2}\omega(l_{p,1})^2$$

$$M_y = M_u - \frac{1}{2}\frac{24M_u}{L^2}l_{p,1} + \frac{1}{2}\frac{24M_u}{L^2}(l_{p,1})^2$$

$$\frac{M_y}{M_u} = 1 - 12 \left(\frac{l_{p,1}}{L} - \left(\frac{l_{p,1}}{L} \right)^2 \right)$$

$$0 = \left(\frac{l_{p,1}}{L} \right)^2 - \frac{l_{p,1}}{L} - \frac{1}{12} \left(\frac{1}{f} - 1 \right)$$

$$l_{p,1} = \frac{1}{2} \left(1 - \sqrt{\frac{1}{3} \left(2 - \frac{1}{f} \right)} \right) L$$

SPAN HINGE LENGTH, $l_{p,2}$

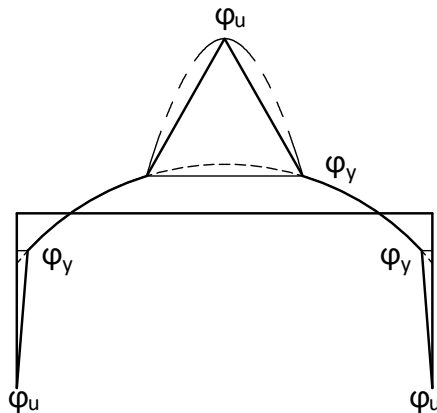
$$\Sigma M_L = 0 = M_u - M_y - \frac{1}{2} \omega \left(\frac{l_{p,2}}{2} \right)^2$$

$$M_y = M_u - \frac{24M_u}{L^2} \frac{1}{8} l_{p,2}^2$$

$$\frac{M_y}{M_u} = 1 - 3 \left(\frac{l_{p,2}}{L} \right)^2$$

$$l_{p,2} = \sqrt{\frac{1}{3} \left(1 - \frac{1}{f} \right)} L$$

A.2.2 Plastic Deflections



SUPPORT HINGE

$$\Delta_i = \frac{1}{2} (\phi_u - \phi_y f) (l_{p,1}) \frac{2}{3} l_{p,1}$$

$$\Delta_i = \frac{1}{3} \left(\frac{\phi_u}{\phi_y} - f \right) \left(\frac{l_{p,1}}{L} \right)^2 [\phi_y L^2]$$

SPAN HINGE

$$\Delta_{i'} = \frac{1}{2} (\phi_u - \phi_y f) \left(\frac{l_{p,2}}{2} \right) \frac{2}{3} \frac{l_{p,2}}{2}$$

$$\Delta_{i'} = \frac{1}{12} \left(\frac{\phi_u}{\phi_y} - f \right) \left(\frac{l_{p,2}}{L} \right)^2 [\phi_y L^2]$$

TOTAL PLASTIC DEFLECTION

$$\Delta_T = \Delta_i + \Delta_{i'}$$

$$\Delta_T = \left[\frac{1}{3} \left(\frac{l_{p,1}}{L} \right)^2 + \frac{1}{12} \left(\frac{l_{p,2}}{L} \right)^2 \right] (\phi_u - \phi_y f) [\phi_y L^2]$$

Appendix B

Warning of Failure Expansions

B.1 Ratio of Moment Capacities

The following example is intended to demonstrate the impacts of differing positive and negative moment capacities on deflections at incipient failure. Key parameters that are affected by the different positive and negative capacities are the curvature ductility ratios and shape factors. All are roughly proportional to the ratio of the reinforcement ratios at each cross section, and will be discussed with reference to the values representing the cross section in positive bending.

The deflections presented in Chapter 4 are computed assuming that the positive and negative flexural capacities are equal. In reality a range of capacity ratios from 1.0 to 2.0 can be expected for single-span beams. The bounding configurations are fixed-ended beams subjected to a single concentrated load, and a UDL, respectively.

For a flexural capacity ratio of 2.0, the ratio of curvature ductility ratios at the critical location for negative bending is approximately 0.45, or $\phi_u^-/\phi_y^- = 0.45\phi_u^+/\phi_y^+$. Similarly, the yield curvature at the negative cross section, ϕ_y^- is $0.90\phi_y^+$. Finally, the shape factor, f^- , can range from approximately 0.82 to 0.91 of f^+ . A value of $0.86f^+$ will be assumed.

Figure B.1 shows the comparison of normalized total deflections at incipient failure for an element with $\rho^+ = 0.004$ and $\rho^- = 0.008$, giving a ratio of moments, M^-/M^+ of approximately

2.0 and the cross section parameters above. Many simplifications have been made for to facilitate this illustration, but the scale of the resulting deflections is sufficiently representative. For sections with the minimum reinforcement ratio of 0.002 at the critical positive cross section and 0.004 at the critical negative cross section, the maximum deflection is approximately 70% of that expected where the cross sections have equal capacities. The difference between the two cases decreases at higher reinforcing ratios.

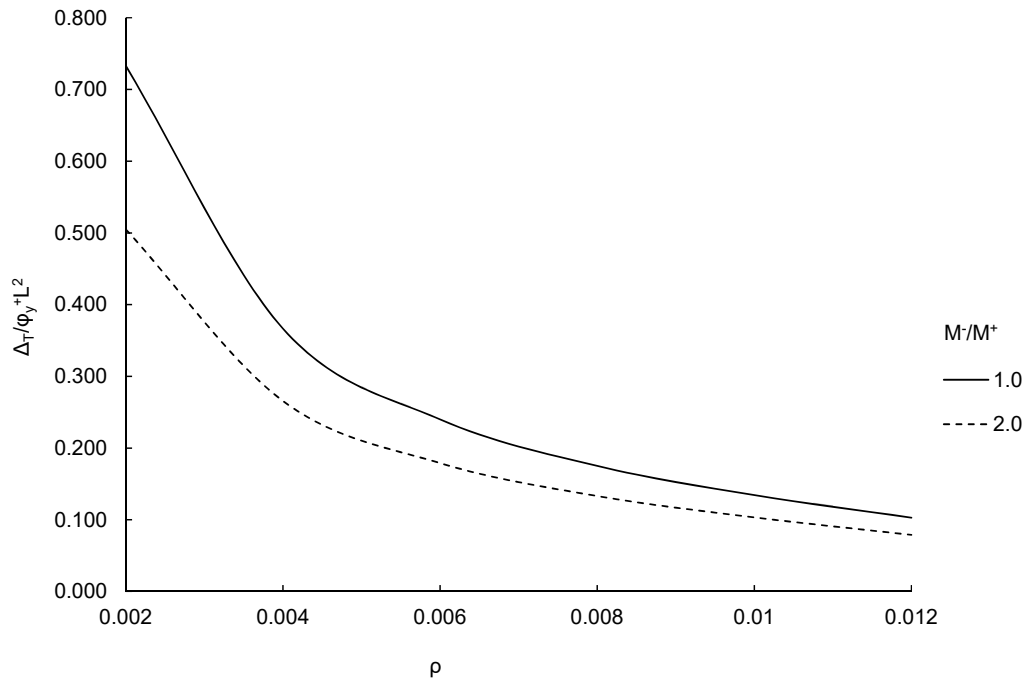


Figure B.1: Comparison of deflections at incipient failure for M^-/M^+ from 1.0 to 2.0

B.2 Two Span Beam Analysis

The analysis results of a two-span beam that is continuous over the middle support and subjected to symmetric loading yields the same response as a single-span propped cantilever. Therefore, analysis of only the two-span case with differently loaded spans will be outlined below.

Figure B.2 shows the load patterns for a two-span beam, Case (a) with symmetrical loading, and Case (b) where one span is loaded more heavily than the other. This will produce

several possible structural responses, from which designs are typically proportioned in line with response envelopes. For a two-span system, two additive components of loading must be considered: that applied to both spans, w_2 , and that applied to only one span, w_1 . Generally w_2 will consist of dead loads (and live loads where symmetrically loaded) and w_1 will consist of live loads. The path to failure is dependent on the ratio $\alpha = w_1/w_2$.

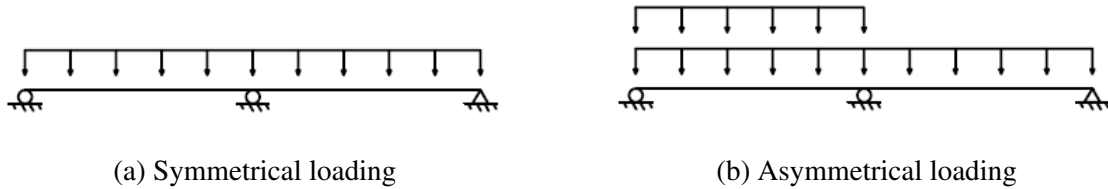


Figure B.2: Load patterns for two-span beams

In the analysis of two span beams, the consideration of the ductility ratio for the critical cross sections in both positive and negative bending, φ_u^+/φ_y^+ , and φ_u^-/φ_y^- , is required, along with the ratio of yield curvatures in positive and negative bending φ_y^-/φ_y^+ . The moment area method is used to calculate deflections at incipient failure, and the effect of varying curvature ductility ratios and plastic hinges can be observed.

Depending on the ratio of the w_1 and w_2 , the first plastic hinge to form may be the support hinge or the span hinge. If the support hinge forms first, the second stage of loading is essentially applied to two separate simply supported beams, until the formation of span hinges. If the span hinge forms first, the second stage of loading applies to single span beam with an overhang.

The elastic deflection curves for these two cases are shown in Figure B.3. Case 2 has large elastic deflections in the second stage of loading due to the large additional rotations after the formation of the span hinge.

Figure B.4 shows the deflections of equivalent beams when calculated according to Case 1 and Case 2 procedures. The deflections at incipient failure for the asymmetrical case are consistently markedly higher than for the symmetrically loaded case. The figure is derived for



Figure B.3: Elastic curves for two-span beams

the condition where w_1 and w_2 are equal, or $\alpha=1.0$. The cross-section properties used assume equal positive and negative reinforcement ratios.

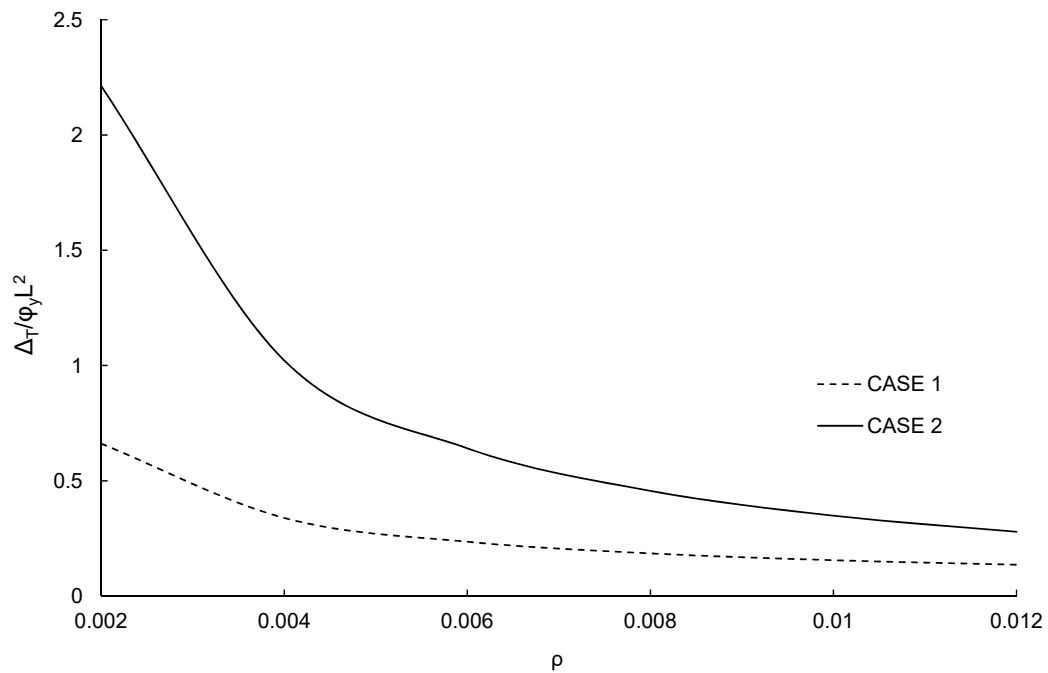


Figure B.4: Comparison of deflections at imminent failure two span beams with asymmetrical loading

Expansion of these concepts can provide further insight into the effects of load ratio, and the flexural capacity ratio on the total deflections in two-span systems. This can eventually be used to improve the accuracy with which the warning factor represents their failure behaviours.

Curriculum Vitae

Name: Marcie van Weerdhuizen

**Post-Secondary
Education and
Degrees:** University of Waterloo
Waterloo, Ontario
2011 - 2016 B.A.Sc.

University of Western Ontario
London, Ontario
2016 - 2018 M.E.Sc.

**Related Work
Experience:** Teaching Assistant
University of Western Ontario
2016 - 2018

Publications:

van Weerdhuizen, M., & Bartlett, F. M. (2018). Curvature Ductility of Concrete Columns with Low Axial Loads. In *Proc. CSCE 2018 Fredericton Annual Conference*. Canadian Society of Civil Engineers.